Environ. Sci. Technol. **2008,** *42,* 1017–1023

Impact of Artificial Recharge on Dissolved Noble Gases in Groundwater in California

BRADLEY D. CEY,*,† G. BRYANT HUDSON,‡ JEAN E. MORAN,‡ AND BRIDGET R. SCANLON§

Department of Geological Sciences, Jackson School of Geosciences, University of Texas at Austin, Austin, Texas 78712, Bureau of Economic Geology, Jackson School of Geosciences, University of Texas at Austin, Austin, Texas 78712, and Chemical Sciences Division, Lawrence Livermore National Laboratory, Livermore, California 94550

Received March 9, 2007. Revised manuscript received November 19, 2007. Accepted November 26, 2007.

Dissolved noble gas concentrations in groundwater can provide valuable information on recharge temperatures and enable $^3H-^3He$ age-dating with the use of physically based interpretive models. This study presents a large (905 samples) data set of dissolved noble gas concentrations from drinking water supply wells throughout California, representing a range of physiographic, climatic, and water management conditions. Three common interpretive models (unfractionated air, UA; partial re-equilibration, PR; and closed system equilibrium, CE) produce systematically different recharge temperatures or ages; however, the ability of the different models to fit measured data within measurement uncertainty indicates that goodness-of-fit is not a robust indicator for model appropriateness. Therefore caution is necessary when interpreting model results. Samples from multiple locations contained significantly higher Ne and excess air concentrations than reported in the literature, with maximum excess air tending toward 0.05 cm^3 STP g^{-1} (ΔNe ~400%). Artificial recharge is the most plausible cause of the high excess air concentrations. The ability of artificial recharge to dissolve greater amounts of atmospheric gases has important implications for oxidation–reduction dependent chemical reactions. Measured gas concentration ratios suggest that diffusive degassing may have occurred. Understanding the physical processes controlling gas dissolution during groundwater recharge is critical for optimal management of artificial recharge and for predicting changes in water quality that can occur following artificial recharge.

Introduction

Concentrations of atmospherically derived noble gases dissolved in groundwater are used to determine recharge temperatures which are useful for paleoclimatic studies of glacial−interglacial temperature variation (*1–5*). Concentrations of dissolved noble gases in groundwater are virtually always greater than equilibrium solubility. The portion of gas in excess of equilibrium solubility is referred to as "excess air" because of its compositional similarity to air, although it is commonly fractionated relative to air (heavy gases more enriched than light gases) (*6*). Because determinations of recharge temperature and $^3H-^3He$ age are based on equilibrium gas solubility, total measured gas must be corrected for excess air. Entrapped soil air near the water table is generally considered to be the source of excess air (*6*). These bubbles dissolve during downward water flux and during water table fluctuations. Early interpretations of dissolved gas data assumed excess air resulted from complete dissolution of entrapped air (*4, 7*). Subsequent research suggested that the commonly observed elemental fractionation of excess air was caused by complete dissolution of entrapped air and subsequent diffusive degassing (*2*) or by incomplete dissolution of entrapped air (*8*).

Three physically based models are used to interpret dissolved noble gas concentration data in groundwater: (1) unfractionated air, UA, model based on complete dissolution of entrapped air (*7*), (2) partial re-equilibration, PR, model based on complete dissolution of entrapped air bubbles followed by diffusive degassing (*2*), and (3) closed system equilibrium, CE, model based on incomplete dissolution of entrapped air (*8*). The PR and CE models both simulate excess air elemental fractionation, but PR fractionation is controlled by diffusivity whereas CE fractionation is controlled by gas solubility.

It is generally believed that the CE model best represents physical processes occurring during recharge (*6*), although few studies have systematically compared all three models. Aeschbach-Hertig et al. (*8*) showed that the CE model provided the best fit when comparing models using dissolved noble gas data from four diverse sites. Peeters et al. (*9*) used data from an aquifer in Niger to compare the three models and found that the CE and PR models both adequately fit elemental data; however, only the CE model fit isotopic data.

The process interpreted to control gas dissolution during groundwater recharge can have a significant impact on calculated recharge temperatures and $^3H-^3He$ groundwater ages (*6, 8, 9*). For example, incorrectly assuming complete dissolution of entrapped air (unfractionated excess air) results in erroneously low $^3H-^3He$ ages. Accurate determination of $^3H-^3He$ ages require an understanding of the processes affecting gas dissolution during groundwater recharge.

Understanding gas dissolution during groundwater recharge has broad implications for water resources management. Regions suffering from water shortages and poor water quality increasingly rely on (1) reclaimed municipal wastewater as a source of water, and (2) artificial recharge to store surface water for later reuse and to improve water quality (*10*) (herein we limit the definition of artificial recharge to recharge from surface sources actively managed to maximize recharge). Water quality improvement by artificial recharge largely results from microbially mediated, oxidation–reduction (redox) dependent degradation of organic compounds (e.g., trihalomethanes and endocrine-disrupting compounds) (*11*). Because of the importance of dissolved oxygen as a terminal electron acceptor, understanding gas dissolution processes is especially important for artificially recharged treated wastewater.

Objectives of this study were as follows: (1) quantify variability in observed dissolved noble gas concentrations across the study area, (2) compare measured data to previously published data, (3) examine possible causes of

* Corresponding author phone: (512) 535-5516; fax: (512) 471-9425; e-mail: bdc@mail.utexas.edu.
† Department of Geological Sciences, Jackson School of Geosciences, University of Texas at Austin.
‡ Lawrence Livermore National Laboratory.
§ Bureau of Economic Geology, Jackson School of Geosciences, University of Texas at Austin.

10.1021/es0706044 CCC: $40.75 © 2008 American Chemical Society
Published on Web 01/16/2008

observed variability in dissolved noble gas concentrations, (4) evaluate ability of interpretive models to fit measured gas data, and (5) assess implications of these results for groundwater age-dating and groundwater management. This study is based on dissolved noble gas data from groundwater basins throughout California. Unique aspects of the study include the following: (1) the size of study area which is nearly twice that of any previous study of dissolved noble gases in groundwater, (2) the large range of physiographic (Coastal Plain, Central Valley, Sierra Nevada) and climatic (arid to humid) regimes, (3) the range of water management regimes (artificial recharge versus natural recharge), and (4) application of various interpretive models to a large and highly variable data set. The size of this study provides a unique opportunity to assess factors controlling excess air generation during groundwater recharge.

Materials and Methods

Overview of Study. Samples evaluated in this study were collected as part of a statewide, comprehensive assessment of groundwater contamination vulnerability in California (www.swrcb.ca.gov/gama). $^3H-^3He$ groundwater age was used in combination with analyses of ubiquitous contaminants at ultralow levels to assess the relative probability that drinking water aquifers will become contaminated with anthropogenic pollutants. Dissolved noble gas analyses were used to calculate $^3H-^3He$ groundwater ages (*12*).

Nearly all of the wells in this study are public drinking water supply wells. There are ~16,000 public supply wells in California; wells sampled for this study are a subset from large metropolitan areas (Los Angeles, San Jose, and Sacramento), as well as several smaller population centers (e.g., Bakersfield, Chico, Stockton) and rural areas that rely on groundwater for drinking water supply (see Supporting Information for sample locations). Wells were selected according to the following criteria: (1) spatial distribution for the groundwater basin, including depth distribution that represents the exploited aquifers, (2) availability of well information such as total depth, open intervals, typical pumping rate, and year of construction, and (3) availability for sampling during the study period. The sample set almost exclusively comprises deep (>50 m total depth below ground surface), long-screened/perforated (>50 m open interval), high production ($>10^{-2}$ m^3 s^{-1}) wells actively used for drinking water supply.

Sampling and Analysis. Dissolved noble gas samples were collected using standard sampling techniques. Samples were collected by connecting the sample vessel (8 mm i.d. copper tubing, 250 mm long) to the wellhead of operating (pumping) wells with clear tygon tubing at full wellhead pressure. Water flowed for several minutes to purge air bubbles. The copper tubing was tapped lightly to dislodge bubbles and a visual inspection for bubbles was made. Steel clamps pinched the copper tubing flat in two locations to secure the water sample. Tritium samples were collected in 1 L glass bottles.

Sample analyses were performed at Lawrence Livermore National Laboratory (LLNL). Reactive gases were removed with multiple reactive metal getters. Known quantities of isotopically enriched ^{22}Ne, ^{86}Kr, and ^{136}Xe were added to provide internal standards. The isotope dilution protocol used for measuring noble gas concentrations is insensitive to potential isotopic composition variation in dissolved gases (especially Ne) from diffusive gas exchange. Noble gases were separated from one another using cryogenic adsorption. Helium was analyzed using a VG-5400 noble gas mass spectrometer. Other noble gas isotopic compositions were measured using a quadrupole mass spectrometer. The Ar abundance was determined by measuring the total noble gas sample pressure using a high-sensitivity capacitive manometer. The procedure was calibrated using water samples equilibrated with the atmosphere at a known temperature and pressure. Tritium concentrations were determined on 500 g subsamples by the ^3He in-growth method (approximately 15 day accumulation time). Analytical uncertainties are approximately 1% for $^3He/^4He$, 2% for He, Ne, and Ar, and 3% for Kr and Xe.

Modeling. The total measured concentration of dissolved noble gas is the sum of equilibrium, excess air, and radiogenic components (*6*). Helium may have an additional radiogenic component, tritiogenic ^3He (*6, 12*). Addition of excess air has the greatest relative impact on He and Ne concentrations because the equilibrium component is relatively small. A common way to represent the amount of excess air is as percent Ne, ΔNe (excess Ne relative to equilibrium component) (*6*).

Helium is commonly excluded from noble gas modeling because of the presence of radiogenic or tritiogenic sources. Calculation of equilibrium and excess air components of He are required to quantify tritiogenic ^3He which is used to calculate $^3H-^3He$ groundwater ages (*12*). Helium concentrations are impacted more by excess air than Ne; therefore, the model used to determine excess air can have a significant impact on calculated $^3H-^3He$ ages (*6*).

Measured Ne, Ar, Kr, and Xe concentrations were fitted by UA, PR, and CE models using NOBLE90 to solve for excess air, degree of excess air fractionation (in CE and PR models only), and recharge temperature. NOBLE90 is an error weighted, least-squares fitting, inverse modeling program (*8, 13*). Additional details of the modeling and goodness of fit criteria are presented in the Supporting Information.

Results and Discussion

Dissolved Ne, Ar, Kr, and Xe were measured on 905 samples. Dissolved He and $^3He/^4He$ were measured in all but one of the samples, and ^3H was measured in all but six samples (see Supporting Information for measured data and sample locations).

Spatial Characterization. To spatially characterize the data, samples were grouped into six geographic regions: (1) San Francisco Bay Area (SFBA), (2) Los Angeles Basin (LAB), (3) igneous/volcanic aquifers of northern California (NC), (4) Mojave Desert Basin (MDB), (5) northern portion of the Central Valley (NCV), and (6) southern portion of the Central Valley (SCV) (see Supporting Information for sample locations). All of the regions are alluvial basins with the exception of NC. Seasonal timing of precipitation is similar for all regions, with ≥80% of precipitation occurring from November through April. The total amount of precipitation varies greatly among the six regions (~150 mm yr^{-1} in MDB to ~1000 mm yr^{-1} for some NC sample locations).

Dense population and large-scale irrigated agriculture have led to significant modification of the natural hydrologic cycle in California. Water is transferred from northern and eastern portions of California to heavily populated coastal areas (e.g., SFBA and LAB). Irrigated agriculture has considerably altered the natural groundwater and surface water flow regimes throughout the Central Valley, where many areas are severely overdrafted and recharge is dominated by net irrigation return flow (*14*). The current situation masks natural environmental forcing such as precipitation, temperature, and vegetative cover. Furthermore, because sampled wells all have long open intervals, samples are composites of waters recharged under various conditions. Detailed spatial characterization is therefore unrealistic, yet regional differences in dissolved gas concentrations are apparent.

High Ne concentrations are most commonly associated with locations having long-term artificial recharge. Major artificial recharge facilities in LAB, SFBA, and Bakersfield (which is in the SCV region) have been operational for decades (*15–18*). High Ne concentrations in areas impacted by artificial

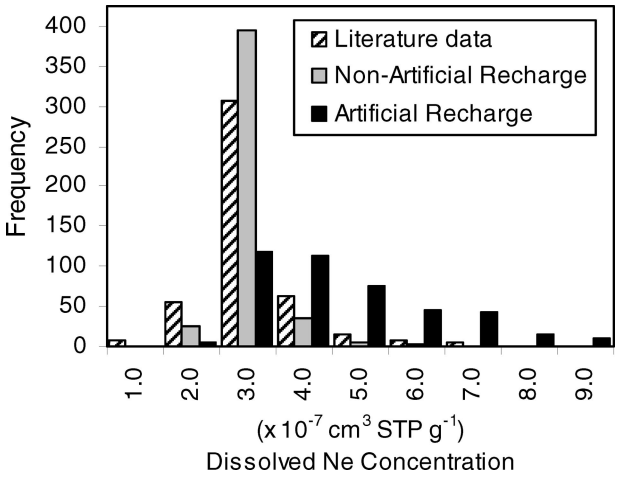

FIGURE 1. Histogram of Ne concentrations for: literature data (*1–5, 19–36*), artificial recharge impacted areas (SFBA, LAB, and Bakersfield), and nonartificial recharge impacted areas.

recharge contrast sharply with both the remainder of this data set and also literature data (Figure 1). Literature data are from studies in a wide range of climatic and hydrogeologic settings (463 samples from 23 different studies) (*1–5, 19–36*). Median Ne concentration in areas impacted by artificial recharge is 50% greater than that in the literature evaluated, while in areas not impacted by artificial recharge it is 3% less than the literature value. In contrast to Ne, all Xe concentrations fall in a relatively narrow range. Spatial differences in gas concentrations decrease with increasing molecular weight.

Data from the SCV region point to artificial recharge as the cause of high Ne concentrations. The SCV region is relatively uniform in terms of land use (irrigated agriculture), geology, and climate. However, Bakersfield is the only SCV area in our study that has a history of intensive artificial recharge. The mean Ne concentration of samples from Bakersfield ($n = 43$) is 49% greater than samples from the remainder of SCV ($n = 182$).

As noted earlier, excess air has the greatest relative impact on the lightest gases. The unique data from areas impacted by artificial recharge indicate large amounts of excess air that cannot be attributed to sampling (e.g., trapped bubbles in sampling device) or analytical problems because many of the samples with high gas concentrations were reanalyzed and showed good replication.

Noble Gas Models. The UA model is a limiting case of both models incorporating fractionation; therefore, fractionation models always fit more samples than the UA model. The fractionation models fit slightly more samples than the UA model for all regions; however, the greatest difference is for areas impacted by artificial recharge (Table 1).

Correlation between measured and modeled gas concentrations for samples fit by fractionation models was greatest for Ne ($R^2_{CE} = 0.9998$, $R^2_{PR} = 0.9997$) and least for Kr ($R^2_{CE} = 0.982$, $R^2_{PR} = 0.984$) (see Supporting Information for plots of modeled versus measured gas concentrations). Model errors (relative difference between measured and modeled gas concentrations) between the gases provide additional insight. Visual inspection of model error scatter plots reveals correlations (Figure 2). Negative correlation exists between gases with similar molecular weights (e.g., Kr−Xe), which is consistent with model errors produced when modeling synthetic data.

Excess Air. Of samples fit by the CE model, those in artificially recharging areas had much higher median excess air (89% ΔNe) than samples from nonartificial recharging areas (28% ΔNe) (results of the other models are comparable, see Supporting Information). Samples not fit by the models

TABLE 1. Number of Samples Fit by Each Model for a Given Region According to Criteria Discussed in the Supporting Information (AR refers to artificial recharge impacted areas (i.e., SFBA, LAB, and Bakersfield))

		samples fit		
area	number of samples	UA	CE	PR
SFBA	221	147	148	147
LAB	170	129	147	149
NC	31	27	31	31
MDB	64	57	63	63
NCV	194	179	182	182
SCV	225	195	216	211
AR	434	305	337	338
non-AR	471	429	450	445
total	905	734	787	783

tended to have greater average Ne concentrations (by a factor of 1.6). Inability of the models to fit samples with large Ne concentrations is reflected in the lower proportion of samples from artificial recharge areas fit by the models (Table 1). The reason that models do not fit samples with large Ne concentrations may be nonequilibrium effects (e.g., gas dissolution stopping prior to attaining equilibrium between entrapped gas and dissolved gas). Kinetic factors may control dissolved gas concentrations (*37*), especially in locations with high recharge flux.

Neon, Ar, Kr, and Xe concentrations do not allow one to clearly differentiate between the CE and PR models. Peeters et al. (*9*) explain the benefit of isotopic data for distinguishing between the CE and PR models; however, isotopic data are not available in this study. In the absence of isotopic data, an examination of model-predicted He concentrations can help differentiate the models. Helium data were not used for modeling but NOBLE90 outputs predicted He concentrations. The range of predicted He:Ne ratios from the CE model is limited because He:Ne in the excess air component can only range from that of air (0.288) to that of air saturated water (0.230 at 10 °C), whereas the PR model has a theoretical lower limit of zero. Over 160 samples—the majority of which are fit by the PR model—have low measured He:Ne ratios that cannot be readily explained by either the UA or CE models (Figure 3). Approximately two-thirds of these samples are from areas impacted by artificial recharge. The 160 samples represent a minimum number as some samples may have had low He:Ne ratios immediately after recharge followed by addition of radiogenic He. These results are consistent with diffusive degassing; however, elemental ratios alone can not be considered conclusive evidence of diffusive degassing. The authors of the present study are unaware of any groundwater studies that present evidence of dissolved noble gas fractionation by diffusive degassing, although studies have shown degassing caused by CO_2/CH_4 gas stripping (*32, 38*).

It is clear that for high excess air concentrations, excess air is less fractionated (e.g., lower CE model fractionation factor F values, where $F = v/q$, v is the ratio of entrapped gas volumes in final and initial states, and q is the ratio of dry gas pressures in entrapped air to that in the atmosphere (*8*)) (Figure 4). This is expected because pore spaces hold a finite amount of entrapped air in bubbles and as dissolution of entrapped air continues the excess air component becomes decreasingly fractionated until the entrapped air completely dissolves. The upper bound of excess air observed in this study is 400−500% ΔNe or ~0.05 cm^3 at standard temperature and pressure (STP) per gram of water, cm^3 STP g^{-1} (as air; Figure 4). This is reasonable given that the amount of entrapped air in quasi-saturated porous media is >0.05 cm^3 STP g^{-1}, as reported from laboratory pycnometer measure-

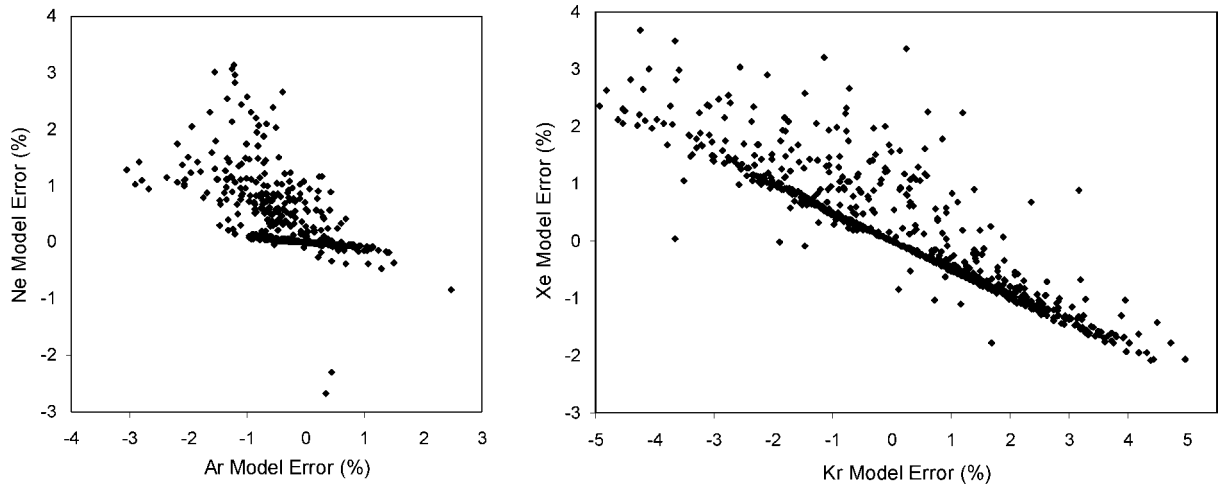

FIGURE 2. Scatter plots of model error (relative difference between modeled and measured gas concentrations) for samples fit by the CE model. Results from the other models are comparable. Note that analytical uncertainties are approximately 2% for Ne and Ar, and 3% for Kr and Xe.

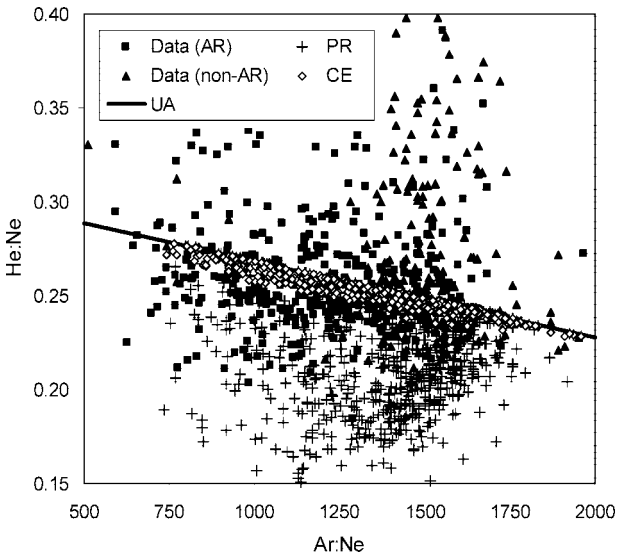

FIGURE 3. Element ratios for (1) measured gas concentrations for artificial recharge impacted areas (AR) and non-AR areas, and (2) total model-predicted gas concentrations (UA, CE, and PR). Measured ratios below the cluster of CE points can not be explained by the UA or CE models and are consistent with diffusive degassing or other fractionating processes. The UA model-predicted ratios lie on the line shown. Not all data are shown at this scale.

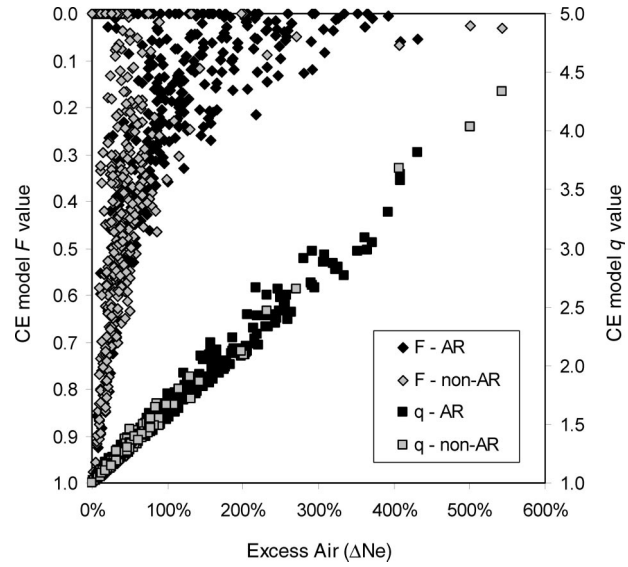

FIGURE 4. Relationship between CE model parameters and excess air. As excess air increases, the degree of fractionation decreases. Note that the CE model reduces to the UA model when $F = 0$. One data point is not shown at the given scale ($\Delta Ne = 737\%$, $F = 0.031$, $q = 5.8$).

ments (*39*) and field experiments using a neutron probe (*40*). Stonestrom and Rubin (*39*) measured entrapped air in alluvium (i.e., Oakley sand) from the NCV region and reported a range of 0.09−0.14 $cm^3\ g^{-1}$ under capillary saturation at 21 °C (STP values would be even greater because the pressure of entrapped air was unknown).

Excess air concentrations are strongly correlated with the CE model parameter q (Figure 4), consistent with results of Aeschbach-Hertig et al. (*41*). Aeschbach-Hertig et al. (*41*) and Kipfer et al. (*6*) assert that q is a semiquantitative measure of hydrostatic pressure exerted on entrapped air and therefore of water table fluctuations. The upper range of these data would then indicate water table fluctuations of >20 m assuming all the pressure was generated hydrostatically (interfacial tension only produces such high pressures for bubble radii <0.001 mm). It is unlikely that such large water table fluctuations naturally occur in any of the study regions. An alternative mechanism that could generate large q values (large hydrostatic pressures) is entrainment of entrapped bubbles in areas of high recharge. Bubbles could be transported to sufficient depths to cause dissolution of large amounts of excess air.

$^3H-^3He$ Age-Dating. The choice of excess air model has an impact on interpreted $^3H-^3He$ groundwater ages, especially for the youngest waters (*12*). Normally the excess air component of He is determined based on Ne data alone and assumes no gas fractionation (*6*, *12*). Kipfer et al. (*6*) and Aeschbach-Hertig et al. (*8*) demonstrate that the assumption of no gas fractionation may give unreasonably low ages (even negative values of tritiogenic He).

The interpreted ages resulting from each of the three excess air models vary systematically as discussed by Peeters et al. (*9*). The oldest age is calculated by PR, the youngest age is calculated by UA, while the CE model yields ages between the PR and UA models (see Supporting Information for histogram of calculated $^3H-^3He$ ages). The reason is that the interpreted excess air component of He is maximized for unfractionated conditions. A larger excess air component of He results in a lower interpreted tritiogenic He component

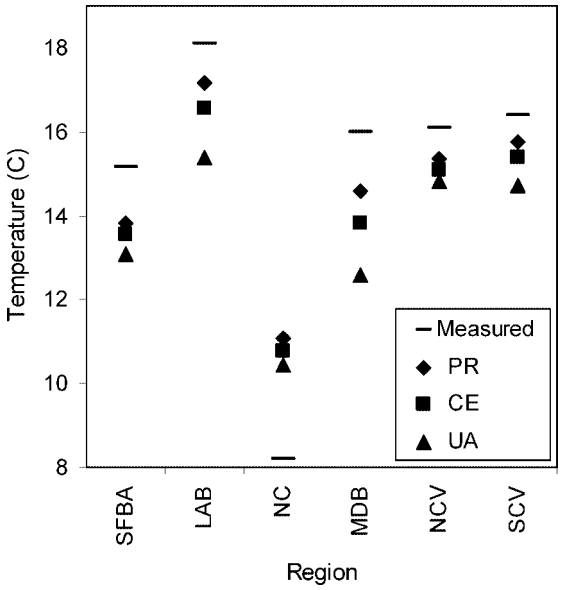

FIGURE 5. Median calculated recharge temperatures from each of the three models. The measured data are mean annual air temperatures taken from the United States Historical Climatology Network (data available at http://www.ncdc.noaa.gov/ol/climate/research/ushcn/ushcn.html) and are the medians of stations nearest each sample location.

for a given total measured amount of He, and a younger interpreted age. As expected the difference between PR and CE calculated ages is more pronounced for samples having higher excess air, for artificial recharge areas the mean difference is 4.1 yr (n = 170) versus 3.6 yr for nonartificial recharge areas (n = 144). Samples with ^3H < 3 pCi L^{-1}, negative calculated tritiogenic ^3He, or calculated ages >55 yr were excluded. Age-dating calculations assumed radiogenic $^3He/^4He = 2.0 \times 10^{-8}$ and no mantle derived He.

The differences in interpreted groundwater ages were greatest for (1) younger samples, and (2) samples with fractionated excess air. These results are consistent with the literature (*6*) and suggest calculating groundwater age without considering gas fractionation will underestimate groundwater age, especially if diffusive degassing occurs.

Recharge Temperature. Model recharge temperatures generally range from lowest to highest in the following order; UA, CE, PR (Figure 5 and Supporting Information). Because Xe solubility increases substantially with decreasing temperature, calculated recharge temperature (which is based on the equilibrium solubility component) tends to be higher for fractionation models than for the UA model. In other words, fractionation models tend to produce higher calculated recharge temperatures than the UA model because more of the total Xe is attributed to the excess air component (and less to the equilibrium component) in fractionation models. An evaluation of the relationship between model recharge temperature differences and amount of excess air did not reveal a clear correlation.

The mean calculated recharge temperature of each region broadly tracks the measured mean annual air temperature (MAAT) for each of the three models (Figure 5). In virtually all cases soil temperatures are slightly greater (1−3 °C) than MAAT; therefore, it is common for NGTs to be greater than MAAT (*6*). These data show the opposite relationship, which is unusual but not unprecedented (*33*). There are possible reasons that NGTs are less than MAAT. Groundwater recharge may reflect winter temperatures rather than MAAT because of focused seasonal recharge. Spring snowmelt runoff from uplands (e.g., Sierra Nevada) into the alluvial basins causes focused recharge from surface channels (rivers, streams, canals). Also, MAAT data used in this analysis are referenced to well location rather than recharge location. Detailed analyses of recharge areas for each well are beyond the scope of this study; however, it is likely that some groundwater recharged near basin edges at higher elevations and cooler temperatures than the wellhead (especially MDB). Furthermore, the assumption that the recharge elevation is the wellhead elevation may yield incorrect NGTs.

Artificial Recharge. The most plausible reason for the large excess air concentrations is artificial recharge. Presently LAB and SFBA artificially recharge ~4.0×10^8 and >1.0×10^8 $m^3 yr^{-1}$, respectively; which is greater than half of groundwater pumping for each area (*16, 42, 43*). Operational procedures of large-capacity artificial recharge facilities in LAB provide the necessary conditions to dissolve large amounts of air (*18*). Specifically Reichard et al. (*42*) present data from shallow wells near artificial recharge facilities in LAB with annual head fluctuations >10 m (well 2S/12W-14J1 1590F) and Mills (*18*) notes a sustained percolation rate of 1.2 m s^{-1} at an artificial recharge facility in LAB. Furthermore, Anders and Schroeder (*17*) suggest that a measured increase in redox potential of an artificially recharged groundwater plume in LAB may be caused by large amounts of excess air.

Management of artificial recharge facilities can have a major impact on the amount of dissolved gas in recharging water. Continual buildup of clogging layers on the bottom of spreading basins necessitates periodic drying to allow degradation and/or removal of clogging layers (*18*). Optimal management balances the effects of increased recharge flux caused by removal of low permeability clogging layers against the interruption to recharge caused by basin drying/cleaning. An additional operational consideration is reduced hydraulic conductivity following basin drying caused by the presence of newly entrapped air. Therefore, frequency and duration of basin drying strongly influence the amount of excess air in groundwater recharged from artificial recharge facilities.

The majority of samples not fit by the models (75–82% depending on model) are from areas impacted by artificial recharge (Table 1). Using such models to determine recharge parameters of samples in areas impacted by artificial recharge is challenging. Artificial recharge may occur at temperatures different from the local average water table temperature due to seasonal recharging activities and heating of water in spreading basins. For example, temperatures of surface water used for artificial recharge in LAB can vary from 10 to 35 °C annually (*44*). It is also likely that many well water samples are mixtures of naturally recharged and artificially recharged waters. Furthermore, it is unlikely that gas dissolution occurs under equilibrium conditions under very high recharge fluxes. Nonequilibrium gas dissolution during groundwater recharge has received relatively little attention (*37*), but is likely to occur during artificial recharge and other rapid infiltration scenarios (e.g., highly conductive river beds).

California, like many other regions with water supply challenges, is increasingly using reclaimed wastewater as a source for artificial recharge (*17, 42*). Fate and transport of organic compounds such as disinfection byproducts (e.g., trihalomethanes) and endocrine-disrupting compounds in artificially recharged wastewater is a major water quality concern in California (*10, 17*) and in many other areas (*11*). California has proposed that artificially recharged wastewater have a minimum subsurface residence time of 6 months to allow degradation of contaminants (*10*). The contribution of dissolved O_2 in excess air plays a critical role in the redox chemistry of groundwater and therefore the fate of many organic pollutants (*11*). The proportion of dissolved O_2 added by excess air relative to equilibrium solubility, ΔO_2, is less than ΔNe (ΔO_2:ΔNe is ~0.3 for unfractionated air, but can exceed 0.5 for fractionated conditions). Therefore artificially

recharged groundwater could have a dissolved O_2 concentration up to twice that of equilibrium solubility.

Improved understanding of excess air generation is key for both managing the physical process of artificial recharge and predicting water quality changes related to artificial recharge. Few studies have addressed the issue of gas dissolution during artificial recharge (*43, 45*). Long-term field studies in well characterized media would be particularly helpful in assessing the impact of dissolved gases on artificially recharged groundwater.

Three main noble gas models exist to interpret dissolved gas concentrations. Parameters deduced from model output (recharge temperatures or $^3H-^3He$ ages) systematically differ among models because of the different physical processes upon which the models are based. As demonstrated in this study, all three models may adequately fit measured data. This suggests that goodness-of-fit is not a robust indicator for model appropriateness and caution is necessary when interpreting results from noble gas modeling. Furthermore, gas concentration ratios suggest that diffusive degassing may have occurred. Further research aimed at understanding the physical processes controlling gas dissolution during groundwater recharge is warranted. For example, analyses of dissolved gas isotopic ratios would provide information on the possible occurrence of diffusive degassing at artificial recharge sites.

Acknowledgments

Funding was provided by the California State Water Resources Control Board Groundwater Ambient Monitoring and Assessment Program, the Jackson School of Geosciences, and the Glenn T. Seaborg Institute at LLNL (fellowship to B.D.C.). We acknowledge the USGS for assistance in sample collection, Mr. Wayne Culham for sample analyses, Dr. Andrew Manning for reviewing an earlier version of this manuscript, and two anonymous reviewers for insightful and constructive comments.

Supporting Information Available

Details of noble gas models and their application using NOBLE90, tabulation and statistical summary of dissolved gas concentrations and calculated quantities, and figures showing sample locations, modeled versus measured gas concentrations, differences between calculated recharge temperatures, and calculated $^3H-^3He$ ages for each of three models. This information is available free of charge via the Internet at http://pubs.acs.org.

Literature Cited

(1) Aeschbach-Hertig, W.; Stute, M.; Clark, J. F.; Reuter, R. F.; Schlosser, P. A paleotemperature record derived from dissolved noble gases in groundwater of the Aquia Aquifer (Maryland, USA). *Geochim. Cosmochim. Acta* **2002**, *66*, 797–817.

(2) Stute, M.; Forster, M.; Frischkorn, H.; Serejo, A.; Clark, J. F.; Schlosser, P.; Broecker, W. S.; Bonani, G. Cooling of tropical Brazil (5 °C) during the last glacial maximum. *Science* **1995**, *269*, 379–383.

(3) Weyhenmeyer, C. E.; Burns, S. J.; Waber, N. H.; Aeschbach-Hertig, W.; Kipfer, R.; Loosli, H. H.; Matter, A. Cool glacial temperatures and changes in moisture source recorded in Oman groundwaters. *Science* **2000**, *287*, 842–845.

(4) Andrews, J. N.; Fontes, J.-C.; Aranyossy, J.-F.; Dodo, A.; Edmunds, W. M.; Joseph, A.; Travi, Y. The evolution of alkaline groundwaters in the continental intercalaire aquifer of the Irhazer Plain, Niger. *Water Resour. Res.* **1994**, *30*, 45–61.

(5) Clark, J. F.; Davisson, M. L.; Hudson, G. B.; Macfarlane, P. A. Noble gases, stable isotopes, and radiocarbon as tracers of flow in the Dakota aquifer, Colorado and Kansas. *J. Hydrol.* **1998**, *211*, 151–167.

(6) Kipfer, R.; Aeschbach-Hertig, W.; Peeters, F.; Stute, M. Noble gases in lakes and ground waters. In *Noble Gases in Geochemistry and Cosmochemistry*; Porcelli, D., Ballentine, C. J., Wieler, R., Eds.; Mineralogical Society of America: Washington, DC, 2002.

(7) Heaton, T. H. E.; Vogel, J. C. "Excess air" in groundwater. *J. Hydrol.* **1981**, *50*, 201–216.

(8) Aeschbach-Hertig, W.; Peeters, F.; Beyerle, U.; Kipfer, R. Palaeotemperature reconstruction from noble gases in ground water taking into account equilibration with entrapped air. *Nature* **2000**, *405*, 1040–1044.

(9) Peeters, F.; Beyerle, U.; Aeschbach-Hertig, W.; Holocher, J. O.; Brennwald, M. S.; Kipfer, R. Improving noble gas based paleoclimate reconstruction and groundwater dating using $^{20}Ne/^{22}Ne$ ratios. *Geochim. Cosmochim. Acta* **2002**, *67*, 587–600.

(10) Asano, T.; Cotruvo, J. A. Groundwater recharge with reclaimed municipal wastewater: health and regulatory considerations. *Water Res.* **2004**, *38*, 1941–1951.

(11) Greskowiak, J.; Prommer, H.; Massmann, G.; Johnston, C. D.; Nützmann, G.; Pekdeger, A. The impact of variably saturated conditions on hydrogeochemical changes during artificial recharge of groundwater. *Appl. Geochem.* **2005**, *20*, 1409–1426.

(12) Solomon, D. K.; Cook, P. G. ^3H and ^3He. In *Environmental Tracers in Subsurface Hydrology*; Cook, P. G., Herczeg, A. L., Eds.; Kluwer Academic Publishers: Norwell, MA, 2000.

(13) Aeschbach-Hertig, W.; Peeters, F.; Beyerle, U.; Kipfer, R. Interpretation of dissolved atmospheric noble gases in natural waters. *Water Resour. Res.* **1999**, *35*, 2779–2792.

(14) Bertoldi, G. L.; Johnston, R. H.; Evenson, K. D. *Ground Water in the Central Valley, California: A Summary Report*; U.S. Geological Survey Professional Paper 1401-A; U.S. Geological Survey: Washington, DC, 1991.

(15) City of Bakersfield, California. *Urban Water Management Plan*; Bakersfield, CA, 2005. Available at http://www.bakersfieldcity.us/cityservices/water/pdfs/URBAN_WATER_MANAGEMENT_PLAN.pdf.

(16) Santa Clara Valley Water District. *Santa Clara Valley Water District Groundwater Management Plan*; San Jose, CA, 2001. Available at http://www.valleywater.org/media/pdf/Groundwater%20Management%20Plan.pdf.

(17) Anders, R. A.; Schroeder, R. A. *Use of water-quality indicators and environmental tracers to determine the fate and transport of recycled water in Los Angeles County, California*;U.S. Geological Survey Water-Resources Investigations Report 2003-4279; U.S. Geological Survey: Sacramento, CA, 2003.

(18) Mills, W. R. The quest for water through artificial recharge and wastewater recycling. In *Management of Aquifer Recharge for Sustainability*; Dillon, P. J. , Ed.; A.A. Balkema: Exton, PA, 2002.

(19) Zuber, A.; Weise, S. M.; Osenbrück, K.; Pajnowska, H.; Grabczak, J. Age and recharge pattern of water in the Oligocene of the Mazovian basin (Poland) as indicated by environmental tracers. *J. Hydrol.* **2000**, *233*, 174–188.

(20) Stute, M.; Clark, J. F.; Schlosser, P.; Broecker, W. S.; Bonani, G. A 30,000 yr continential paleotemperature record derived from noble gases dissolved in groundwater from the San Juan Basin, New Mexico. *Quat. Res.* **1995**, *43*, 209–220.

(21) Clark, J. F.; Stute, M.; Schlosser, P.; Drenkard, S.; Bonani, G. A tracer study of the Floridian aquifer in southeastern Georgia: implications for groundwater flow and paleoclimate. *Water Resour. Res.* **1997**, *33*, 281–289.

(22) Dennis, F.; Andrews, J. N.; Parker, A.; Poole, J.; Wolf, M. Isotopic and noble gas study of Chalk groundwater in the London Basin, England. *Appl. Geochem.* **1997**, *12*, 763–773.

(23) Stute, M.; Sonntag, C. Palaeotemperatures derived from noble gases dissolved in groundwater and in relation to soil temperature. In *Proceedings of Isotopes of Noble Gases as Tracers in Environmental Studies*. IAEA, Vienna, 1992; pp 111–122.

(24) Andrews, J. N.; Drimmie, R. J.; Loosli, H. H.; Hendry, M. J. Dissolved gases in the Milk River aquifer, Alberta, Canada. *Appl. Geochem.* **1991**, *6*, 393–403.

(25) Fontes, J.-C.; Andrews, J. N.; Edmunds, W. M.; Guerre, A.; Travi, Y. Paleorecharge by the Niger River (Mali) deduced from groundwater geochemistry. *Water Resour. Res.* **1991**, *27*, 199–214.

(26) Kulongoski, J. T.; Hilton, D. R.; Selaolo, E. T. Climate variability in the Botswana Kalahari from the late Pleistocene to the present day. *Geophys. Res. Lett.* **2004**, *31*, L10204 doi:10210.11029/12003GL019238.

(27) Ma, L.; Castro, M. C.; Hall, C. M. A late Pleistocene—Holocene noble gas paleotemperature record in southern Michigan. *Geophys. Res. Lett.* **2004**, *31*, L23204 doi:23210.21029/22004GL021766.

(28) Saar, M. O.; Castro, M. C.; Hall, C. M.; Manga, M.; Rose, T. P. Quantifying magmatic, crustal, and atmospheric helium contributions to volcanic aquifers using all stable noble gases:

Implications for magmatism and groundwater flow. *Geochem. Geophys. Geosyst.* **2005**, *6*, Q03008 doi:03010.01029/02004-GC000828.
(29) Zuber, A.; Weise, S. M.; Motyka, J.; Osenbrück, K.; Rózanski, K. Age and flow pattern of groundwater in Jurassic limestone aquifer and related Tertiary sands derived from combined isotope, noble gas and chemical data. *J. Hydrol.* **2004**, *286*, 87–112.
(30) Wilson, G. B.; Andrews, J. N.; Bath, A. H. The nitrogen isotope composition of groundwater nitrates from the East Midlands Triassic Sandstone aquifer, England. *J. Hydrol.* **1994**, *157*, 35–46.
(31) Wilson, G. B.; Andrews, J. N.; Bath, A. H. Dissolved gas evidence from denitrification in the Lincolnshire Limestone Groundwaters, Eastern England. *J. Hydrol.* **1990**, *113*, 51–60.
(32) Thomas, J. M.; Hudson, G. B.; Stute, M.; Clark, J. F. Noble gas loss may indicate groundwater flow across flow barriers in southern Nevada. *Environ. Geol.* **2003**, *43*, 568–579.
(33) Hall, C. M.; Castro, M. C.; Lohmann, K. C.; Ma, L. Noble gases and stable isotopes in a shallow aquifer in southern Michigan: implications for noble gas paleotemperature reconstructions for cool climates. *Geophys. Res. Lett.* **2005**, *32*, L18404 doi: 18410.11029/12005GL023582.
(34) Beyerle, U.; Purtschert, R.; Aeschbach-Hertig, W.; Imboden, D. M.; Loosli, H. H.; Wieler, R.; Kipfer, R. Climate and groundwater recharge during the last glaciation in an ice-covered region. *Science* **1998**, *282*, 731–734.
(35) Beyerle, U.; Rueedi, J.; Leuenberger, M.; Aeschbach-Hertig, W.; Peeters, F.; Kipfer, R.; Dodo, A. Evidence for periods of wetter and cooler climate in the Sahel between 6 and 40 kyr BP derived from groundwater. *Geophys. Res. Lett.* **2003**, *30*, 1173 doi: 1110.1029/2002GL016310.
(36) Stute, M.; Deak, J. Environmental isotope study (^{14}C,^{13}C,^{18}O, D, noble gases) on deep groundwater circulation systems in Hungary with reference to paleoclimate. *Radiocarbon* **1989**, *31*, 902–918.
(37) Holocher, J. O.; Peeters, F.; Aeschbach-Hertig, W.; Kinzelbach, W.; Kipfer, R. Kinetic model of gas bubble dissolution in groundwater and its implications for the dissolved gas composition. *Environ. Sci. Technol.* **2003**, *37*, 1337–1343.
(38) Klump, S.; Kipfer, R.; Cirpka, O. A.; Harvey, C. F.; Brennwald, M. S.; Ashfaque, K. N.; Badruzzaman, A. B. M.; Hug, S. J.; Imboden, D. M. Groundwater dynamics and arsenic mobilization in Bangladesh assessed using noble gases and tritium. *Environ. Sci. Technol.* **2006**, *40*, 243–250.
(39) Stonestrom, D. A.; Rubin, J. Water content dependence of trapped air in two soils. *Water Resour. Res.* **1989**, *25*, 1947–1958.
(40) Fayer, M. J.; Hillel, D. Air encapsulation: I. measurement in a field soil. *Soil Sci. Soc. Am. J.* **1986**, *50*, 568–572.
(41) Aeschbach-Hertig, W.; Beyerle, U.; Holocher, J. O.; Peeters, F.; Kipfer, R. Excess air in groundwater as a potential indicator of past environmental changes. In *Proceedings of Study of Environmental Change using Isotope Techniques*; IAEA: Vienna, 2002; pp 174–183.
(42) Reichard, E. G.; Land, M.; Crawford, S. M.; Johnson, T.; Everett, R. R.; Kulshan, T. V.; Ponti, D. J.; Halford, K. L.;Johnson, T. A.; Paybins, K. S.; Nishikawa, T. *Geohydrology, geochemistry, and ground-water simulation-optimization of the Central and West Coast Basins, Los Angeles County, California*;U.S. Geological Survey Water-Resources Investigation 2003-4065; U.S. Geological Survey: Sacramento, CA, 2003.
(43) Clark, J. F.; Hudson, G. B.; Davisson, M. L.; Woodside, G.; Herndon, R. Geochemical imaging of flow near an artificial recharge facility, Orange County, California. *Ground Water* **2004**, *42*, 167–174.
(44) Davisson, M. L.; Hudson, G. B.; Clark, J. F.; Woodside, G.; Herndon, R. *Final report on isotope tracer investigations in the Forebay of the Orange County groundwater basin*; UCRL-TR-201735; Lawrence Livermore National Laboratory: Livermore, CA, 2004.
(45) Clark, J. F.; Hudson, G. B.; Avisar, D. Gas transport below artificial recharge ponds: insights from dissolved noble gases and a dual gas (SF_6 and^3He) tracer experiment. *Environ. Sci. Technol.* **2005**, *39*, 3939–3945.

ES0706044

Supporting Information for:

Impact of Artificial Recharge on Dissolved Noble Gases in Groundwater in California, USA

Bradley D. Cey*, G. Bryant Hudson, Jean E. Moran, and Bridget R. Scanlon

*Corresponding Author

The following is the list of supporting materials for the article:

Materials and Methods
Results and Discussion
Supporting References
Figures and Tables
Figure S1. Map showing sampled well locations
Figure S2. Plots showing modeled (CE) versus measured gas concentrations
Figure S3. Plots showing modeled (PR) versus measured gas concentrations
Figure S4. Plots showing modeled (UA) versus measured gas concentrations
Figure S5. Histogram of calculated ^{3}H-^{3}He ages
Figure S6. Plot showing modeled recharge temperatures
Table S1. Summary of excess air concentrations and recharge temperatures
Table S2. Measured data and model results

Number of pages: 36

Materials and Methods

The equilibrium solubility of a given gas *i*, $C_{i,eq}$, is given by Henry's Law as

$$C_{i,eq} = \frac{p_i}{H_i(T,S)} \quad [1]$$

where p_i is partial pressure of gas *i* and H_i is Henry's Law constant which is a function of temperature *T* and salinity *S*. The total measured concentration of dissolved gas *i*, $C_{i,m}$, is the sum of multiple components

$$C_{i,m} = C_{i,eq} + C_{i,exc} + C_{i,rad} + C_{i,ter} \quad [2]$$

where subscripts *exc*, *rad*, and *ter* refer to excess air, radiogenic, and terrigenic components, respectively. It was assumed that Ne, Ar, Kr, and Xe did not have significant radiogenic or terrigenic components in the study area (*1*).

Three physically-based models are used to interpret dissolved noble gas concentration data in groundwater: 1) unfractionated air, UA, model (*2*), 2) partial re-equilibration, PR, model (*3*), and 3) closed system equilibrium, CE, model (*4*). The UA model is the simplest as it assumes the excess air component is atmospheric air resulting from the complete dissolution of entrapped air bubbles during recharge (*2,5,6*). The total concentration of gas *i* as given by the UA model is

$$C_{i,m}^{UA} = C_{i,eq} + A_d \cdot z_i \quad [3]$$

where A_d is concentration of dry air dissolved, and z_i is volume fraction of gas *i* in dry air. Stute et al. (*3*) found elemental fractionation in the excess air component (whereby lighter gases are depleted relative to heavier gases) and suggested that this fractionation was caused by complete bubble dissolution followed by diffusive degassing (PR model). The total concentration of gas *i* as given by the PR model is

$$C_{i,m}^{PR} = C_{i,eq} + \left(A_d \cdot z_i\right) \cdot e^{\frac{-R \cdot D_i}{D_{Ne}}} \qquad [4]$$

where A_d is initial concentration of dissolved excess air, R is degree of re-equilibration, D_i is molecular diffusivity of gas i, and D_{Ne} is molecular diffusivity of Ne. Kipfer et al. (*7*) extended the PR model to include multiple dissolution-degassing cycles. Aeschbach-Hertig et al. (*4*) suggested that fractionation of excess air is the result of incomplete dissolution of entrapped air bubbles and fractionation is related to differing gas solubilities (CE model). The total concentration of gas i as given by the CE model is

$$C_{i,m}^{CE} = C_{i,eq} + \frac{\left(1 - F\right) \cdot A_e \cdot z_i}{1 + \left(\frac{F \cdot A_e \cdot z_i}{C_{i,eq}}\right)} \qquad [5]$$

where F is a fractionation parameter and A_e is the initial concentration of entrapped air

$$A_e = \frac{V_g^0}{\rho\left(T,S\right) \cdot V_w} \cdot \frac{\left(P_g - e_s\right)}{P_0} \qquad [6]$$

where V_g^0 is initial volume of entrapped air, ρ is water density as a function of temperature T and salinity S, V_w is volume of water, P_g is pressure of entrapped air, e_s is the saturation water vapor pressure, and P_0 is standard pressure (1 atm). The fractionation parameter is

$$F = \frac{v}{q} = \frac{\left(\frac{V_g}{V_g^0}\right)}{\left(\frac{P_g - e_s}{P_{atm} - e_s}\right)} \qquad [7]$$

where P_{atm} is atmospheric pressure, v is fraction of entrapped air remaining, and q is the ratio of dry entrapped air pressure to dry atmospheric pressure (which is approximately the pressure on the entrapped air).

The UA model is a limiting case of both the CE model (when $F = 0$) and the PR model (when $R = 0$). CE and PR models can give similar results as underlying physical processes for these two models vary similarly among gases. Peeters et al. (*8*) suggested that in addition to noble gas concentration data, isotopic data (especially Ne) are helpful in distinguishing between diffusive degassing (PR model) and incomplete bubble dissolution (CE model).

Inverse modeling of dissolved noble gas data allows determination of various parameters affecting gas dissolution. Calculation of recharge temperature relies heavily on $C_{Xe,m}$ because Xe solubility is highly temperature dependent. Strong correlation between recharge temperature and recharge elevation leads many researchers to define recharge elevation and solve for recharge temperature, which greatly reduces uncertainty of recharge temperature (*7*). This is a reasonable approach given that recharge elevation is usually relatively straightforward to estimate.

Measured noble gas concentrations were modeled using the UA, PR, and CE models. For all modeling the recharging water was assumed to be fresh ($S = 0$) and recharge elevation was assumed to be the wellhead elevation. It is common to assume the recharging water is fresh in noble gas studies (*4,9*). The assumption that the recharge elevation is the wellhead elevation is less accurate and may introduce error into the analysis.

The measured dissolved noble gas concentrations were modeled using NOBLE90, an error weighted, least squares fitting, inverse modeling program (downloaded from http://www.eawag.ch/research_e/w+t/UI/interpretation.html#download). NOBLE90

solves for parameter combinations for the selected interpretive model that match measured data within experimental error by minimizing χ^2, the sum of the weighted squared deviations between the modeled and measured concentrations. The ability of the selected model to describe the observed data (i.e. the goodness of fit of the model) is judged on the probability of χ^2 being greater than a given value obtained from the χ^2 distribution (for the appropriate number of degrees of freedom). If this probability is lower than a predetermined cutoff value then the solution is rejected and it is concluded that the selected model is unable to describe the measured data (*10*). This approach allows assessment of the likelihood that differences between modeled and measured values result from experimental error. In this study solutions with probabilities (p) <0.05 are rejected. The gas solubility data used in the NOBLE90 calculations came from multiple sources (*11-14*). Additional details of NOBLE90 are given by Aeschbach-Hertig et al. (*4,10*) and Peeters et al. (*8*).

Results and Discussion

Noble gas concentrations were measured on 905 groundwater samples. Statistical summaries of excess air and recharge temperature are given in Table S1 while data and extensive modeling results are given in Table S2.

Three measures were used to evaluate NOBLE90 output; 1) χ^2 test (exclude if p <0.05), 2) physically reasonable A values (exclude if A >1 cm^3 STP g^{-1}), and 3) physically reasonable recharge temperatures (exclude if modeled recharge temperature is either greater than 2°C above the greatest average monthly air temperature or less than 2°C below the lowest average monthly air temperature). Aeschbach-Hertig et al.

(*15*) note that samples that fit according to χ^2 but with large *A* are likely an artifact of the fitting procedure, because of correlation between *A* and *T*.

Correlation between measured and modeled gas concentrations for samples fit by models was greatest for Ne and least for either Kr (CE and PR models, Figure S2 and Figure S3) or Xe (UA model, Figure S4).

The interpreted ages resulting from each of the three excess air models vary systematically as discussed by Peeters et al. (*8*). The oldest age is calculated by PR, the youngest age by UA, while the CE model yields ages between the PR and UA models (Figure S5). CE model recharge temperatures are almost always lower than those calculated by the PR model, and UA model temperatures are almost always lower than those of the CE model (Figure S6).

Supporting References

(1) Lehmann, B. E.; Davis, S. N.; Fabryka-Martin, J. T. Atmospheric and subsurface sources of stable and radioactive nuclides used for groundwater dating. *Water Resour. Res.* **1993**, *29*, 2027-2040.

(2) Heaton, T. H. E.; Vogel, J. C. "Excess air" in groundwater. *J. Hydrol.* **1981**, *50*, 201-216.

(3) Stute, M.; Forster, M.; Frischkorn, H.; Serejo, A.; Clark, J. F.; Schlosser, P.; Broecker, W. S.; Bonani, G. Cooling of tropical Brazil (5°C) during the last glacial maximum. *Science* **1995**, *269*, 379-383.

(4) Aeschbach-Hertig, W.; Peeters, F.; Beyerle, U.; Kipfer, R. Palaeotemperature reconstruction from noble gases in ground water taking into account equilibration with entrapped air. *Nature* **2000**, *405*, 1040-1044.

(5) Andrews, J. N.; Fontes, J.-C.; Aranyossy, J.-F.; Dodo, A.; Edmunds, W. M.; Joseph, A.; Travi, Y. The evolution of alkaline groundwaters in the continental intercalaire aquifer of the Irhazer Plain, Niger. *Water Resour. Res.* **1994**, *30*, 45-61.

(6) Beyerle, U.; Purtschert, R.; Aeschbach-Hertig, W.; Imboden, D. M.; Loosli, H. H.; Wieler, R.; Kipfer, R. Climate and groundwater recharge during the last glaciation in an ice-covered region. *Science* **1998**, *282*, 731-734.

(7) Kipfer, R.; Aeschbach-Hertig, W.; Peeters, F.; Stute, M. Noble gases in lakes and ground waters. In *Noble Gases in Geochemistry and Cosmochemistry*; Porcelli, D., Ballentine, C. J., Wieler, R., Eds.; Mineralogical Society of America: Washington, DC, 2002.

(8) Peeters, F.; Beyerle, U.; Aeschbach-Hertig, W.; Holocher, J. O.; Brennwald, M. S.; Kipfer, R. Improving noble gas based paleoclimate reconstruction and groundwater dating using $^{20}Ne/^{22}Ne$ ratios. *Geochim. Cosmochim. Acta* **2002**, *67*, 587-600.

(9) Aeschbach-Hertig, W.; Stute, M.; Clark, J. F.; Reuter, R. F.; Schlosser, P. A paleotemperature record derived from dissolved noble gases in groundwater of the Aquia Aquifer (Maryland, USA). *Geochim. Cosmochim. Acta* **2002**, *66*, 797-817.

(10) Aeschbach-Hertig, W.; Peeters, F.; Beyerle, U.; Kipfer, R. Interpretation of dissolved atmospheric noble gases in natural waters. *Water Resour. Res.* **1999**, *35*, 2779-2792.

(11) Weiss, R. F. The solubility of nitrogen, oxygen and argon in water and seawater. *Deep-Sea Res.* **1970**, *17*, 721-735.

(12) Weiss, R. F. Solubility of helium and neon in water and seawater. *J. Chem. Eng. Data* **1971**, *16*, 235-241.

(13) Weiss, R. F.; Kyser, T. K. Solubility of krypton in water and seawater. *J. Chem. Eng. Data* **1978**, *23*, 69-72.

(14) Clever, H. L., Ed. *Krypton, Xenon and Radon*; Pergamon Press: Elmsford, NY, 1979; Vol. 2.

(15) Aeschbach-Hertig, W.; Beyerle, U.; Holocher, J. O.; Peeters, F.; Kipfer, R. Excess air in groundwater as a potential indicator of past environmental changes. In Proceedings of *Study of Environmental Change using Isotope Techniques*. IAEA, Vienna, 2002; pp 174-183.

Figures and Tables

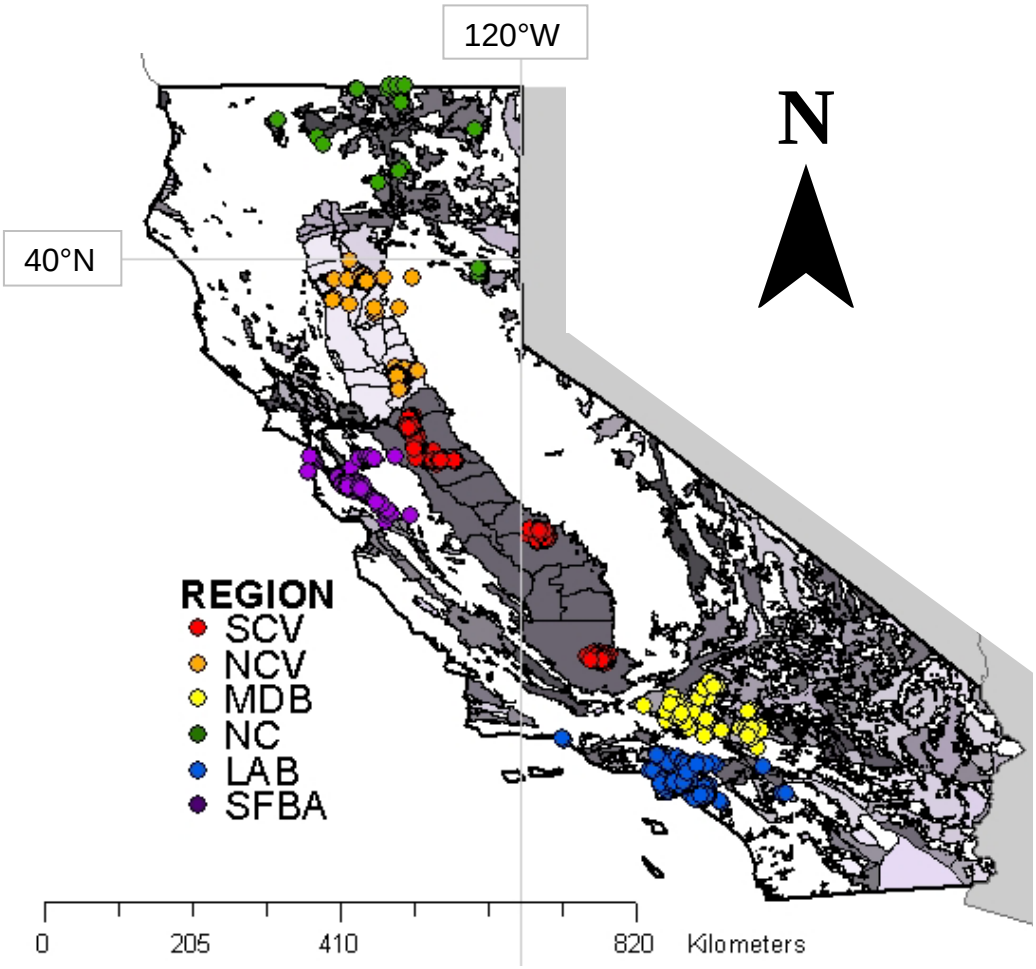

Figure S1. Map of California showing sample locations in each of the six regions: Los Angeles Basin (LAB), Mojave Desert Basin (MDB), northern California (NC), northern portion of the Central Valley (NCV), southern portion of the Central Valley (SCV), and San Francisco Bay Area (SFBA).

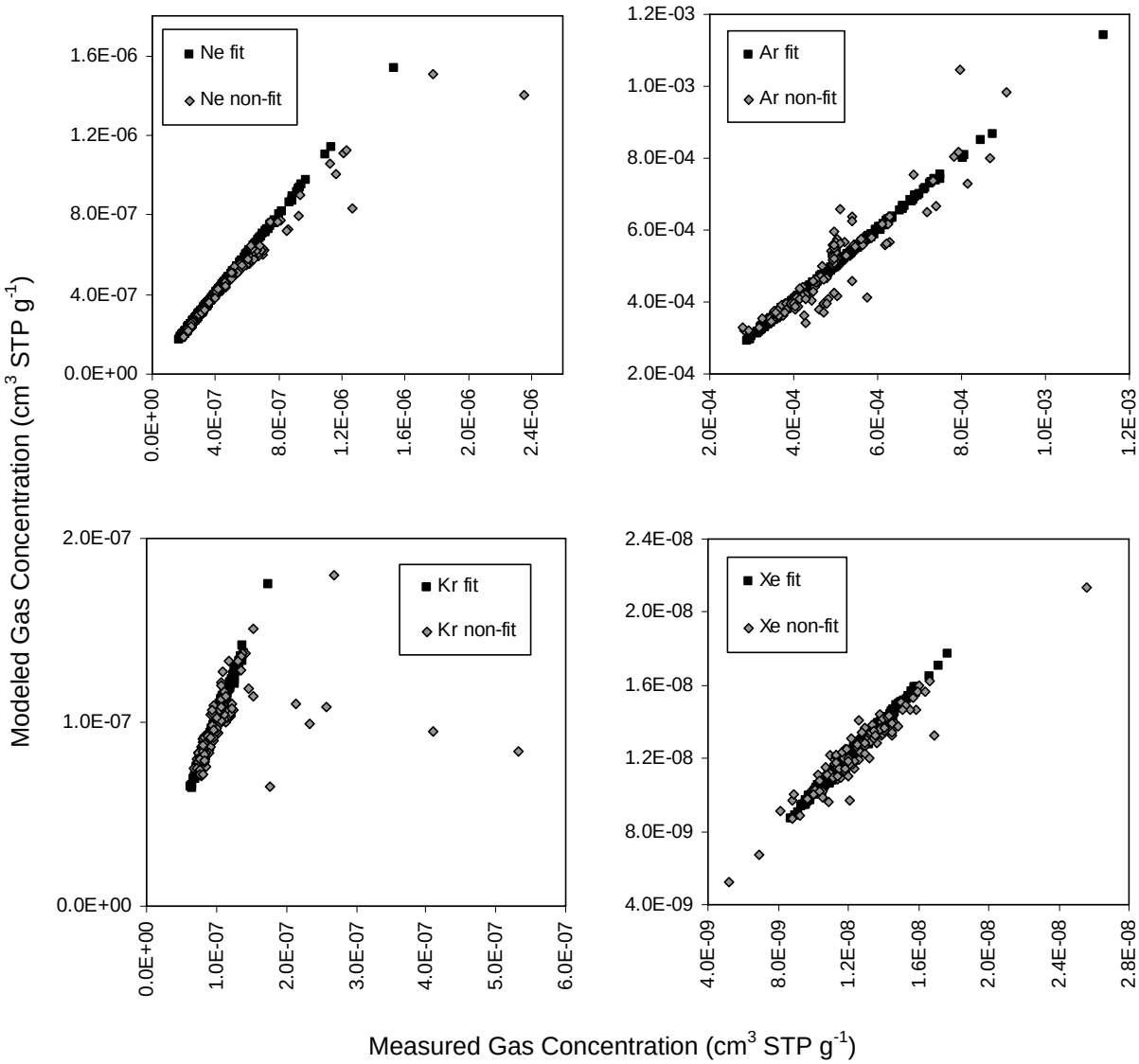

Figure S2. CE modeled versus measured gas concentrations. Note that sample 100706 plots off scale for Kr.

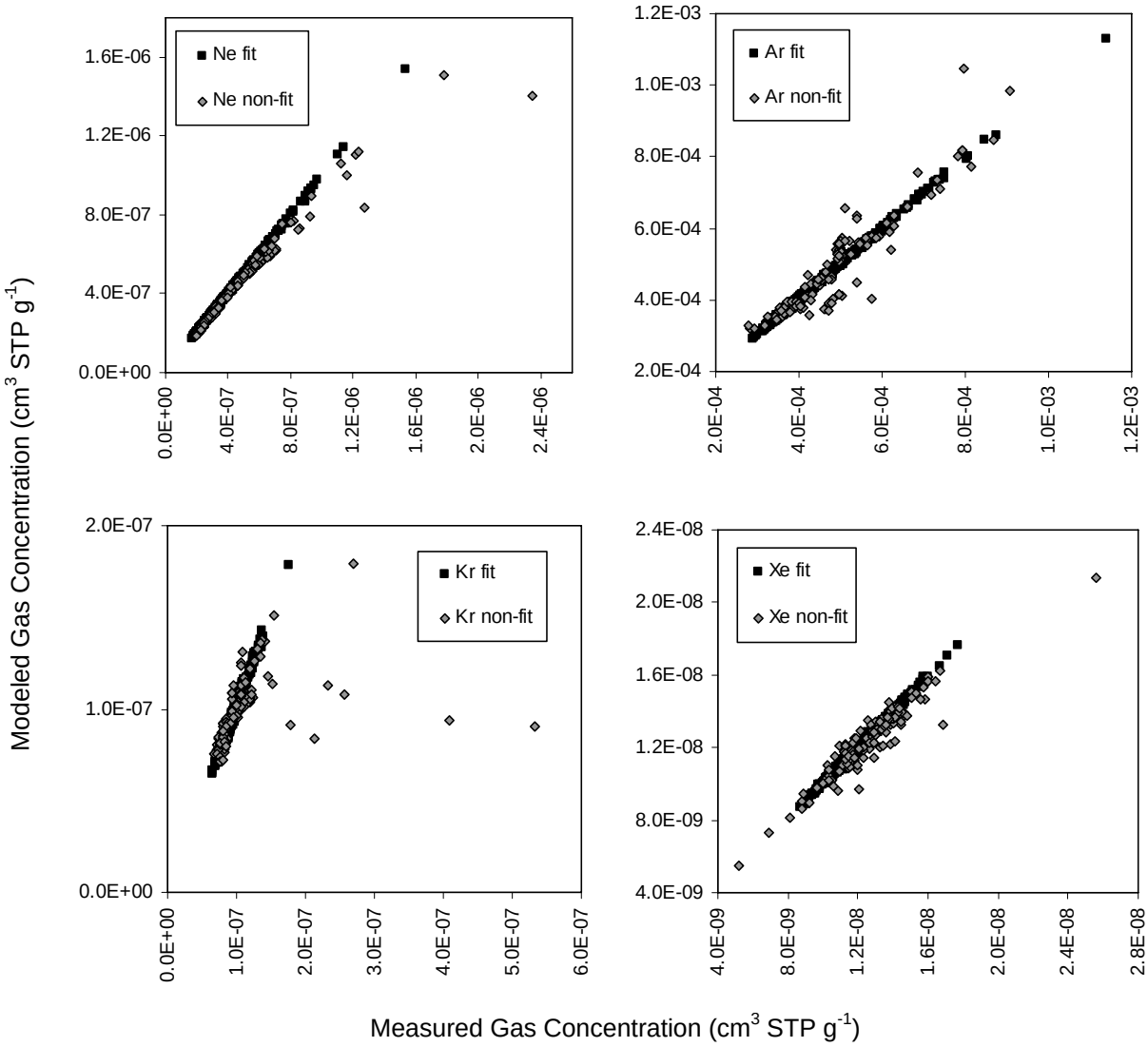

Figure S3. PR modeled versus measured gas concentrations. Note that sample 100706 plots off scale for Kr.

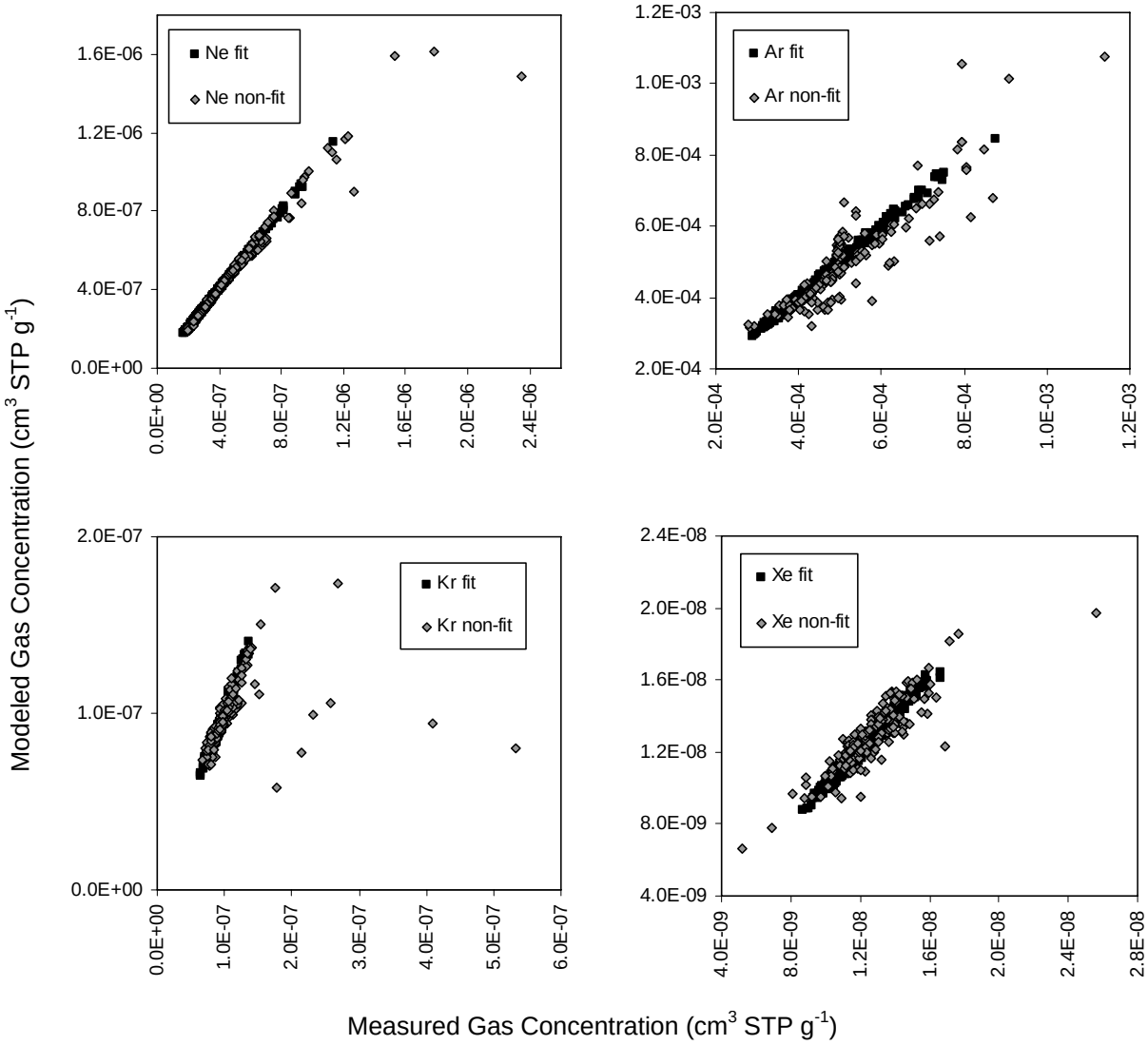

Figure S4. UA modeled versus measured gas concentrations. Note that sample 100706 plots off scale for Kr.

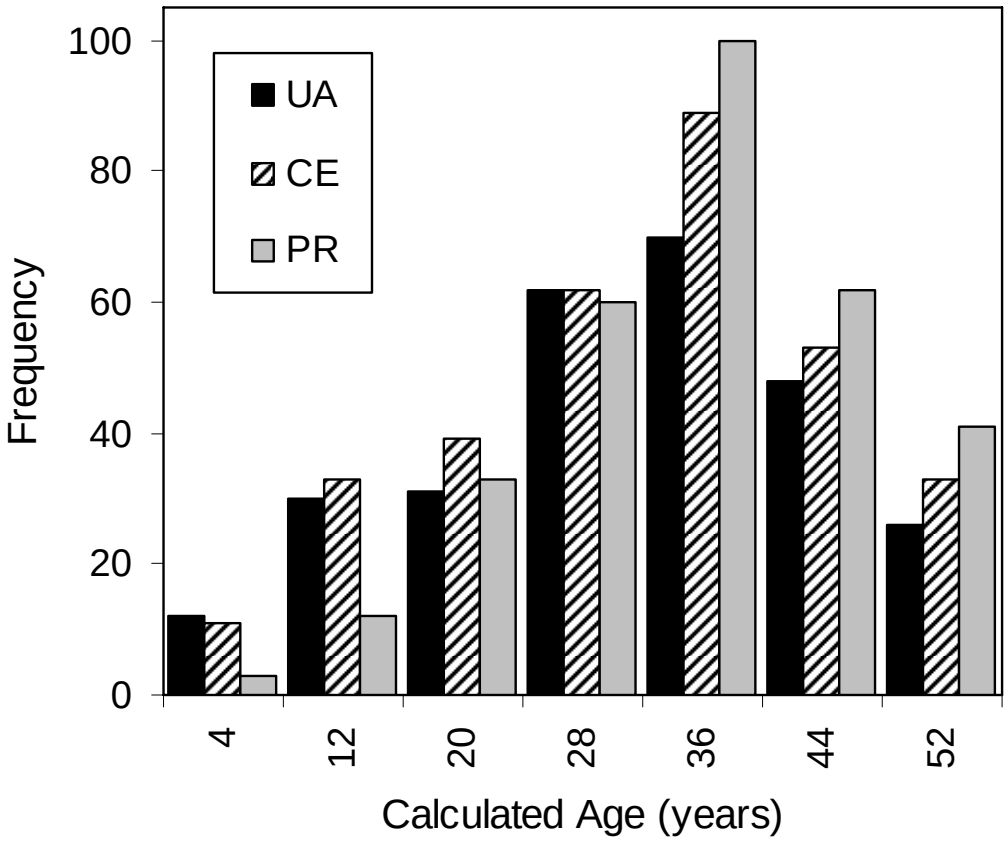

Figure S5. Histogram of calculated ^{3}H-^{3}He ages for each of three models.

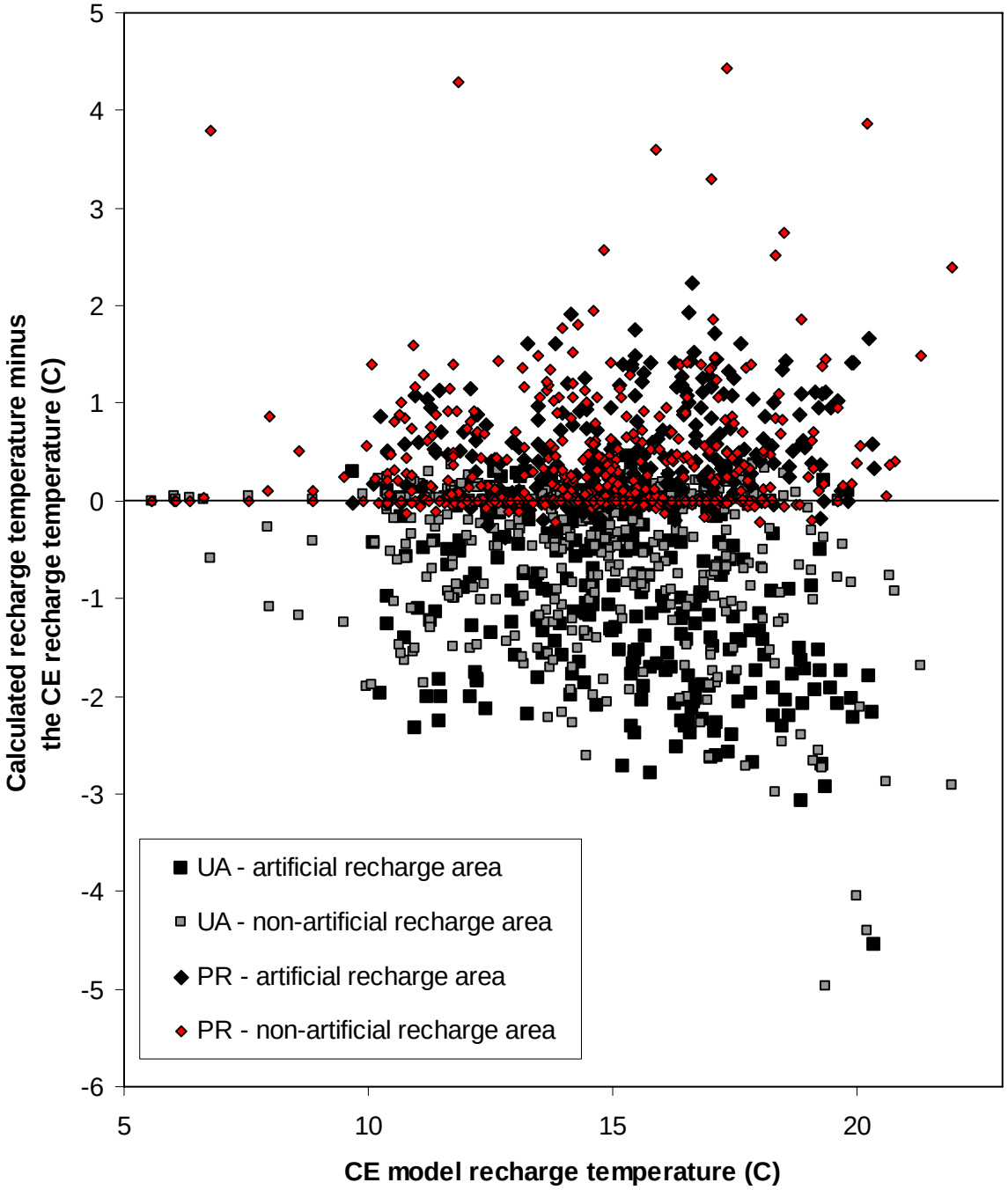

Figure S6. Modeled recharge temperatures for samples fit by all three excess air models. In general, the PR recharge temperature > CE recharge temperature > UA recharge temperature.

Table S1. Statistical summary of excess air concentrations (% ΔNe) and recharge temperatures (°C). AR refers to artificial recharge impacted areas (i.e. SFBA, LAB, and Bakersfield).

Excess Air (% ΔNe)	Area	Mean	Std. dev.	Median	Lower quartile	Upper quartile
UA Model	SFBA	150	86	132	87	203
	LAB	66	48	57	31	85
	NC	20	14	16	11	26
	MDB	47	29	45	31	60
	NCV	25	25	19	12	32
	SCV	46	55	33	23	49
	AR	108	83	85	46	147
	non-AR	33	35	26	16	40
	All	64	70	38	21	77
CE Model	SFBA	146	82	124	87	194
	LAB	80	64	66	33	94
	NC	26	21	19	12	35
	MDB	63	82	47	33	64
	NCV	26	28	19	12	33
	SCV	58	82	35	25	55
	AR	113	84	89	50	154
	non-AR	38	57	28	17	45
	All	70	79	42	22	85
PR Model	SFBA	146	83	126	86	195
	LAB	79	63	67	34	94
	NC	27	23	19	13	35
	MDB	64	84	49	33	66
	NCV	27	28	19	12	33
	SCV	60	85	36	25	57
	AR	113	84	89	51	152
	non-AR	39	59	28	17	45
	All	71	80	42	22	86
Recharge Temp. (°C)	**Area**	**Mean**	**Std. dev.**	**Median**	**Lower quartile**	**Upper quartile**
UA Model	SFBA	12.9	2.0	13.1	11.4	14.3
	LAB	15.4	1.6	15.4	14.2	16.4
	NC	10.4	3.7	10.4	7.2	11.8
	MDB	12.9	2.6	12.6	11.8	14.4
	NCV	14.9	2.1	14.8	13.4	16.3
	SCV	14.5	2.4	14.7	12.7	16.4
	AR	14.2	2.2	14.3	12.9	15.8
	non-AR	14.1	2.7	14.4	12.3	16.1
	All	14.1	2.5	14.4	12.5	15.9
CE Model	SFBA	13.7	2.0	13.6	12.5	14.8
	LAB	16.7	2.0	16.6	15.3	18.1
	NC	10.2	3.6	10.4	7.2	11.7
	MDB	13.7	2.3	13.8	11.8	14.9
	NCV	15.1	2.2	15.1	13.8	16.5
	SCV	15.5	2.6	15.6	13.8	17.4
	AR	15.4	2.4	15.4	13.7	17.1
	non-AR	14.6	2.9	14.8	12.7	16.7
	All	14.9	2.7	15.0	13.2	16.9
PR Model	SFBA	14.2	2.1	14.1	12.8	15.3
	LAB	17.5	2.4	17.5	15.8	18.9
	NC	11.0	3.6	10.7	7.9	12.8
	MDB	14.4	2.4	14.7	12.5	15.7
	NCV	15.4	2.5	15.4	13.9	16.9
	SCV	16.2	3.0	16.1	14.2	18.2
	AR	16.1	2.8	15.8	14.1	18.1
	non-AR	15.1	3.0	15.2	13.0	17.0
	All	15.5	3.0	15.4	13.6	17.6

Table S2. Measured data and model results for all 905 samples.

Sample Number	Region[a]	AR area[b]	MAAT[c] (ºC)	Atmo. pres.[d] (atm)	^{3}H (piC/L)[e]	^{4}He (x 10^{-7})[ef]	$^{3}He/^{4}He$ (x 10^{-6})[e]	Ne (x 10^{-7})[f]	Ar (x 10^{-4})[f]	Kr (x 10^{-8})[f]	Xe (x 10^{-8})[f]	ΔNe_{UA} (%)	NGT_{UA} (ºC)	ΔNe_{CE} (%)	NGT_{CE} (ºC)	CE *F* value	$L_{ex,CE}$[g]	ΔNe_{PR} (%)	NGT_{PR} (ºC)	PR *R* value	$L_{ex,PR}$[g]
100595	LAB	Y	18.1	0.995	40.8	0.773	3.00	3.45	3.53	8.22	0.970	-	-	-	-	-	-	-	-	-	-
100598	LAB	Y	18.3	0.995	19.9	0.839	1.54	3.48	4.21	8.55	1.07	87	17.2	88	19.2	0.26	0.272	90	20.3	0.84	0.142
100599	LAB	Y	18.1	0.995	40.3	0.809	2.57	3.34	4.18	8.81	1.15	75	15.2	75	15.7	0.13	0.281	76	16.0	0.32	0.218
100613	LAB	Y	17.7	0.971	14.5	1.93	1.59	8.59	5.39	14.5	1.59	-	-	-	-	-	-	-	-	-	-
100618	LAB	Y	18.2	0.993	25.9	0.836	1.91	3.38	4.24	9.07	1.13	78	15.1	79	16.4	0.26	0.273	80	17.6	0.83	0.140
100620	LAB	Y	18.2	0.993	23.3	0.746	2.97	2.85	3.99	8.95	1.10	-	-	-	-	-	-	54	20.0	1.82	0.062
100624	LAB	Y	18.2	0.993	19.9	0.621	1.61	2.55	3.67	8.27	1.05	35	16.6	36	17.3	0.43	0.273	37	18.4	1.10	0.112
100627	LAB	Y	16.9	0.998	0.1	1.19	0.786	2.15	3.46	7.55	1.10	13	16.5	12	16.5	0.00	0.288	12	16.5	0.00	0.288
100628	LAB	Y	18.1	0.995	0.4	0.621	1.25	2.36	3.60	8.15	1.17	22	14.8	21	14.6	0.00	0.288	21	14.6	0.00	0.288
100630	LAB	Y	18.1	0.996	0.0	0.684	1.19	2.42	3.66	8.35	1.22	24	14.0	23	13.8	0.00	0.288	23	13.8	0.00	0.288
100634	LAB	Y	18.1	0.996	30.1	0.871	2.33	3.61	4.49	9.53	1.20	87	13.6	88	15.1	0.24	0.272	90	16.3	0.82	0.140
100635	LAB	Y	18.3	0.996	34.8	0.882	2.56	3.69	4.53	9.44	1.20	92	13.9	93	15.5	0.23	0.272	94	16.5	0.79	0.145
100636	LAB	Y	18.1	0.995	0.2	0.618	1.30	2.47	3.64	8.22	1.10	29	15.8	29	15.7	0.00	0.288	29	15.7	0.00	0.288
100637	LAB	Y	18.1	0.996	0.0	1.68	0.539	2.32	3.74	8.56	0.883	-	-	-	-	-	-	-	-	-	-
100638	LAB	Y	18.1	0.996	0.4	1.03	1.36	2.15	3.47	7.63	1.01	15	17.5	16	19.6	0.83	0.250	17	20.6	2.55	0.034
100640	LAB	Y	18.1	0.995	10.5	0.866	1.95	3.54	4.25	8.85	1.17	85	15.4	85	15.5	0.03	0.287	86	15.6	0.07	0.270
100641	LAB	Y	18.1	0.996	2.0	0.757	1.56	3.00	4.15	8.47	1.16	57	14.6	58	16.2	0.39	0.267	59	16.4	0.82	0.141
100642	LAB	Y	18.1	0.995	17.6	1.23	1.54	4.82	4.83	9.19	1.14	158	17.7	159	18.6	0.06	0.282	160	19.0	0.24	0.235
100643	LAB	Y	18.1	0.996	0.7	0.655	1.41	2.57	3.80	8.02	1.17	34	14.9	33	14.9	0.00	0.288	33	14.8	0.00	0.288
100644	LAB	Y	18.1	0.996	29.2	0.955	2.62	3.71	4.50	8.37	1.16	-	-	-	-	-	-	-	-	-	-
100645	LAB	Y	17.6	0.993	16.1	1.40	1.49	5.59	5.43	11.2	1.13	-	-	-	-	-	-	-	-	-	-
100646	LAB	Y	18.1	0.995	17.8	0.802	1.63	3.32	4.21	8.39	1.12	76	16.2	78	17.9	0.29	0.271	78	18.4	0.73	0.154
100647	LAB	Y	18.1	0.995	25.1	0.872	2.28	3.68	4.48	9.63	1.18	91	13.9	92	15.5	0.23	0.272	94	17.0	0.87	0.136
100648	LAB	Y	18.1	0.995	0.0	0.717	1.41	2.94	4.05	8.11	1.11	56	15.9	57	17.8	0.43	0.265	58	18.1	0.95	0.128
100649	LAB	Y	18.1	0.995	24.5	0.899	2.02	3.75	4.40	8.61	1.14	99	16.3	100	17.5	0.16	0.277	100	17.7	0.40	0.204
100650	LAB	Y	18.1	0.995	13.8	0.842	2.11	3.35	4.34	8.62	1.17	76	14.8	78	16.7	0.31	0.268	78	17.1	0.78	0.147
100651	LAB	Y	18.1	0.993	13.2	2.01	1.76	6.98	5.01	10.3	1.26	-	-	-	-	-	-	-	-	-	-
100652	LAB	Y	18.1	0.993	21.9	0.615	1.43	2.59	3.61	7.34	1.03	40	18.8	40	19.3	0.31	0.278	40	19.1	0.21	0.241
100654	LAB	Y	18.1	0.996	3.9	0.744	1.58	3.16	4.21	8.96	1.14	65	14.6	67	16.7	0.38	0.265	69	18.2	1.22	0.101
100656	LAB	Y	18.1	0.996	2.3	0.764	1.53	3.12	4.26	8.64	1.18	62	14.1	63	15.8	0.37	0.267	64	16.1	0.84	0.138
100659	LAB	Y	18.1	0.996	6.9	0.844	1.72	3.42	4.57	9.42	1.22	76	12.5	79	15.2	0.37	0.262	81	16.6	1.25	0.097
100660	LAB	Y	18.1	0.995	19.8	0.894	2.33	3.69	4.54	9.13	1.24	91	13.6	92	14.6	0.18	0.276	92	14.8	0.42	0.198
100661	LAB	Y	17.6	0.986	18.4	0.749	1.61	3.07	4.00	8.06	1.07	65	16.9	66	18.7	0.35	0.269	67	19.2	0.83	0.142
100662	LAB	Y	18.1	0.996	16.7	0.781	2.26	3.16	4.14	8.55	1.09	68	16.2	69	18.5	0.38	0.266	71	19.8	1.17	0.107
100663	LAB	Y	18.1	0.995	0.1	0.597	1.30	2.31	3.58	7.73	1.05	23	16.9	23	18.0	0.68	0.261	24	18.4	1.34	0.091
100664	LAB	Y	18.1	0.995	55.0	0.830	3.56	3.37	4.22	8.74	1.18	76	14.9	76	15.2	0.10	0.283	76	15.3	0.17	0.248
100665	LAB	Y	18.2	0.995	23.8	0.593	1.80	2.55	3.65	8.20	1.05	35	16.8	36	17.2	0.34	0.278	36	17.9	0.76	0.150
100666	LAB	Y	18.2	0.995	22.4	2.14	1.56	6.59	5.87	9.92	1.24	256	18.0	257	19.7	0.05	0.281	259	19.8	0.23	0.238
100667	LAB	Y	18.1	0.995	0.8	0.644	1.40	2.80	3.96	9.13	1.14	45	14.0	-	-	-	-	47	16.3	1.16	0.104
100669	LAB	Y	17.6	0.995	16.4	0.896	1.44	3.61	4.28	9.12	1.12	91	15.9	91	16.8	0.16	0.278	92	17.8	0.58	0.175
100670	LAB	Y	18.1	0.995	37.1	1.00	2.66	4.01	4.55	9.04	1.16	112	15.8	113	17.0	0.14	0.278	114	17.5	0.42	0.200
100671	LAB	Y	18.1	0.995	0.0	0.691	1.40	2.90	3.99	8.36	1.11	53	15.6	54	17.1	0.41	0.268	55	17.7	0.94	0.128
100672	LAB	Y	18.1	0.995	0.1	0.740	1.24	2.30	3.59	7.84	1.11	21	15.8	21	15.8	0.03	0.288	20	15.8	0.00	0.288
100673	LAB	Y	18.1	0.995	23.9	1.18	2.10	4.80	4.60	8.76	1.10	160	19.9	158	19.8	0.00	0.288	158	19.8	0.00	0.288
100674	LAB	Y	18.2	0.995	30.2	0.802	1.86	3.13	4.09	8.31	1.11	66	16.2	67	17.6	0.31	0.271	68	18.0	0.70	0.158

Table S2. Measured data and model results for all 905 samples.

Sample Number	Region[a]	AR area[b]	MAAT[c] (ºC)	Atmo. pres.[d] (atm)	^{3}H (piC/L)[e]	^{4}He (x 10^{-7})[ef]	$^{3}He/^{4}He$ (x 10^{-6})[e]	Ne (x 10^{-7})[f]	Ar (x 10^{-4})[f]	Kr (x 10^{-8})[f]	Xe (x 10^{-8})[f]	ΔNe_{UA} (%)	NGT_{UA} (ºC)	ΔNe_{CE} (%)	NGT_{CE} (ºC)	CE *F* value	$L_{ex,CE}$[g]	ΔNe_{PR} (%)	NGT_{PR} (ºC)	PR *R* value	$L_{ex,PR}$[g]
100675	LAB	Y	18.1	0.996	0.2	0.671	1.25	2.34	3.57	7.77	1.10	23	16.4	22	16.3	0.00	0.288	22	16.3	0.00	0.288
100676	LAB	Y	18.1	0.995	23.8	0.661	1.69	2.39	3.54	8.01	1.05	27	17.0	27	17.2	0.26	0.283	27	17.6	0.55	0.179
100679	LAB	Y	18.1	0.996	42.4	0.808	3.70	3.38	4.40	9.05	1.22	74	13.4	75	14.6	0.25	0.273	76	14.9	0.58	0.173
100680	LAB	Y	18.1	0.996	12.6	0.638	2.23	2.67	3.97	8.68	1.18	38	13.6	38	14.5	0.46	0.269	39	14.9	0.87	0.133
100682	LAB	Y	18.1	0.995	0.0	1.57	0.564	2.41	5.04	8.13	1.12	-	-	-	-	-	-	-	-	-	-
100683	LAB	Y	18.3	0.996	41.1	0.842	3.05	3.40	4.42	8.94	1.16	78	14.4	80	17.0	0.35	0.264	82	18.2	1.12	0.110
100684	LAB	Y	18.1	0.996	43.4	0.923	3.21	3.68	4.55	9.06	1.23	91	13.8	92	15.1	0.20	0.274	92	15.3	0.49	0.186
100685	LAB	Y	16.9	0.998	9.3	0.752	1.61	2.14	4.64	7.48	1.03	-	-	-	-	-	-	-	-	-	-
100686	LAB	Y	18.1	0.995	25.8	0.755	1.76	3.21	3.99	8.84	1.08	70	16.7	-	-	-	-	72	18.2	0.56	0.179
100688	LAB	Y	18.1	0.996	19.9	0.708	2.43	2.91	4.04	8.25	1.14	52	15.2	53	16.4	0.38	0.270	54	16.6	0.66	0.162
100689	LAB	Y	18.1	0.995	29.4	0.951	1.90	3.78	4.47	8.85	1.12	101	16.1	103	18.3	0.24	0.271	104	19.3	0.80	0.146
100690	LAB	Y	18.1	0.995	39.7	0.782	2.55	3.29	4.17	8.35	1.14	74	15.9	74	16.8	0.21	0.277	75	16.8	0.37	0.208
100691	LAB	Y	18.1	0.996	0.4	0.665	1.38	2.81	4.04	8.37	1.11	48	15.2	50	17.9	0.53	0.259	51	18.9	1.51	0.079
100692	LAB	Y	18.1	0.996	0.2	0.549	1.30	2.12	3.48	8.33	1.19	9	14.1	-	-	-	-	-	-	-	-
100693	LAB	Y	16.2	0.998	13.2	1.00	1.15	2.18	3.48	7.93	1.12	14	15.8	13	15.7	0.00	0.288	13	15.7	0.00	0.288
100694	LAB	Y	16.2	0.998	10.3	0.698	1.52	3.19	3.64	8.23	1.01	-	-	-	-	-	-	-	-	-	-
100695	LAB	Y	18.3	0.995	18.6	0.950	2.42	3.08	4.09	8.40	1.17	61	15.0	61	15.5	0.19	0.280	62	15.4	0.21	0.239
100696	LAB	Y	17.1	0.998	61.7	0.600	5.43	2.11	3.42	7.68	1.05	11	17.0	11	17.1	0.55	0.280	11	17.2	0.45	0.194
100697	LAB	Y	18.3	0.995	0.4	0.619	1.39	2.65	3.86	8.19	1.15	38	15.0	39	15.4	0.33	0.277	39	15.4	0.33	0.216
100698	LAB	Y	18.3	0.995	0.3	0.708	1.18	2.54	3.75	8.11	1.11	33	15.6	34	16.2	0.43	0.273	34	16.4	0.60	0.171
100699	LAB	Y	17.1	0.998	0.0	0.616	1.34	2.50	3.65	7.82	1.07	32	17.0	32	17.5	0.39	0.276	33	17.6	0.44	0.197
100700	LAB	Y	18.1	0.996	0.0	0.535	1.38	2.46	3.71	8.19	1.11	29	15.4	29	15.6	0.33	0.280	29	15.8	0.38	0.206
100701	LAB	Y	16.2	0.998	13.5	0.642	1.54	2.45	3.53	7.66	1.04	31	18.1	31	18.1	0.01	0.288	31	18.1	0.01	0.287
100702	LAB	Y	18.3	0.995	30.8	0.768	2.88	2.94	4.12	8.60	1.12	55	14.8	56	17.4	0.48	0.260	58	18.7	1.44	0.084
100703	LAB	Y	17.1	0.998	0.9	0.726	1.35	3.04	3.91	8.50	1.11	60	16.4	59	16.3	0.00	0.288	60	16.4	0.00	0.288
100704	LAB	Y	18.3	0.995	0.2	0.609	1.39	2.38	3.78	8.20	1.09	25	15.1	27	17.5	0.72	0.251	28	18.6	2.12	0.047
100705	LAB	Y	18.3	0.995	0.3	0.794	1.32	3.00	4.11	8.85	1.19	55	13.7	55	14.3	0.24	0.277	56	14.5	0.44	0.195
100706	LAB	Y	17.1	0.998	31.6	0.662	3.46	2.79	3.79	116	1.04	-	-	-	-	-	-	-	-	-	-
100707	LAB	Y	17.1	0.998	2.6	0.658	1.34	2.22	5.76	8.01	1.10	-	-	-	-	-	-	-	-	-	-
100708	LAB	Y	18.1	0.993	3.2	0.979	1.50	3.62	4.20	8.74	1.10	93	17.1	94	17.7	0.11	0.282	94	18.2	0.35	0.214
100710	LAB	Y	16.9	0.998	61.8	0.697	5.73	1.98	3.31	7.39	0.976	6	18.5	8	20.3	0.92	0.245	9	21.9	3.67	0.014
100719	LAB	Y	18.1	0.993	12.9	2.50	1.51	8.48	5.05	10.7	1.23	-	-	-	-	-	-	-	-	-	-
100721	LAB	Y	18.1	0.995	1.0	0.540	1.41	2.34	3.84	8.47	1.13	22	13.8	24	16.3	0.77	0.248	25	17.5	2.39	0.036
100722	LAB	Y	17.1	0.993	0.1	0.808	1.15	2.87	4.08	8.57	1.09	-	-	54	18.5	0.53	0.257	57	20.6	1.83	0.062
100724	LAB	Y	18.1	0.996	8.9	0.638	1.32	2.08	3.50	7.76	1.03	10	16.6	12	19.3	0.88	0.244	13	20.4	3.24	0.019
100726	LAB	Y	18.1	0.995	9.2	0.625	1.86	2.66	4.02	8.84	1.18	37	13.1	38	14.5	0.54	0.262	39	15.4	1.35	0.087
100727	LAB	Y	17.6	0.986	18.2	0.608	1.50	2.37	3.61	7.83	1.07	27	16.3	27	16.9	0.53	0.271	27	17.1	0.75	0.150
100728	LAB	Y	17.1	0.993	18.5	2.20	1.81	4.76	5.29	9.82	1.21	-	-	156	18.7	0.21	0.266	161	20.8	1.05	0.120
100729	LAB	Y	17.1	0.993	20.5	12.3	1.88	3.88	4.55	8.93	1.10	-	-	111	19.7	0.26	0.268	114	21.5	1.06	0.119
100730	LAB	Y	18.1	0.995	30.9	0.961	1.74	4.11	4.61	9.52	1.08	-	-	-	-	-	-	128	23.6	1.22	0.106
100731	LAB	Y	17.1	0.993	0.0	1.06	0.982	3.23	4.30	8.88	1.14	70	14.5	72	17.1	0.39	0.263	74	18.6	1.27	0.097
100732	LAB	Y	18.3	0.995	32.0	1.00	2.96	4.11	4.80	9.73	1.22	114	13.6	115	15.6	0.20	0.271	118	16.9	0.78	0.146
100733	LAB	Y	18.1	0.996	1.5	1.06	0.726	2.08	3.62	8.05	1.09	9	14.9	11	17.1	0.90	0.242	11	17.7	3.10	0.020
100734	LAB	Y	17.1	0.993	2.0	1.64	2.11	2.45	3.75	7.93	1.04	31	16.4	33	19.4	0.68	0.253	34	20.5	2.02	0.053
100735	LAB	Y	17.6	0.986	18.2	0.664	1.82	2.68	3.85	8.29	1.08	43	15.7	44	17.5	0.52	0.262	45	18.7	1.43	0.085

Table S2. Measured data and model results for all 905 samples.

Sample Number	Region[a]	AR area[b]	MAAT[c] (ºC)	Atmo. pres.[d] (atm)	^{3}H (piC/L)[e]	^{4}He (x 10^{-7})[ef]	^{3}He/^{4}He (x 10^{-6})[e]	Ne (x 10^{-7})[f]	Ar (x 10^{-4})[f]	Kr (x 10^{-8})[f]	Xe (x 10^{-8})[f]	ΔNe_{UA} (%)	NGT_{UA} (ºC)	ΔNe_{CE} (%)	NGT_{CE} (ºC)	CE *F* value	$L_{ex,CE}$[g]	ΔNe_{PR} (%)	NGT_{PR} (ºC)	PR *R* value	$L_{ex,PR}$[g]
100736	LAB	Y	18.1	0.995	0.8	0.460	1.38	2.06	3.55	8.13	1.12	7	14.5	7	14.8	0.86	0.263	7	15.1	1.61	0.069
100737	LAB	Y	16.9	0.998	75.9	0.638	9.11	2.12	3.41	7.74	1.04	12	17.1	12	17.3	0.60	0.278	12	17.6	0.90	0.132
100738	LAB	Y	18.1	0.995	48.7	0.944	2.90	3.61	4.46	8.86	1.11	-	-	95	19.2	0.32	0.265	98	21.0	1.21	0.105
100739	LAB	Y	18.1	0.996	0.2	0.652	1.24	2.41	3.66	7.81	1.06	28	16.7	28	18.0	0.64	0.262	29	18.5	1.27	0.097
100740	LAB	Y	18.1	0.996	0.0	0.702	1.14	2.43	3.71	7.96	1.09	28	15.9	29	16.9	0.58	0.266	29	17.1	0.96	0.125
100742	LAB	Y	17.1	0.998	0.4	2.60	0.458	1.94	3.15	7.01	0.986	4	19.6	3	19.3	0.00	0.288	3	19.3	0.00	0.288
100743	LAB	Y	17.1	0.998	67.5	0.988	3.66	2.16	4.02	7.96	1.14	-	-	-	-	-	-	-	-	-	-
100744	LAB	Y	17.1	0.998	21.9	0.781	2.03	2.07	4.26	7.13	1.04	-	-	-	-	-	-	-	-	-	-
100745	LAB	Y	18.3	0.996	41.9	1.11	2.90	4.04	4.61	9.58	1.22	110	14.2	110	14.7	0.08	0.283	111	15.1	0.27	0.227
100746	LAB	Y	18.1	0.996	32.1	0.792	2.99	3.12	4.22	8.76	1.14	63	14.6	65	16.9	0.40	0.264	67	18.0	1.19	0.104
100747	LAB	Y	18.1	0.995	35.9	0.797	2.22	3.18	4.24	8.36	1.08	-	-	73	20.0	0.43	0.261	75	21.3	1.43	0.087
100748	LAB	Y	18.2	0.995	29.8	0.670	2.22	2.75	4.01	8.16	1.08	-	-	49	19.2	0.57	0.256	50	20.2	1.70	0.069
100749	LAB	Y	18.1	0.996	0.0	0.681	1.14	2.40	3.74	8.28	1.14	25	14.6	25	14.8	0.42	0.277	25	15.0	0.43	0.196
100750	LAB	Y	18.3	0.995	19.7	0.855	1.54	3.46	4.22	8.64	1.10	84	16.6	85	18.1	0.25	0.273	86	19.0	0.73	0.154
100751	LAB	Y	18.2	0.995	16.4	1.13	1.63	4.60	4.76	9.31	1.22	141	15.7	140	15.6	0.00	0.288	139	15.6	0.00	0.288
100753	LAB	Y	18.2	0.993	24.3	0.557	1.96	2.46	3.57	7.95	1.05	31	17.1	31	17.1	0.00	0.288	31	17.2	0.12	0.260
100755	LAB	Y	18.2	0.995	23.4	0.892	1.58	3.99	4.43	8.90	1.07	115	17.9	116	19.9	0.18	0.274	119	21.3	0.74	0.155
100756	LAB	Y	18.2	0.995	22.2	0.803	1.51	3.45	4.20	8.19	1.08	85	17.5	87	19.3	0.25	0.273	87	19.6	0.63	0.169
100757	LAB	Y	18.2	0.987	24.3	0.616	1.84	2.70	3.76	7.92	1.01	46	17.7	48	19.9	0.51	0.263	49	21.3	1.46	0.085
100758	LAB	Y	18.2	0.995	-	0.759	1.47	3.34	4.12	8.34	1.06	80	17.6	81	19.5	0.29	0.271	82	20.4	0.85	0.141
100759	LAB	Y	18.1	0.996	1.7	0.622	1.38	2.55	3.88	8.39	1.19	32	13.8	32	14.1	0.31	0.279	32	14.0	0.20	0.241
100760	LAB	Y	18.1	0.996	0.3	0.615	1.33	2.57	3.88	8.45	1.17	33	14.0	33	14.5	0.42	0.274	33	14.6	0.53	0.181
100761	LAB	Y	18.1	0.996	0.7	0.631	1.24	2.47	3.81	8.08	1.07	30	15.8	33	18.9	0.69	0.252	34	20.0	2.09	0.049
100762	LAB	Y	18.1	0.996	18.2	0.695	2.61	2.85	4.10	8.73	1.14	49	14.2	50	16.6	0.51	0.259	52	18.0	1.55	0.076
100763	LAB	Y	18.1	0.996	0.2	0.721	1.32	2.89	4.18	9.40	1.20	48	12.4	49	13.8	0.45	0.264	51	15.4	1.39	0.084
100764	LAB	Y	18.1	0.996	0.0	0.700	1.16	2.42	3.87	8.56	1.14	25	13.8	27	15.7	0.71	0.253	28	17.0	2.07	0.048
100765	LAB	Y	18.3	0.995	1.6	0.621	1.40	2.42	3.81	8.72	1.17	25	13.4	25	13.7	0.46	0.275	25	14.2	0.84	0.137
100767	LAB	Y	18.1	0.996	17.1	0.701	2.19	2.85	4.08	8.58	1.14	49	14.4	50	16.5	0.49	0.261	51	17.3	1.30	0.094
100768	LAB	Y	18.1	0.993	19.0	0.959	2.40	3.92	4.65	9.26	1.22	105	14.0	106	15.5	0.19	0.274	107	16.1	0.57	0.176
100771	LAB	Y	18.1	0.993	22.3	1.45	1.95	5.59	5.02	10.5	1.25	-	-	-	-	-	-	-	-	-	-
100772	LAB	Y	18.1	0.995	3.5	0.735	1.50	3.18	3.96	8.47	1.17	66	15.8	62	15.4	0.00	0.288	62	15.4	0.00	0.288
100773	LAB	Y	18.1	0.993	24.8	1.13	2.21	4.42	4.75	9.75	1.25	129	14.1	128	14.0	0.00	0.288	129	14.1	0.00	0.288
100775	LAB	Y	18.1	0.993	8.3	1.02	1.60	4.14	4.64	10.3	1.16	-	-	-	-	-	-	-	-	-	-
100776	LAB	Y	18.1	0.993	16.4	1.15	1.78	4.55	4.63	9.72	1.19	139	15.9	135	15.7	0.00	0.288	136	15.8	0.00	0.288
100777	LAB	Y	18.1	0.993	13.4	1.07	1.99	4.43	4.81	9.46	1.21	133	15.0	134	16.1	0.10	0.279	135	16.5	0.35	0.212
100778	LAB	Y	17.6	0.993	17.4	0.816	1.53	3.33	4.21	8.60	1.15	76	15.4	76	16.4	0.22	0.276	77	16.7	0.48	0.190
100779	LAB	Y	18.1	0.995	2.9	0.665	1.54	2.79	4.04	8.41	1.13	46	14.7	48	16.7	0.51	0.261	49	17.4	1.26	0.097
100780	LAB	Y	18.1	0.995	1.1	0.685	1.44	2.97	4.09	8.27	1.12	57	15.6	58	17.6	0.43	0.265	59	18.1	1.02	0.119
100781	LAB	Y	18.1	0.996	0.0	0.621	1.38	2.60	3.85	7.82	1.08	38	16.4	40	18.6	0.58	0.259	40	18.9	1.29	0.096
100782	LAB	Y	18.1	0.995	10.0	1.20	1.58	4.80	4.98	9.21	1.16	157	16.8	159	18.9	0.12	0.276	161	19.5	0.48	0.191
100783	LAB	Y	18.1	0.995	22.4	1.36	2.06	5.66	5.95	10.2	1.28	-	-	206	19.3	0.16	0.267	-	-	-	-
100784	LAB	Y	18.1	0.995	3.2	3.39	1.84	6.70	5.98	10.9	1.30	253	15.5	254	16.7	0.04	0.282	256	17.3	0.25	0.233
100785	LAB	Y	18.1	0.996	63.7	0.599	2.01	2.37	3.72	7.65	1.07	26	16.4	27	18.3	0.70	0.256	27	18.3	1.41	0.086
100786	LAB	Y	18.1	0.995	5.7	1.23	1.46	4.87	5.01	9.70	1.13	-	-	165	20.0	0.15	0.273	169	22.1	0.80	0.149
100787	LAB	Y	18.1	0.995	33.6	0.824	2.23	3.44	4.38	9.06	1.10	-	-	85	18.8	0.37	0.263	89	21.5	1.48	0.084

Table S2. Measured data and model results for all 905 samples.

Sample Number	Region[a]	AR area[b]	MAAT[c] (ºC)	Atmo. pres.[d] (atm)	^{3}H (piC/L)[e]	^{4}He (x 10^{-7})[ef]	$^{3}He/^{4}He$ (x 10^{-6})[e]	Ne (x 10^{-7})[f]	Ar (x 10^{-4})[f]	Kr (x 10^{-8})[f]	Xe (x 10^{-8})[f]	ΔNe_{UA} (%)	NGT_{UA} (ºC)	ΔNe_{CE} (%)	NGT_{CE} (ºC)	CE *F* value	$L_{ex,CE}$[g]	ΔNe_{PR} (%)	NGT_{PR} (ºC)	PR *R* value	$L_{ex,PR}$[g]
100825	SCV	N	16.4	0.995	3.4	1.08	1.59	2.20	3.42	7.80	1.08	16	16.6	15	16.5	0.00	0.288	15	16.5	0.00	0.288
100827	SCV	N	16.4	0.995	16.6	0.788	1.70	3.18	4.08	8.62	1.15	66	15.3	66	15.5	0.08	0.285	67	15.6	0.14	0.254
100828	SCV	N	16.4	0.995	3.6	3.62	1.09	4.67	5.05	10.3	1.26	142	13.3	143	14.7	0.12	0.277	145	15.7	0.53	0.180
100830	SCV	N	16.4	0.995	7.4	0.863	1.40	2.23	3.48	8.08	1.05	18	16.5	17	16.5	0.00	0.288	18	16.9	0.62	0.169
100831	SCV	N	15.4	0.995	32.1	1.76	1.42	2.21	3.55	7.98	1.12	15	15.3	14	15.2	0.00	0.288	14	15.2	0.00	0.288
100832	SCV	N	16.4	0.995	20.5	4.72	0.932	2.46	3.75	8.29	1.11	29	15.0	29	15.8	0.55	0.268	30	16.3	1.03	0.117
100833	SCV	N	16.4	0.995	38.3	0.781	3.39	2.92	4.03	8.59	1.11	54	15.3	55	17.1	0.44	0.265	56	18.4	1.25	0.099
100834	SCV	N	16.4	0.995	17.7	2.07	0.962	2.08	3.63	7.90	1.09	9	14.9	11	17.0	0.89	0.243	11	16.8	2.56	0.031
100835	SCV	N	16.4	0.995	34.2	0.607	3.18	2.55	3.83	8.26	1.16	32	14.5	33	14.9	0.37	0.277	33	14.9	0.33	0.214
100836	SCV	N	16.4	0.995	5.4	5.06	1.11	2.40	3.84	8.22	1.15	25	14.0	26	15.2	0.67	0.259	26	15.3	1.18	0.102
100837	SCV	N	16.4	0.995	9.8	4.03	1.04	2.78	3.90	7.90	1.12	47	16.0	47	16.9	0.35	0.273	47	16.7	0.40	0.204
100838	SCV	N	16.4	0.995	18.7	0.955	1.72	2.52	3.97	8.77	1.22	29	12.5	30	13.2	0.54	0.267	30	13.5	0.88	0.131
100839	SCV	N	16.4	0.995	1.8	20.1	0.807	2.17	3.69	8.44	1.19	11	13.1	11	13.1	0.32	0.285	11	13.2	0.13	0.255
100840	SCV	N	16.4	0.995	11.1	2.07	1.05	2.74	3.98	8.72	1.19	42	13.6	42	14.0	0.30	0.277	42	14.3	0.47	0.190
100841	SCV	N	16.4	0.995	13.1	3.21	1.08	2.40	3.74	8.27	1.15	25	14.4	25	14.6	0.34	0.280	25	14.6	0.26	0.229
100842	SCV	N	16.4	0.995	18.0	1.51	1.20	2.16	3.76	8.79	1.20	10	12.2	10	12.7	0.83	0.257	12	14.1	2.59	0.028
100843	SCV	N	16.4	0.995	16.5	15.5	0.828	2.44	3.83	8.65	1.19	25	13.1	25	13.2	0.13	0.286	25	13.3	0.17	0.248
100844	SCV	N	16.4	0.995	9.7	1.55	1.87	2.71	3.87	8.24	1.11	43	15.6	43	16.6	0.43	0.270	44	17.0	0.81	0.142
100845	SCV	N	16.4	0.995	9.3	38.0	0.719	2.27	3.94	9.34	1.33	13	10.0	12	9.9	0.00	0.288	12	9.9	0.00	0.288
100846	SCV	N	16.4	0.995	22.8	14.1	0.800	2.19	3.48	8.13	1.14	14	15.1	13	15.0	0.00	0.288	13	15.0	0.00	0.288
100847	SCV	N	16.4	0.995	32.1	2.42	1.21	2.18	3.64	8.44	1.10	14	14.4	18	19.4	0.85	0.242	19	20.8	3.63	0.014
100848	SCV	N	16.4	0.995	2.2	16.6	0.801	2.39	3.58	8.19	1.14	24	15.3	23	15.2	0.00	0.288	23	15.2	0.00	0.288
100849	SCV	N	15.4	0.995	5.3	6.55	1.03	2.46	3.68	8.25	1.12	28	15.3	28	15.2	0.00	0.288	28	15.2	0.00	0.288
100850	SCV	N	16.4	0.995	1.6	64.3	0.622	2.25	3.82	9.12	1.36	12	10.3	-	-	-	-	-	-	-	-
100851	SCV	N	16.4	0.995	21.5	4.35	0.968	2.28	3.56	8.16	1.13	19	15.2	18	15.1	0.00	0.288	18	15.1	0.00	0.288
100853	SCV	N	16.4	0.995	1.0	3.48	0.961	3.96	4.47	9.64	1.29	102	13.3	-	-	-	-	-	-	-	-
100854	SCV	N	16.4	0.995	26.6	0.797	2.34	2.58	3.86	8.68	1.17	34	13.8	34	14.0	0.24	0.281	34	14.3	0.41	0.200
100855	SCV	N	16.4	0.995	5.4	1.52	1.05	2.12	3.67	8.71	1.23	8	12.3	7	12.1	0.00	0.288	7	12.1	0.00	0.288
100856	SCV	N	16.4	0.995	0.8	0.883	1.21	2.41	3.85	8.88	1.22	23	12.4	23	12.4	0.00	0.288	23	12.4	0.00	0.288
100857	SCV	N	16.4	0.995	24.3	8.50	0.865	2.45	3.64	7.98	1.14	28	15.5	26	15.4	0.00	0.288	26	15.4	0.00	0.288
100858	SCV	N	16.4	0.995	9.3	1.49	1.39	2.94	4.18	9.30	1.28	49	11.7	49	11.7	0.01	0.288	49	11.8	0.05	0.276
100859	SCV	N	16.4	0.995	72.6	10.9	0.750	2.59	3.78	8.20	1.17	34	14.7	33	14.7	0.00	0.288	33	14.6	0.00	0.288
100860	SCV	N	16.4	0.995	6.0	6.14	0.812	2.16	3.71	8.39	1.17	12	13.3	12	14.0	0.83	0.255	12	14.3	1.67	0.065
100861	SCV	N	16.4	0.995	2.8	41.7	0.727	2.12	3.74	8.61	1.23	8	12.0	8	12.0	0.00	0.288	7	12.0	0.00	0.288
100862	SCV	N	16.4	0.995	24.7	19.6	0.813	2.35	3.54	7.77	1.12	23	16.1	22	16.0	0.00	0.288	22	16.0	0.00	0.288
100863	SCV	N	15.4	0.995	18.9	1.93	1.56	2.56	3.74	8.47	1.15	33	14.7	31	14.6	0.00	0.288	31	14.6	0.00	0.288
100864	SCV	N	16.4	0.995	15.4	16.3	0.806	2.33	3.60	8.44	1.13	21	14.9	20	14.7	0.00	0.288	20	14.7	0.00	0.288
100865	SFBA	Y	15.2	0.979	9.3	1.09	1.29	3.69	4.80	9.06	1.19	-	-	101	18.0	0.36	0.259	-	-	-	-
100866	SFBA	Y	15.2	0.979	1.5	1.35	0.893	3.26	4.58	9.24	1.19	-	-	76	17.1	0.46	0.254	80	19.3	1.84	0.060
100867	SFBA	Y	15.2	0.979	18.6	1.37	1.40	4.16	4.91	9.60	1.21	-	-	123	16.3	0.24	0.266	126	17.8	0.99	0.123
100868	SFBA	Y	15.2	0.979	35.9	1.15	1.87	4.08	4.69	9.25	1.20	117	14.3	118	15.9	0.17	0.274	120	16.6	0.57	0.175
100869	SFBA	Y	15.2	0.979	13.3	1.27	1.18	3.44	4.33	8.96	1.24	79	13.1	80	13.3	0.06	0.285	80	13.2	0.05	0.277
100875	SFBA	Y	14.0	0.998	0.5	1.05	1.03	2.67	4.16	9.10	1.29	35	11.1	35	11.6	0.41	0.272	35	11.7	0.48	0.186
100876	SFBA	Y	14.0	0.998	0.4	0.809	1.11	2.40	3.80	8.09	1.18	24	14.2	24	14.6	0.53	0.271	24	14.5	0.33	0.214
100877	SFBA	Y	14.0	0.998	0.0	1.05	0.843	2.52	4.06	9.67	1.25	27	10.9	-	-	-	-	31	15.8	2.60	0.029

Table S2. Measured data and model results for all 905 samples.

Sample Number	Region[a]	AR area[b]	MAAT[c] (ºC)	Atmo. pres.[d] (atm)	^{3}H (piC/L)[e]	^{4}He (x 10^{-7})[ef]	^{3}He/^{4}He (x 10^{-6})[e]	Ne (x 10^{-7})[f]	Ar (x 10^{-4})[f]	Kr (x 10^{-8})[f]	Xe (x 10^{-8})[f]	ΔNe_{UA} (%)	NGT_{UA} (ºC)	ΔNe_{CE} (%)	NGT_{CE} (ºC)	CE *F* value	$L_{ex,CE}$[g]	ΔNe_{PR} (%)	NGT_{PR} (ºC)	PR *R* value	$L_{ex,PR}$[g]
100878	SFBA	Y	14.0	0.998	0.0	0.680	1.40	2.96	4.53	9.96	1.17	-	-	-	-	-	-	-	-	-	-
100880	SFBA	Y	14.0	0.999	7.4	0.551	1.47	2.14	4.72	8.19	1.13	-	-	-	-	-	-	-	-	-	-
100881	SFBA	Y	14.0	0.999	3.6	0.566	1.37	1.98	4.60	7.80	1.13	-	-	-	-	-	-	-	-	-	-
100882	SFBA	Y	13.1	0.993	5.7	0.591	1.56	2.21	4.82	8.31	1.18	-	-	-	-	-	-	-	-	-	-
100883	SFBA	Y	14.0	0.999	0.1	1.48	0.707	2.37	5.40	9.25	1.38	-	-	-	-	-	-	-	-	-	-
100884	SFBA	Y	13.1	0.993	5.8	0.566	1.52	2.15	4.78	8.11	1.13	-	-	-	-	-	-	-	-	-	-
100885	SFBA	Y	13.1	0.993	1.5	0.646	1.41	2.40	4.98	8.37	1.17	-	-	-	-	-	-	-	-	-	-
100886	SFBA	Y	13.1	0.993	0.9	0.601	1.34	2.57	3.76	8.65	1.14	33	14.5	33	14.5	0.00	0.288	33	14.5	0.00	0.288
100888	SFBA	Y	13.1	0.993	0.3	0.686	1.37	2.52	4.95	8.05	1.13	-	-	-	-	-	-	-	-	-	-
100891	SFBA	Y	15.1	0.998	36.9	0.946	2.36	3.56	4.53	9.55	1.24	82	12.7	83	13.9	0.23	0.273	84	14.7	0.68	0.157
100892	SFBA	Y	15.1	0.998	21.5	0.822	1.46	3.16	3.70	8.62	1.18	-	-	-	-	-	-	-	-	-	-
100893	SFBA	Y	15.1	0.998	29.5	0.649	2.25	2.60	3.80	8.13	1.16	35	15.0	35	15.0	0.00	0.288	34	14.9	0.00	0.288
100894	SFBA	Y	15.1	0.998	23.5	0.842	1.53	3.25	4.12	8.38	1.18	70	15.5	69	15.5	0.00	0.288	68	15.4	0.00	0.288
100895	SFBA	Y	15.1	0.998	22.9	0.856	1.62	3.12	4.14	8.42	1.17	63	15.0	63	15.8	0.23	0.277	64	15.7	0.34	0.214
100896	SFBA	Y	15.1	0.998	19.4	0.772	1.41	3.02	4.06	8.45	1.23	55	14.2	54	14.1	0.00	0.288	53	14.0	0.00	0.288
100897	SFBA	Y	15.1	0.998	19.9	0.730	1.40	2.87	4.00	8.38	1.19	49	14.5	49	14.6	0.08	0.285	48	14.5	0.00	0.288
100898	SFBA	Y	15.1	0.998	17.6	0.699	1.41	2.83	4.04	9.23	1.18	45	13.3	46	14.1	0.37	0.272	47	15.3	1.06	0.113
100899	SFBA	Y	15.1	0.998	19.9	0.711	1.43	2.85	3.99	9.11	1.19	46	13.6	46	13.5	0.00	0.288	47	13.8	0.15	0.252
100900	SFBA	Y	15.1	0.998	19.7	0.840	1.47	3.21	4.30	9.23	1.18	66	13.6	67	15.4	0.36	0.267	69	16.8	1.12	0.108
100901	SFBA	Y	15.1	0.998	20.3	0.678	1.50	2.73	3.88	8.37	1.14	42	15.1	43	15.4	0.23	0.280	43	15.5	0.29	0.223
100902	SFBA	Y	15.1	0.998	18.7	0.811	1.44	3.12	4.16	8.49	1.20	62	14.4	62	14.8	0.14	0.282	62	14.6	0.09	0.266
100903	SFBA	Y	14.4	0.999	6.1	9.54	1.24	9.26	5.38	25.7	1.19	-	-	-	-	-	-	-	-	-	-
100904	SFBA	Y	14.4	0.999	6.5	2.04	1.43	4.50	5.04	10.4	1.30	130	12.3	131	13.5	0.12	0.277	132	14.3	0.50	0.185
100905	SFBA	Y	15.2	0.979	36.0	1.10	1.55	3.82	4.49	9.31	1.17	102	14.3	103	15.5	0.16	0.276	104	16.3	0.56	0.176
100906	SFBA	Y	15.2	0.979	15.2	0.968	1.83	3.78	4.79	8.39	1.23	-	-	-	-	-	-	-	-	-	-
100907	SFBA	Y	15.2	0.979	46.2	1.10	2.04	3.96	4.55	9.27	1.14	112	15.1	114	17.0	0.19	0.273	116	18.3	0.75	0.151
100908	SFBA	Y	15.2	0.979	27.3	1.21	1.55	4.15	4.82	9.91	1.21	119	13.1	121	15.5	0.21	0.269	124	17.2	0.92	0.130
100909	SFBA	Y	12.6	0.996	10.0	0.633	1.41	2.92	4.21	23.3	1.26	-	-	-	-	-	-	-	-	-	-
100910	SFBA	Y	12.6	0.996	10.4	0.783	1.16	3.22	4.30	17.7	0.519	-	-	-	-	-	-	-	-	-	-
100911	SFBA	Y	12.6	0.996	11.1	0.633	1.41	2.93	4.44	8.27	0.812	-	-	-	-	-	-	-	-	-	-
100912	SFBA	Y	12.6	0.996	9.4	0.682	1.40	3.02	4.46	53.2	0.888	-	-	-	-	-	-	-	-	-	-
100915	SFBA	Y	15.7	0.995	12.6	1.75	0.887	2.95	4.01	8.96	1.20	52	13.7	51	13.7	0.00	0.288	51	13.7	0.00	0.288
100916	SFBA	Y	15.0	0.995	13.8	1.92	1.49	6.97	4.96	21.4	0.694	-	-	-	-	-	-	-	-	-	-
100918	SFBA	Y	12.3	0.995	13.3	0.723	1.51	2.97	4.10	8.99	1.12	55	14.5	57	16.6	0.45	0.262	59	18.9	1.56	0.076
100919	SFBA	Y	15.0	0.995	12.5	1.68	1.45	6.18	4.99	11.3	1.39	-	-	-	-	-	-	-	-	-	-
100920	SFBA	Y	15.0	0.995	13.4	1.34	1.67	4.94	4.95	11.4	1.41	-	-	-	-	-	-	-	-	-	-
100923	SFBA	Y	14.4	0.999	15.2	1.24	1.47	4.64	4.99	11.9	1.30	-	-	-	-	-	-	-	-	-	-
100924	SFBA	Y	14.4	0.999	1.2	5.83	1.22	4.18	4.94	11.4	1.50	102	8.3	-	-	-	-	-	-	-	-
100925	SFBA	Y	14.4	0.999	0.1	9.83	1.25	4.07	4.96	11.6	1.33	-	-	-	-	-	-	-	-	-	-
100926	SFBA	Y	14.4	0.999	3.6	4.28	1.36	5.32	4.94	12.0	1.39	-	-	-	-	-	-	-	-	-	-
100927	SFBA	Y	14.4	0.999	1.6	6.48	1.22	5.05	5.05	12.0	1.27	-	-	-	-	-	-	-	-	-	-
100928	NCV	N	16.0	0.998	0.4	18.4	0.545	2.08	3.57	8.05	1.12	8	14.7	8	15.1	0.85	0.262	9	15.2	1.19	0.100
100929	NCV	N	16.0	0.998	2.1	14.6	0.571	2.22	3.71	8.37	1.20	13	13.2	13	13.1	0.00	0.288	13	13.1	0.00	0.288
100930	NCV	N	16.0	0.998	0.5	7.32	0.624	2.17	3.66	8.11	1.20	12	13.7	11	13.6	0.00	0.288	11	13.6	0.00	0.288
100931	NCV	N	16.0	0.998	0.5	11.9	0.622	2.21	3.76	8.40	1.26	12	12.4	12	12.3	0.00	0.288	12	12.3	0.00	0.288

Table S2. Measured data and model results for all 905 samples.

Sample Number	Region[a]	AR area[b]	MAAT[c] (ºC)	Atmo. pres.[d] (atm)	^{3}H (piC/L)[e]	^{4}He (x 10^{-7})[ef]	^{3}He/^{4}He (x 10^{-6})[e]	Ne (x 10^{-7})[f]	Ar (x 10^{-4})[f]	Kr (x 10^{-8})[f]	Xe (x 10^{-8})[f]	ΔNe_{UA} (%)	NGT_{UA} (ºC)	ΔNe_{CE} (%)	NGT_{CE} (ºC)	CE *F* value	$L_{ex,CE}$[g]	ΔNe_{PR} (%)	NGT_{PR} (ºC)	PR *R* value	$L_{ex,PR}$[g]
100932	NCV	N	16.0	0.998	0.8	12.6	0.624	2.30	3.85	8.66	1.25	17	12.0	17	12.0	0.00	0.288	16	12.0	0.00	0.288
100933	NCV	N	16.0	0.998	0.4	10.6	0.648	2.23	3.80	8.47	1.24	13	12.4	13	12.4	0.00	0.288	13	12.3	0.00	0.288
100934	NCV	N	16.0	0.998	0.5	2.63	0.810	2.19	3.72	8.44	1.20	12	13.0	12	13.0	0.00	0.288	12	13.0	0.00	0.288
100935	NCV	N	16.0	0.998	0.0	6.78	0.725	2.19	3.77	8.53	1.26	11	12.1	10	12.0	0.00	0.288	10	12.0	0.00	0.288
100936	NCV	N	16.0	0.998	18.9	3.17	1.04	2.24	3.82	8.63	1.27	13	11.8	12	11.7	0.00	0.288	12	11.6	0.00	0.288
100937	NCV	N	16.0	0.998	17.0	0.849	2.00	2.27	3.80	8.39	1.21	16	12.9	16	13.1	0.55	0.276	16	13.0	0.17	0.246
100938	NCV	N	16.0	0.998	19.0	0.542	1.71	2.24	3.86	8.76	1.28	13	11.4	12	11.4	0.00	0.288	12	11.3	0.00	0.288
100939	NCV	N	16.0	0.998	13.9	2.40	1.04	2.31	3.82	8.65	1.23	17	12.4	17	12.4	0.00	0.288	17	12.4	0.00	0.288
100940	NCV	N	16.0	0.998	22.3	0.707	2.11	2.24	3.90	8.99	1.33	11	10.5	10	10.2	0.00	0.288	10	10.2	0.00	0.288
100941	NCV	N	16.0	0.998	0.0	19.5	0.517	2.05	3.53	7.96	1.15	6	14.5	6	14.5	0.00	0.288	6	14.5	0.00	0.288
100943	NCV	N	16.0	0.998	0.8	33.6	0.691	2.41	3.95	8.32	1.22	23	12.8	24	13.8	0.67	0.259	24	13.6	0.86	0.133
100944	NCV	N	16.0	0.998	3.3	1.40	1.02	2.24	3.62	8.10	1.13	16	15.0	16	15.1	0.42	0.281	16	15.1	0.26	0.229
100945	NCV	N	16.0	0.998	1.0	7.47	0.734	2.29	3.74	8.36	1.18	18	13.6	18	13.8	0.45	0.279	18	13.8	0.26	0.229
100946	NCV	N	16.0	0.998	0.3	9.78	0.684	2.21	3.75	8.55	1.25	12	12.3	12	12.1	0.00	0.288	12	12.1	0.00	0.288
100947	NCV	N	16.0	0.998	16.2	18.6	0.591	2.28	3.91	8.94	1.31	14	10.8	13	10.8	0.00	0.288	13	10.6	0.00	0.288
100948	NCV	N	16.0	0.998	21.1	1.95	1.07	2.39	3.97	9.24	1.30	20	10.7	19	10.7	0.00	0.288	19	10.7	0.00	0.288
100949	NCV	N	16.0	0.998	1.9	11.7	0.658	2.23	3.80	8.70	1.26	12	11.9	12	11.8	0.00	0.288	12	11.8	0.00	0.288
100950	NCV	N	16.0	0.998	1.6	16.7	0.604	2.27	3.70	8.06	1.13	18	14.8	19	15.7	0.73	0.259	19	15.8	1.19	0.101
100951	NCV	N	16.0	0.998	2.5	4.24	0.728	2.25	3.59	8.18	1.14	16	14.8	16	14.8	0.00	0.288	16	14.8	0.00	0.288
100952	NCV	N	16.0	0.998	0.8	6.99	0.720	2.21	3.79	8.64	1.24	12	12.1	12	12.1	0.00	0.288	12	12.1	0.00	0.288
100953	NCV	N	16.0	0.998	1.5	2.63	0.809	2.33	3.72	8.37	1.19	20	13.8	19	13.7	0.00	0.288	19	13.7	0.00	0.288
100954	NCV	N	16.0	0.998	1.6	4.42	0.707	2.21	3.67	8.30	1.14	14	14.3	15	14.8	0.75	0.263	15	15.2	1.38	0.085
100955	NCV	N	16.0	0.998	0.1	7.80	0.682	2.26	3.87	8.85	1.24	14	11.7	14	12.1	0.73	0.264	15	12.4	1.12	0.104
100956	NCV	N	16.0	0.998	2.6	3.32	0.806	2.31	3.75	8.60	1.19	18	13.2	18	13.2	0.00	0.288	18	13.2	0.00	0.288
100957	SFBA	Y	15.0	0.995	16.0	1.57	1.58	6.06	4.98	11.3	1.45	-	-	-	-	-	-	-	-	-	-
100958	SFBA	Y	15.0	0.995	11.5	1.62	1.55	6.12	4.99	11.9	1.47	-	-	-	-	-	-	-	-	-	-
100961	SFBA	Y	14.4	0.993	6.0	1.82	0.928	3.32	4.59	10.1	1.33	67	10.1	68	11.3	0.31	0.268	69	12.2	0.92	0.125
100963	SFBA	Y	14.4	0.993	11.8	0.871	1.50	4.00	4.54	10.1	1.28	104	12.8	-	-	-	-	-	-	-	-
100965	SFBA	Y	14.4	0.993	2.2	1.52	1.54	6.13	4.90	12.0	1.36	-	-	-	-	-	-	-	-	-	-
100966	SFBA	Y	15.0	0.993	7.2	3.46	1.47	12.7	5.09	15.2	1.69	-	-	-	-	-	-	-	-	-	-
100967	SFBA	Y	14.4	0.993	2.0	2.07	1.31	8.93	7.50	12.6	1.55	359	12.0	361	13.6	0.03	0.281	363	13.8	0.20	0.241
100968	SFBA	Y	15.0	0.993	4.1	1.78	1.34	8.20	6.81	11.9	1.45	325	13.8	326	14.3	0.01	0.286	326	14.2	0.05	0.277
100969	SFBA	Y	15.0	0.993	13.2	1.09	1.30	5.36	5.27	10.0	1.32	178	14.1	177	14.1	0.00	0.288	176	14.1	0.00	0.288
100970	SFBA	Y	15.0	0.993	7.0	1.53	1.42	6.43	6.03	11.1	1.41	231	12.6	231	13.4	0.03	0.283	232	13.6	0.16	0.250
100973	LAB	Y	18.1	0.947	11.2	2.11	1.43	7.48	8.69	11.9	1.39	-	-	-	-	-	-	-	-	-	-
100974	LAB	Y	18.1	0.947	7.3	2.10	1.24	6.36	5.20	12.2	1.39	-	-	-	-	-	-	-	-	-	-
100975	LAB	Y	18.0	0.947	0.4	1.21	0.891	2.94	4.30	9.40	1.20	-	-	59	13.6	0.49	0.255	63	16.1	1.86	0.057
100976	LAB	Y	18.1	0.947	7.6	0.863	1.39	3.25	4.29	9.36	1.17	75	12.2	77	14.2	0.34	0.265	79	16.1	1.24	0.097
100977	SFBA	Y	15.2	0.982	26.4	1.38	1.54	5.23	7.39	10.6	1.38	-	-	-	-	-	-	-	-	-	-
100978	SFBA	Y	15.2	0.982	30.7	1.40	1.56	5.66	5.75	10.9	1.40	192	11.2	193	12.5	0.07	0.278	194	12.9	0.33	0.215
100979	NCV	N	16.0	0.998	0.6	0.713	1.12	2.18	3.54	8.12	1.14	13	14.9	12	14.9	0.00	0.288	12	14.9	0.00	0.288
100980	NCV	N	16.0	0.998	0.0	14.4	0.642	2.25	3.77	8.72	1.25	14	12.1	13	11.9	0.00	0.288	13	11.9	0.00	0.288
100981	NCV	N	16.0	0.998	1.4	11.9	0.597	2.19	3.71	8.46	1.19	12	13.2	12	13.3	0.36	0.284	12	13.3	0.20	0.241
100982	NCV	N	16.0	0.998	0.3	3.03	0.744	2.29	3.56	7.66	1.07	21	16.8	22	17.3	0.57	0.272	22	17.3	0.53	0.182
100983	NCV	N	16.0	0.998	0.1	7.50	0.677	2.32	3.84	8.52	1.21	19	12.7	19	13.1	0.59	0.271	19	13.1	0.50	0.183

Table S2. Measured data and model results for all 905 samples.

Sample Number	Region[a]	AR area[b]	MAAT[c] (ºC)	Atmo. pres.[d] (atm)	^{3}H (piC/L)[e]	^{4}He (x 10^{-7})[ef]	^{3}He/^{4}He (x 10^{-6})[e]	Ne (x 10^{-7})[f]	Ar (x 10^{-4})[f]	Kr (x 10^{-8})[f]	Xe (x 10^{-8})[f]	ΔNe_{UA} (%)	NGT_{UA} (ºC)	ΔNe_{CE} (%)	NGT_{CE} (ºC)	CE *F* value	$L_{ex,CE}$[g]	ΔNe_{PR} (%)	NGT_{PR} (ºC)	PR *R* value	$L_{ex,PR}$[g]
100984	NCV	N	16.0	0.998	0.9	5.37	0.709	2.20	3.61	8.30	1.21	12	13.6	12	13.6	0.00	0.288	12	13.6	0.00	0.288
100985	NCV	N	16.0	0.998	1.8	9.05	0.565	2.14	3.60	7.98	1.12	11	14.9	11	15.4	0.80	0.262	12	15.4	1.00	0.119
100986	NCV	N	16.0	0.998	0.0	15.9	0.508	2.13	3.53	7.97	1.16	10	14.7	9	14.7	0.00	0.288	9	14.7	0.00	0.288
100987	NCV	N	16.0	0.998	0.2	8.83	0.371	2.02	3.33	7.77	1.12	5	16.1	5	16.0	0.00	0.288	5	16.0	0.00	0.288
100988	NCV	N	16.0	0.998	0.2	5.74	0.398	2.12	3.53	7.81	1.12	11	15.4	10	15.4	0.00	0.288	10	15.4	0.00	0.288
100989	NCV	N	16.5	0.998	0.5	11.9	0.371	2.15	3.50	7.36	1.14	-	-	-	-	-	-	-	-	-	-
100990	NCV	N	16.5	0.998	1.0	0.558	1.22	2.06	3.38	7.56	1.06	9	17.0	8	16.9	0.00	0.288	8	16.9	0.00	0.288
100991	NCV	N	16.5	0.998	0.2	20.5	0.427	1.94	3.48	7.66	1.09	2	15.6	2	16.1	0.98	0.241	2	15.9	2.39	0.035
100992	NCV	N	16.5	0.998	0.1	22.1	0.426	2.05	3.50	7.71	1.16	6	15.0	6	15.0	0.00	0.288	6	15.0	0.00	0.288
100993	NCV	N	16.0	0.998	0.1	13.4	0.463	5.66	5.31	9.85	1.26	197	16.2	197	16.2	0.00	0.288	196	16.2	0.00	0.288
100994	NCV	N	16.0	0.998	0.2	23.1	0.476	2.05	3.50	8.10	1.09	7	15.3	8	15.9	0.90	0.252	10	19.5	3.86	0.011
100995	NCV	N	16.0	0.998	0.9	0.728	1.12	2.31	3.85	8.79	1.17	18	12.8	19	14.3	0.78	0.250	21	16.1	2.53	0.031
100996	NCV	N	16.0	0.998	15.9	2.02	0.844	2.37	3.79	8.52	1.14	23	14.1	23	15.2	0.69	0.258	25	16.2	1.75	0.062
100997	NCV	N	16.0	0.998	32.0	3.06	1.08	2.31	3.72	8.77	1.26	17	12.5	16	12.3	0.00	0.288	16	12.3	0.00	0.288
100998	NCV	N	16.0	0.998	14.4	0.619	1.66	2.27	3.89	8.60	1.32	14	11.3	13	11.1	0.00	0.288	13	11.0	0.00	0.288
100999	SFBA	Y	12.3	0.995	13.3	0.699	1.74	2.94	4.00	8.86	1.21	51	13.7	49	13.6	0.00	0.288	49	13.5	0.00	0.288
101000	SFBA	Y	12.3	0.995	13.3	0.707	1.52	2.91	4.10	8.48	1.15	52	14.5	54	16.2	0.43	0.265	54	16.7	0.98	0.122
101001	SFBA	Y	12.3	0.995	12.4	0.604	1.48	2.53	3.82	7.71	1.03	-	-	38	20.8	0.65	0.254	39	21.3	1.89	0.060
101002	SFBA	Y	15.7	0.995	13.3	0.712	1.52	2.85	3.98	8.33	1.16	49	14.8	49	15.3	0.26	0.278	49	15.3	0.29	0.223
101003	SFBA	Y	15.7	0.995	13.6	0.721	1.51	2.95	3.98	8.56	1.11	55	15.6	56	16.7	0.33	0.272	57	17.5	0.82	0.141
101004	SFBA	Y	15.7	0.995	14.5	0.957	1.43	3.97	4.51	9.28	1.26	104	14.0	102	13.8	0.00	0.288	101	13.8	0.00	0.288
101005	SFBA	Y	15.7	0.995	13.5	0.989	1.43	3.61	4.29	7.43	0.878	-	-	-	-	-	-	-	-	-	-
101006	SFBA	Y	15.7	0.995	4.6	0.754	1.48	2.95	4.12	6.66	0.921	-	-	-	-	-	-	-	-	-	-
101007	SFBA	Y	15.7	0.995	15.6	0.706	1.45	3.26	4.22	8.04	1.15	-	-	-	-	-	-	-	-	-	-
101008	SFBA	Y	15.7	0.995	13.5	0.724	1.53	3.08	4.16	8.13	1.19	-	-	-	-	-	-	-	-	-	-
101009	SFBA	Y	12.3	0.995	14.2	1.06	1.45	4.12	4.75	9.36	1.24	114	13.9	115	14.9	0.13	0.278	115	15.2	0.35	0.211
101010	SFBA	Y	15.0	0.995	0.8	1.92	1.01	4.64	4.67	10.8	1.45	-	-	-	-	-	-	-	-	-	-
101011	SFBA	Y	15.0	0.995	4.8	4.73	0.976	4.71	5.53	10.5	1.39	-	-	142	13.3	0.21	0.266	145	14.3	0.87	0.133
101012	SFBA	Y	15.0	0.995	13.5	1.80	1.38	6.02	5.89	11.4	1.48	202	10.5	202	10.7	0.01	0.287	202	10.7	0.03	0.280
101013	SFBA	Y	15.0	0.995	8.1	1.52	1.48	6.14	6.04	11.7	1.51	206	9.7	206	10.1	0.02	0.284	207	10.3	0.12	0.258
101014	SFBA	Y	15.0	0.995	13.6	1.64	1.54	6.22	6.05	11.0	1.44	218	11.7	219	13.0	0.05	0.280	220	13.0	0.22	0.235
101015	SFBA	Y	15.0	0.995	14.7	1.56	1.57	6.34	5.74	10.7	1.43	223	13.2	216	12.8	0.00	0.288	-	-	-	-
101016	SFBA	Y	15.0	0.995	7.6	1.76	1.47	6.83	4.99	12.5	1.40	-	-	-	-	-	-	-	-	-	-
101017	SFBA	Y	15.0	0.995	7.7	1.82	1.48	7.05	4.98	12.0	1.45	-	-	-	-	-	-	-	-	-	-
101018	SFBA	Y	15.0	0.995	2.7	1.14	1.34	5.38	5.84	11.5	1.46	170	9.2	171	11.2	0.12	0.272	174	12.3	0.61	0.165
101019	SFBA	Y	15.7	0.995	14.0	1.00	1.50	3.68	4.38	9.01	1.22	91	14.4	90	14.4	0.00	0.288	90	14.4	0.00	0.288
101020	SFBA	Y	15.7	0.995	13.9	0.897	1.48	3.31	4.16	9.12	1.19	71	14.3	71	14.3	0.00	0.288	71	14.3	0.00	0.288
101021	SFBA	Y	15.7	0.995	13.2	1.42	1.63	4.07	4.85	10.1	1.24	-	-	112	15.0	0.23	0.268	115	16.8	0.98	0.122
101022	SFBA	Y	15.7	0.995	12.5	1.49	1.97	5.37	4.97	11.0	1.32	-	-	-	-	-	-	-	-	-	-
101023	SFBA	Y	15.7	0.995	10.7	2.36	2.97	4.15	4.98	10.5	1.27	-	-	115	14.3	0.24	0.266	119	16.5	1.11	0.110
101024	SFBA	Y	15.7	0.995	14.1	1.21	1.49	4.52	4.80	9.94	1.22	135	14.6	136	15.0	0.04	0.284	136	15.5	0.23	0.236
101025	SFBA	Y	15.7	0.995	12.8	0.822	1.46	3.35	4.14	41.0	1.21	-	-	-	-	-	-	-	-	-	-
101026	SFBA	Y	15.7	0.995	8.1	2.81	1.21	4.54	4.98	10.3	1.31	132	12.3	132	12.7	0.04	0.284	133	13.1	0.20	0.241
101027	SFBA	Y	15.7	0.995	14.2	1.30	1.72	4.93	5.00	10.9	1.33	150	12.6	-	-	-	-	-	-	-	-
101028	SFBA	Y	15.7	0.995	14.5	2.03	1.60	7.04	5.09	11.4	1.36	-	-	-	-	-	-	-	-	-	-

Table S2. Measured data and model results for all 905 samples.

Sample Number	Region[a]	AR area[b]	MAAT[c] (ºC)	Atmo. pres.[d] (atm)	^{3}H (piC/L)[e]	^{4}He (x 10^{-7})[ef]	$^{3}He/^{4}He$ (x 10^{-6})[e]	Ne (x 10^{-7})[f]	Ar (x 10^{-4})[f]	Kr (x 10^{-8})[f]	Xe (x 10^{-8})[f]	ΔNe_{UA} (%)	NGT_{UA} (ºC)	ΔNe_{CE} (%)	NGT_{CE} (ºC)	CE *F* value	$L_{ex,CE}$[g]	ΔNe_{PR} (%)	NGT_{PR} (ºC)	PR *R* value	$L_{ex,PR}$[g]
101029	SFBA	Y	15.0	0.995	13.0	1.56	1.62	5.98	4.94	11.6	1.30	-	-	-	-	-	-	-	-	-	-
101030	SFBA	Y	15.0	0.995	10.3	1.77	1.54	6.67	4.94	12.0	1.45	-	-	-	-	-	-	-	-	-	-
101031	SFBA	Y	15.0	0.995	8.0	1.46	1.54	5.93	4.97	11.9	1.37	-	-	-	-	-	-	-	-	-	-
101032	SFBA	Y	15.0	0.995	3.9	1.27	1.43	5.02	4.95	11.4	1.43	-	-	-	-	-	-	-	-	-	-
101033	SFBA	Y	15.0	0.995	10.2	1.70	1.50	6.74	4.99	9.37	1.32	-	-	-	-	-	-	-	-	-	-
101034	SFBA	Y	15.0	0.995	5.8	1.70	1.50	6.95	4.97	11.1	1.28	-	-	-	-	-	-	-	-	-	-
101035	SFBA	Y	15.0	0.995	9.8	1.58	1.45	6.46	4.96	12.1	1.48	-	-	-	-	-	-	-	-	-	-
101036	SFBA	Y	15.0	0.995	2.5	1.33	1.23	4.61	4.97	10.7	1.44	128	10.6	-	-	-	-	-	-	-	-
101037	SFBA	Y	15.0	0.995	9.3	1.42	1.42	6.29	6.16	11.9	1.49	215	9.9	216	11.0	0.05	0.280	218	11.6	0.30	0.219
101038	SFBA	Y	15.0	0.995	0.7	1.11	1.31	4.71	5.43	11.0	1.45	135	9.1	136	10.4	0.12	0.275	137	10.9	0.46	0.189
101039	SFBA	Y	15.0	0.995	7.5	1.56	1.56	5.60	5.84	11.3	1.43	183	10.4	185	12.2	0.10	0.275	188	13.1	0.51	0.182
101040	SFBA	Y	15.0	0.995	13.0	1.58	1.48	6.31	5.87	10.2	1.40	-	-	-	-	-	-	-	-	-	-
101041	SFBA	Y	15.1	0.995	8.9	3.82	1.51	11.6	6.87	13.4	1.55	-	-	-	-	-	-	-	-	-	-
101042	SFBA	Y	15.1	0.995	10.8	2.16	1.32	6.57	6.07	11.0	1.36	242	13.7	243	15.0	0.05	0.281	244	15.4	0.26	0.230
101043	SFBA	Y	15.1	0.995	15.5	0.949	1.54	3.62	4.45	9.06	1.22	88	13.9	88	14.6	0.14	0.279	89	14.7	0.29	0.224
101044	SFBA	Y	15.1	0.995	9.7	1.52	1.44	5.40	5.40	10.7	1.36	175	12.4	175	12.5	0.01	0.287	175	12.6	0.05	0.275
101045	SFBA	Y	15.0	0.995	30.2	1.87	1.36	5.55	5.47	10.8	1.36	183	12.6	183	12.7	0.01	0.287	184	12.8	0.05	0.275
101046	SFBA	Y	15.0	0.995	30.1	1.77	1.46	6.42	5.63	10.8	1.39	228	14.1	-	-	-	-	-	-	-	-
101048	SFBA	Y	15.0	0.995	27.7	2.77	1.16	5.51	4.93	11.2	1.38	-	-	-	-	-	-	-	-	-	-
101049	SFBA	Y	15.0	0.995	32.0	1.65	1.43	5.41	4.93	10.7	1.31	-	-	-	-	-	-	-	-	-	-
101050	SFBA	Y	15.0	0.995	19.5	1.71	1.51	5.73	4.95	10.6	1.30	-	-	-	-	-	-	-	-	-	-
101051	SFBA	Y	15.0	0.995	11.9	1.57	1.37	5.83	5.50	10.6	1.32	202	14.1	202	14.2	0.00	0.288	202	14.3	0.03	0.282
101052	SFBA	Y	15.0	0.995	13.4	2.09	1.43	7.77	6.24	11.5	1.37	304	15.7	295	15.3	0.00	0.288	295	15.3	0.00	0.288
101053	SFBA	Y	15.0	0.995	14.8	1.65	1.46	6.62	5.60	10.8	1.39	-	-	-	-	-	-	-	-	-	-
101054	SFBA	Y	15.7	0.995	14.6	1.46	1.41	5.39	5.35	10.3	1.32	178	13.6	179	14.1	0.03	0.285	179	14.2	0.12	0.259
101055	SCV	N	15.8	0.999	2.2	1.28	1.49	2.77	4.26	9.62	1.30	38	10.4	39	11.2	0.45	0.267	39	11.8	0.98	0.117
101056	SCV	N	15.8	0.999	9.0	1.19	1.91	3.05	4.31	9.35	1.31	53	11.3	53	11.5	0.12	0.283	53	11.5	0.12	0.259
101057	SCV	N	15.8	0.999	9.0	1.45	1.83	3.74	4.58	9.50	1.31	90	12.4	90	12.4	0.02	0.287	90	12.3	0.00	0.288
101064	SFBA	Y	14.4	0.995	7.8	1.88	1.49	8.91	6.90	12.1	1.46	362	15.1	353	14.7	0.00	0.288	351	14.7	0.00	0.288
101065	SFBA	Y	14.4	0.995	6.5	1.32	1.49	5.97	5.79	10.6	1.43	204	12.2	205	12.5	0.01	0.287	204	12.2	0.00	0.288
101066	SFBA	Y	14.4	0.995	-	0.897	1.49	4.29	5.01	9.78	1.28	122	12.6	123	14.7	0.19	0.271	125	15.4	0.67	0.159
101067	SFBA	Y	14.4	0.999	3.8	31.9	1.17	5.67	6.04	11.2	1.47	-	-	187	12.3	0.12	0.272	190	12.9	0.55	0.175
101068	SFBA	Y	15.7	0.995	11.3	1.00	1.54	4.20	4.71	8.65	1.23	-	-	-	-	-	-	-	-	-	-
101070	SFBA	Y	15.7	0.995	12.5	0.748	1.47	3.50	4.11	8.56	1.19	83	15.9	78	15.5	0.00	0.288	78	15.5	0.00	0.288
101071	SFBA	Y	14.4	0.995	4.4	2.30	1.46	9.31	7.51	13.6	1.58	372	11.4	372	11.9	0.01	0.286	374	12.4	0.12	0.259
101072	SFBA	Y	14.4	0.995	4.5	2.70	1.36	11.2	7.83	14.1	1.60	-	-	-	-	-	-	-	-	-	-
101073	SFBA	Y	14.4	0.999	3.4	50.1	0.936	5.06	5.65	10.7	1.53	150	9.0	-	-	-	-	-	-	-	-
101074	SFBA	Y	15.0	0.995	11.6	1.68	1.78	6.41	6.07	10.7	1.42	230	12.7	231	13.6	0.04	0.282	231	13.4	0.12	0.260
101075	SFBA	Y	14.4	0.995	4.5	6.56	0.808	6.72	6.19	11.0	1.46	244	12.4	244	12.8	0.01	0.286	244	12.4	0.00	0.288
101077	SFBA	Y	15.0	0.995	9.5	1.59	1.54	6.30	6.25	11.1	1.51	-	-	-	-	-	-	-	-	-	-
101078	SFBA	Y	15.0	0.995	1.4	1.23	1.32	5.65	5.53	11.0	1.31	192	13.3	193	14.5	0.06	0.280	195	15.5	0.37	0.207
101081	SFBA	Y	14.4	0.995	5.6	1.14	1.43	5.11	5.78	11.3	1.35	-	-	166	14.8	0.21	0.263	173	17.8	1.20	0.102
101082	SFBA	Y	14.4	0.995	6.8	2.40	1.43	9.27	7.38	12.7	1.59	370	12.3	366	12.1	0.00	0.288	363	12.0	0.00	0.288
101083	SFBA	Y	14.4	0.995	5.3	0.682	1.37	3.70	4.77	10.1	1.29	88	11.1	90	13.3	0.30	0.265	92	14.9	1.11	0.108
101086	SFBA	Y	15.0	0.995	15.5	2.62	1.54	9.17	6.99	12.1	1.34	391	18.0	392	18.3	0.01	0.287	393	18.7	0.07	0.272

Table S2. Measured data and model results for all 905 samples.

Sample Number	Region[a]	AR area[b]	MAAT[c] (ºC)	Atmo. pres.[d] (atm)	^{3}H (piC/L)[e]	^{4}He (x 10^{-7})[ef]	^{3}He/^{4}He (x 10^{-6})[e]	Ne (x 10^{-7})[f]	Ar (x 10^{-4})[f]	Kr (x 10^{-8})[f]	Xe (x 10^{-8})[f]	ΔNe_{UA} (%)	NGT_{UA} (ºC)	ΔNe_{CE} (%)	NGT_{CE} (ºC)	CE *F* value	$L_{ex,CE}$[g]	ΔNe_{PR} (%)	NGT_{PR} (ºC)	PR *R* value	$L_{ex,PR}$[g]
101087	SFBA	Y	15.0	0.995	15.3	1.55	1.52	5.95	5.65	10.7	1.26	213	15.0	215	16.8	0.07	0.278	218	18.1	0.46	0.194
101088	SFBA	Y	15.7	0.995	11.0	2.75	1.84	8.18	6.80	12.3	1.45	322	13.4	322	13.9	0.01	0.286	324	14.2	0.11	0.262
101090	SFBA	Y	15.7	0.995	15.8	1.51	1.46	5.35	5.35	10.4	1.29	178	13.8	178	14.6	0.05	0.282	179	15.1	0.25	0.230
101091	SFBA	Y	15.7	0.995	12.7	0.792	1.48	3.16	4.05	8.14	1.15	66	16.1	66	16.3	0.07	0.285	66	16.1	0.00	0.288
101092	SFBA	Y	15.7	0.995	14.6	3.41	1.39	12.1	7.94	13.7	1.60	-	-	-	-	-	-	-	-	-	-
101093	SFBA	Y	15.1	0.995	8.8	1.46	1.54	5.83	5.55	10.9	1.36	198	13.0	197	12.9	0.00	0.288	198	12.9	0.00	0.288
101094	SFBA	Y	15.0	0.995	12.2	1.05	1.37	4.48	4.75	9.76	1.25	132	14.4	130	14.2	0.00	0.288	130	14.3	0.00	0.288
101095	SFBA	Y	15.0	0.995	16.0	2.16	1.22	5.38	5.21	10.3	1.35	175	13.5	169	13.2	0.00	0.288	169	13.2	0.00	0.288
101096	SFBA	Y	15.7	0.995	2.2	2.54	0.954	4.27	5.18	10.3	1.37	116	10.3	118	12.4	0.21	0.268	119	13.2	0.75	0.146
101097	SFBA	Y	15.7	0.995	11.9	1.81	1.83	5.39	5.49	10.6	1.38	175	12.1	176	12.7	0.04	0.283	176	12.8	0.15	0.253
101098	SFBA	Y	15.0	0.995	10.3	1.48	1.40	5.72	5.24	10.1	1.33	195	15.0	-	-	-	-	-	-	-	-
101099	SFBA	Y	15.7	0.995	13.8	1.16	1.60	4.64	4.97	10.0	1.31	138	12.9	138	13.0	0.01	0.288	138	13.0	0.02	0.282
101100	SFBA	Y	15.7	0.995	14.2	3.41	1.62	12.3	7.93	13.5	1.57	-	-	-	-	-	-	-	-	-	-
101101	SFBA	Y	15.0	0.995	14.2	2.62	1.38	8.16	6.30	11.3	1.41	323	16.3	-	-	-	-	-	-	-	-
101104	SFBA	Y	15.7	0.995	14.9	1.26	1.56	5.01	5.02	10.0	1.31	158	14.0	154	13.8	0.00	0.288	154	13.7	0.00	0.288
101105	SFBA	Y	15.7	0.995	17.1	5.46	1.53	23.5	7.95	26.9	2.56	-	-	-	-	-	-	-	-	-	-
101106	SFBA	Y	15.7	0.995	3.1	2.15	3.18	3.91	4.90	10.2	1.36	97	10.2	98	11.4	0.18	0.274	99	11.9	0.54	0.176
101107	SFBA	Y	15.0	0.995	11.2	1.46	1.49	5.56	5.70	11.0	1.37	184	11.7	186	13.5	0.10	0.276	189	14.5	0.50	0.185
101108	SFBA	Y	15.7	0.995	7.9	3.14	2.10	6.87	6.35	11.6	1.41	254	12.4	256	14.2	0.06	0.279	259	15.0	0.35	0.210
101109	SFBA	Y	15.7	0.995	16.0	0.874	1.58	3.54	4.37	9.30	1.25	82	13.2	81	13.1	0.00	0.288	81	13.1	0.00	0.288
101110	SFBA	Y	15.0	0.995	1.1	3.01	0.807	4.36	5.06	9.91	1.37	121	11.3	122	12.1	0.10	0.279	122	12.1	0.23	0.234
101111	SFBA	Y	15.7	0.995	14.9	1.55	1.63	5.99	5.67	10.8	1.38	207	12.9	207	12.9	0.00	0.288	207	12.9	0.00	0.288
101112	SFBA	Y	15.0	0.995	3.3	1.81	1.04	4.89	5.29	10.8	1.38	147	11.0	148	11.6	0.06	0.281	148	12.1	0.28	0.224
101113	SFBA	Y	15.0	0.995	14.4	1.66	1.37	6.06	5.57	10.7	1.30	215	14.7	215	14.9	0.01	0.287	216	15.2	0.08	0.268
101127	LAB	Y	18.1	0.996	108.9	0.845	1.87	3.35	4.30	8.94	1.15	75	14.8	77	16.6	0.31	0.269	78	17.6	0.92	0.130
101128	SCV	N	15.6	0.998	23.5	1.56	1.98	2.61	3.96	8.54	1.21	34	13.2	34	13.6	0.36	0.276	34	13.6	0.31	0.217
101129	SFBA	Y	15.0	0.995	12.2	5.56	0.745	6.08	5.46	10.7	1.38	210	13.8	-	-	-	-	-	-	-	-
101130	SFBA	Y	15.1	0.995	10.8	1.99	1.31	6.81	5.62	10.6	1.35	252	16.1	-	-	-	-	-	-	-	-
101131	SCV	N	15.6	0.998	18.2	2.11	1.66	2.58	4.00	9.00	1.24	31	12.1	31	12.3	0.30	0.279	31	12.5	0.37	0.205
101132	SCV	N	15.6	0.998	18.4	0.941	2.46	2.67	3.94	8.61	1.22	37	13.4	36	13.4	0.00	0.288	36	13.3	0.00	0.288
101133	SCV	N	15.6	0.998	5.9	1.04	1.60	2.69	4.20	9.07	1.26	36	11.4	37	12.8	0.56	0.259	38	13.3	1.21	0.096
101134	SFBA	Y	15.7	0.995	14.3	1.50	1.20	4.30	4.68	9.74	1.30	120	13.4	115	13.1	0.00	0.288	115	13.1	0.00	0.288
101136	SCV	N	15.6	0.998	1.3	2.58	1.14	2.52	4.04	9.22	1.28	27	11.1	27	11.3	0.33	0.279	27	11.4	0.42	0.197
101137	SCV	N	15.6	0.998	1.7	2.04	1.49	2.52	3.94	8.69	1.23	28	12.7	28	12.9	0.35	0.278	28	12.9	0.28	0.224
101138	SFBA	Y	15.7	0.995	4.8	3.98	4.98	4.23	4.98	10.3	1.38	113	10.7	113	11.1	0.08	0.282	113	11.3	0.21	0.239
101139	SFBA	Y	15.7	0.995	10.8	1.30	2.31	4.41	5.03	10.2	1.35	124	11.5	124	12.2	0.09	0.280	125	12.5	0.29	0.221
101140	SCV	N	15.6	0.998	4.7	3.09	1.44	2.37	3.82	8.60	1.21	21	13.0	21	13.0	0.28	0.283	21	13.1	0.17	0.248
101141	SCV	N	15.6	0.998	7.6	2.75	1.84	2.31	3.75	8.36	1.17	19	13.8	19	14.1	0.55	0.274	19	14.1	0.51	0.182
101142	SCV	N	15.6	0.998	25.9	2.68	2.42	2.29	3.86	8.95	1.27	15	11.5	15	11.5	0.00	0.288	15	11.5	0.00	0.288
101143	SFBA	Y	15.7	0.995	11.1	1.75	2.23	5.95	5.52	10.7	1.38	204	13.3	198	13.1	0.00	0.288	198	13.1	0.00	0.288
101145	SCV	N	15.6	0.998	24.7	2.55	2.45	2.33	3.78	8.59	1.23	18	12.7	17	12.6	0.00	0.288	17	12.6	0.00	0.288
101146	SCV	N	15.6	0.998	19.2	1.38	2.13	2.67	4.28	9.79	1.40	31	8.9	31	8.9	0.00	0.288	31	8.9	0.00	0.288
101147	SCV	N	15.6	0.998	29.0	6.00	2.20	2.29	3.79	8.36	1.28	16	12.4	15	12.2	0.00	0.288	15	12.2	0.00	0.288
101148	SCV	N	15.6	0.998	24.2	6.90	2.20	2.44	3.86	8.43	1.24	25	12.9	24	12.9	0.00	0.288	23	12.8	0.00	0.288
101149	SCV	N	15.6	0.998	25.5	0.565	2.69	2.68	3.93	8.33	1.29	-	-	-	-	-	-	-	-	-	-

Table S2. Measured data and model results for all 905 samples.

Sample Number	Region[a]	AR area[b]	MAAT[c] (ºC)	Atmo. pres.[d] (atm)	^{3}H (piC/L)[e]	^{4}He (x 10^{-7})[ef]	^{3}He/^{4}He (x 10^{-6})[e]	Ne (x 10^{-7})[f]	Ar (x 10^{-4})[f]	Kr (x 10^{-8})[f]	Xe (x 10^{-8})[f]	ΔNe_{UA} (%)	NGT_{UA} (ºC)	ΔNe_{CE} (%)	NGT_{CE} (ºC)	CE *F* value	$L_{ex,CE}$[g]	ΔNe_{PR} (%)	NGT_{PR} (ºC)	PR *R* value	$L_{ex,PR}$[g]
101150	SCV	N	15.6	0.998	31.3	1.46	2.63	2.25	3.81	9.02	1.30	12	11.2	11	11.0	0.00	0.288	11	10.9	0.00	0.288
101151	SCV	N	15.8	0.999	22.9	0.905	2.05	3.78	4.96	10.6	1.40	88	9.1	89	10.7	0.26	0.268	91	11.7	0.87	0.130
101152	SCV	N	15.8	0.999	0.8	1.50	1.51	2.67	4.17	9.48	1.31	33	10.6	34	10.9	0.35	0.276	34	11.2	0.55	0.174
101153	SCV	N	15.8	0.999	16.0	0.864	2.22	3.00	4.38	9.82	1.33	50	10.2	50	10.8	0.30	0.274	50	11.2	0.63	0.162
101154	SCV	N	15.8	0.999	7.8	1.12	1.83	2.81	4.32	9.70	1.35	39	9.7	40	10.2	0.33	0.275	40	10.4	0.52	0.178
101156	SFBA	Y	15.0	0.993	5.1	1.12	1.42	4.73	5.17	10.3	1.37	140	11.5	140	11.9	0.04	0.284	140	11.9	0.12	0.258
101157	SFBA	Y	15.0	0.993	9.4	1.03	1.40	4.60	5.10	10.2	1.31	136	12.3	137	13.5	0.11	0.277	138	14.1	0.43	0.197
101160	SFBA	Y	14.4	0.995	2.6	1.15	1.38	4.32	5.21	10.8	1.39	117	9.6	118	11.5	0.20	0.270	120	12.6	0.78	0.142
101161	SFBA	Y	14.4	0.995	6.4	0.833	1.46	3.78	4.93	10.3	1.39	89	9.3	90	10.7	0.24	0.270	91	11.3	0.69	0.152
101162	SFBA	Y	14.4	0.995	4.5	1.25	1.46	5.00	5.73	11.4	1.49	148	8.3	150	10.3	0.15	0.270	152	11.1	0.65	0.158
101163	SFBA	Y	14.4	0.995	4.8	8.50	0.784	7.17	6.66	12.6	1.56	258	9.4	259	10.4	0.04	0.281	260	10.9	0.23	0.233
101170	SFBA	Y	15.6	0.991	10.8	0.877	1.49	3.60	4.55	9.71	1.27	84	12.0	85	13.0	0.19	0.276	86	13.6	0.55	0.177
101171	SFBA	Y	15.6	0.991	12.2	0.879	1.43	3.49	4.50	9.43	1.23	80	12.7	81	14.3	0.28	0.269	83	15.2	0.85	0.135
101172	SFBA	Y	15.6	0.991	12.0	0.807	1.40	3.06	4.22	9.11	1.22	58	12.8	58	13.5	0.27	0.275	59	13.9	0.57	0.173
101173	SFBA	Y	15.6	0.991	5.0	1.27	1.34	3.78	4.94	10.3	1.33	-	-	94	12.6	0.31	0.263	97	14.1	1.16	0.102
101174	SFBA	Y	15.6	0.991	13.3	1.53	1.60	5.15	5.36	9.89	1.29	169	13.8	171	15.4	0.10	0.277	172	15.7	0.37	0.208
101175	SFBA	Y	15.6	0.991	3.0	1.33	1.26	3.67	4.81	9.87	1.33	86	10.4	87	12.2	0.28	0.267	89	12.8	0.80	0.140
101176	SFBA	Y	15.6	0.991	12.1	0.702	1.39	3.02	4.15	8.59	1.26	56	13.1	55	13.1	0.00	0.288	54	13.0	0.00	0.288
101177	SCV	N	15.8	0.999	6.7	1.05	1.82	3.21	4.52	9.82	1.36	60	10.0	60	10.6	0.24	0.276	60	10.8	0.43	0.193
101178	SCV	N	15.6	0.998	17.4	0.744	2.18	2.36	3.91	8.98	1.30	18	11.1	17	10.9	0.00	0.288	17	10.9	0.00	0.288
101179	SCV	N	15.6	0.998	12.2	0.536	1.70	2.25	3.85	9.04	1.33	12	10.6	11	10.4	0.00	0.288	11	10.4	0.00	0.288
101182	SFBA	Y	15.0	0.995	11.5	1.87	1.46	7.21	6.36	12.1	1.51	262	11.2	259	11.1	0.00	0.288	259	11.1	0.00	0.288
101183	SFBA	Y	15.0	0.995	14.2	2.39	1.55	9.34	7.32	13.0	1.67	364	11.0	-	-	-	-	-	-	-	-
101184	SFBA	Y	14.4	0.995	11.6	2.31	1.53	8.92	7.29	13.2	1.67	342	10.0	334	9.7	0.00	0.288	333	9.7	0.00	0.288
101185	SFBA	Y	15.0	0.995	7.0	1.72	1.46	6.84	6.53	12.3	1.49	246	10.1	248	12.1	0.07	0.276	251	13.2	0.46	0.190
101186	SFBA	Y	15.0	0.995	13.0	1.66	1.50	6.46	6.06	11.6	1.52	223	10.5	220	10.4	0.00	0.288	220	10.4	0.00	0.288
101187	SFBA	Y	15.0	0.995	2.7	1.90	1.38	7.73	7.12	13.0	1.58	288	9.2	291	11.5	0.06	0.276	295	12.6	0.45	0.192
101188	SFBA	Y	15.0	0.995	4.3	1.88	1.42	7.26	6.60	12.2	1.54	264	10.2	264	10.8	0.02	0.284	265	11.0	0.11	0.260
101198	LAB	Y	15.9	0.996	0.4	0.891	1.34	3.63	4.67	10.3	1.36	-	-	81	10.6	0.11	0.281	82	11.0	0.33	0.212
101199	LAB	Y	15.9	0.996	6.6	1.49	1.51	6.01	5.77	11.2	1.42	204	11.8	204	11.8	0.00	0.288	204	11.9	0.03	0.281
101200	LAB	Y	15.9	0.996	0.0	0.966	1.36	3.97	4.87	10.4	1.39	-	-	98	10.3	0.05	0.284	99	10.5	0.16	0.249
101201	LAB	Y	15.9	0.996	1.0	1.10	1.10	3.77	4.68	10.3	1.32	90	11.0	90	11.4	0.09	0.282	91	11.9	0.35	0.209
101202	SFBA	Y	15.2	0.982	31.2	0.973	1.62	3.58	4.84	9.97	1.36	82	9.5	84	11.5	0.31	0.264	85	12.2	0.94	0.123
101203	SFBA	Y	15.2	0.982	3.6	1.15	1.24	3.97	5.14	10.6	1.40	100	8.6	102	11.0	0.27	0.264	105	12.0	0.98	0.117
101204	SFBA	Y	15.7	0.995	10.5	1.14	1.49	5.39	5.65	10.9	1.41	173	10.9	174	12.2	0.08	0.278	175	12.6	0.35	0.209
101205	SFBA	Y	15.7	0.995	13.1	1.64	1.50	6.62	6.84	12.7	1.60	-	-	232	10.5	0.11	0.268	237	11.9	0.72	0.150
101208	NCV	N	16.0	0.998	1.4	6.88	0.493	2.20	3.64	7.91	1.09	15	15.5	16	17.0	0.81	0.251	17	17.3	1.92	0.055
101209	NCV	N	16.5	0.998	0.1	7.64	0.484	2.25	3.51	7.97	1.11	17	15.9	16	15.8	0.00	0.288	16	15.8	0.00	0.288
101210	NCV	N	16.0	0.998	0.3	1.75	1.28	4.68	4.89	10.0	1.34	137	13.0	131	12.7	0.00	0.288	131	12.7	0.00	0.288
101211	NCV	N	16.0	0.998	0.0	6.16	0.498	2.23	3.55	7.96	1.12	16	15.5	15	15.5	0.00	0.288	15	15.4	0.00	0.288
101212	NCV	N	16.0	0.998	0.2	3.34	0.562	2.24	3.43	7.89	1.16	-	-	-	-	-	-	-	-	-	-
101213	NCV	N	16.0	0.998	2.3	1.50	0.772	2.29	3.58	8.17	1.11	19	15.4	18	15.3	0.00	0.288	18	15.3	0.00	0.288
101214	NCV	N	16.0	0.998	0.0	4.53	0.536	2.03	3.35	7.62	1.09	7	16.6	6	16.5	0.00	0.288	6	16.5	0.00	0.288
101215	NCV	N	16.0	0.998	0.1	8.75	0.449	2.09	2.81	7.83	1.09	-	-	-	-	-	-	-	-	-	-
101216	NCV	N	16.0	0.998	0.1	16.2	0.432	2.00	4.70	7.39	1.07	-	-	-	-	-	-	-	-	-	-

Table S2. Measured data and model results for all 905 samples.

Sample Number	Region[a]	AR area[b]	MAAT[c] (ºC)	Atmo. pres.[d] (atm)	^{3}H (piC/L)[e]	^{4}He (x 10^{-7})[ef]	^{3}He/^{4}He (x 10^{-6})[e]	Ne (x 10^{-7})[f]	Ar (x 10^{-4})[f]	Kr (x 10^{-8})[f]	Xe (x 10^{-8})[f]	ΔNe_{UA} (%)	NGT_{UA} (ºC)	ΔNe_{CE} (%)	NGT_{CE} (ºC)	CE *F* value	$L_{ex,CE}$[g]	ΔNe_{PR} (%)	NGT_{PR} (ºC)	PR *R* value	$L_{ex,PR}$[g]
101217	NCV	N	16.0	0.998	0.1	7.12	0.532	2.07	3.41	7.67	1.08	9	16.5	8	16.4	0.00	0.288	8	16.4	0.00	0.288
101218	NCV	N	16.5	0.998	9.6	0.707	1.48	2.95	3.85	8.57	1.15	53	15.7	50	15.4	0.00	0.288	50	15.4	0.00	0.288
101219	NCV	N	16.5	0.998	4.4	0.653	1.21	2.05	3.27	7.80	1.05	8	17.3	7	17.2	0.00	0.288	7	17.2	0.00	0.288
101220	NCV	N	16.5	0.998	4.7	11.6	0.657	2.49	3.63	8.13	1.11	30	16.1	29	15.9	0.00	0.288	29	15.9	0.00	0.288
101221	NCV	N	16.5	0.998	8.8	9.56	0.690	2.27	3.55	8.10	1.10	18	15.7	18	15.6	0.00	0.288	18	15.6	0.00	0.288
101222	NCV	N	16.5	0.998	21.1	3.39	0.867	1.97	3.39	7.92	1.05	3	16.2	4	17.4	0.96	0.240	8	21.8	4.73	0.006
101223	NCV	N	16.5	0.998	2.9	5.00	0.818	2.36	3.89	8.88	1.27	19	11.6	18	11.6	0.00	0.288	18	11.5	0.00	0.288
101224	NCV	N	16.5	0.998	12.6	1.13	0.979	1.90	3.32	7.58	1.07	0	16.5	0	16.5	0.00	0.288	0	16.5	0.00	0.288
101225	NCV	N	16.5	0.998	0.2	15.0	0.716	2.48	3.97	8.65	1.28	26	11.9	25	11.9	0.00	0.288	25	11.9	0.00	0.288
101226	NCV	N	16.0	0.998	0.5	5.10	0.764	2.08	3.60	8.07	1.17	7	14.0	7	14.0	0.00	0.288	7	14.0	0.00	0.288
101227	NCV	N	16.5	0.998	0.4	13.0	0.709	2.31	3.95	8.99	1.34	15	10.5	14	10.4	0.00	0.288	14	10.3	0.00	0.288
101228	NCV	N	16.5	0.998	0.3	9.01	0.714	2.30	3.77	8.59	1.23	17	12.6	16	12.5	0.00	0.288	16	12.4	0.00	0.288
101229	NCV	N	16.0	0.998	0.6	4.37	0.792	2.09	3.33	7.40	1.06	11	17.6	10	17.4	0.00	0.288	10	17.4	0.00	0.288
101230	NCV	N	16.0	0.998	2.1	2.66	0.928	2.29	3.45	7.78	1.09	20	16.9	19	16.7	0.00	0.288	19	16.7	0.00	0.288
101231	NCV	N	16.0	0.998	1.6	2.75	0.897	2.12	3.37	7.43	1.05	12	17.6	11	17.4	0.00	0.288	11	17.3	0.00	0.288
101232	NCV	N	16.0	0.998	0.0	3.10	0.836	2.03	3.23	7.13	1.02	8	18.8	7	18.5	0.00	0.288	7	18.5	0.00	0.288
101234	NCV	N	16.0	0.998	0.1	5.49	0.753	2.10	3.29	7.15	1.05	12	18.5	11	18.1	0.00	0.288	11	18.1	0.00	0.288
101235	NCV	N	16.0	0.998	16.9	6.18	0.716	3.44	4.86	10.2	1.45	69	8.3	70	9.5	0.31	0.267	71	9.8	0.68	0.153
101236	NCV	N	16.0	0.998	3.5	25.4	0.482	2.19	3.62	8.37	1.12	13	14.5	14	15.0	0.76	0.263	15	16.4	2.21	0.042
101237	NCV	N	16.0	0.998	0.0	15.7	0.511	4.35	5.09	9.89	1.22	-	-	130	17.3	0.25	0.265	135	19.4	1.14	0.109
101238	NCV	N	16.0	0.998	0.4	23.0	0.483	2.51	3.81	8.65	1.14	30	14.2	30	14.7	0.44	0.274	30	15.3	0.89	0.131
101239	NCV	N	16.0	0.998	2.4	13.4	0.477	2.38	3.61	7.82	1.12	25	16.0	23	15.9	0.00	0.288	23	15.8	0.00	0.288
101240	NCV	N	16.0	0.998	0.2	22.9	0.505	3.49	4.79	9.57	1.23	-	-	84	16.7	0.42	0.255	88	18.9	1.71	0.067
101241	NCV	N	16.0	0.998	4.0	13.9	0.483	2.63	4.04	8.61	1.21	35	13.0	36	14.2	0.55	0.263	36	14.4	0.99	0.120
101242	NCV	N	16.0	0.998	4.1	17.9	0.480	2.32	3.64	7.92	1.14	21	15.3	20	15.3	0.00	0.288	20	15.2	0.00	0.288
101243	NCV	N	16.0	0.998	1.4	14.4	0.462	2.58	3.88	8.65	1.17	33	13.8	33	14.2	0.34	0.278	33	14.4	0.51	0.183
101248	NCV	N	16.0	0.998	0.2	8.90	0.585	2.06	3.35	7.70	1.04	9	17.2	8	17.2	0.00	0.288	9	17.2	0.00	0.288
101249	NCV	N	16.5	0.998	2.2	3.73	0.654	2.20	3.39	7.62	1.03	17	17.8	16	17.7	0.00	0.288	16	17.7	0.00	0.288
101250	NCV	N	16.5	0.998	3.3	0.962	0.922	2.01	3.26	7.43	1.03	7	18.0	6	17.9	0.00	0.288	6	17.9	0.00	0.288
101251	NCV	N	16.5	0.998	1.7	4.21	0.513	1.91	3.23	7.37	1.00	2	18.3	2	18.3	0.00	0.288	2	18.3	0.00	0.288
101252	NCV	N	16.5	0.998	1.4	0.481	1.33	1.98	3.26	7.17	0.973	6	19.1	7	19.9	0.92	0.251	7	20.1	2.15	0.047
101253	NCV	N	16.5	0.998	1.9	0.463	1.35	1.96	3.23	7.13	0.969	6	19.3	6	19.7	0.91	0.258	6	19.9	1.72	0.067
101254	NCV	N	16.5	0.998	0.2	1.87	0.524	2.00	3.26	7.38	0.963	8	19.0	10	22.0	0.91	0.245	12	24.3	3.91	0.012
101255	NCV	N	16.5	0.998	1.0	4.92	0.474	2.05	3.29	7.39	0.982	10	18.8	10	19.1	0.77	0.270	11	19.7	1.57	0.076
101256	NCV	N	16.5	0.998	1.5	14.9	0.410	2.06	3.40	7.62	1.09	8	16.4	8	16.4	0.00	0.288	8	16.4	0.00	0.288
101257	NCV	N	16.5	0.998	0.1	29.2	0.429	2.54	3.64	7.86	1.14	33	16.2	31	16.0	0.00	0.288	31	16.0	0.00	0.288
101258	SFBA	Y	15.6	0.989	2.4	1.25	1.48	5.01	5.13	10.5	1.33	157	12.6	156	12.6	0.00	0.288	156	12.6	0.00	0.288
101259	SFBA	Y	15.6	0.989	10.3	1.01	1.63	4.22	4.63	9.85	1.31	115	12.9	110	12.6	0.00	0.288	110	12.6	0.00	0.288
101260	SFBA	Y	15.6	0.989	5.4	1.15	1.67	4.27	5.02	10.0	1.32	119	11.4	120	13.0	0.17	0.273	121	13.6	0.57	0.173
101261	SFBA	Y	15.6	0.989	10.2	1.05	1.63	4.13	4.83	9.95	1.29	112	12.1	113	13.1	0.13	0.277	114	13.6	0.44	0.194
101262	SFBA	Y	15.6	0.989	9.6	1.28	1.44	5.19	5.14	10.5	1.34	166	13.0	161	12.7	0.00	0.288	162	12.8	0.00	0.288
101263	SFBA	Y	15.6	0.989	12.2	1.30	1.50	5.27	5.38	10.6	1.34	172	12.4	172	13.2	0.05	0.282	173	13.6	0.24	0.232
101264	SFBA	Y	15.6	0.989	14.2	1.08	1.62	4.47	4.94	9.88	1.31	130	12.7	130	13.1	0.05	0.284	131	13.2	0.15	0.252
101265	SFBA	Y	15.7	0.995	13.0	0.615	1.38	2.54	3.75	8.38	1.13	33	15.0	33	15.0	0.03	0.288	33	15.1	0.12	0.258
101266	SFBA	Y	15.7	0.995	0.0	45.7	0.543	1.97	3.61	8.34	1.20	1	12.8	1	12.8	0.00	0.288	1	12.8	0.00	0.288

Table S2. Measured data and model results for all 905 samples.

Sample Number	Region[a]	AR area[b]	MAAT[c] (ºC)	Atmo. pres.[d] (atm)	^{3}H (piC/L)[e]	^{4}He (x 10^{-7})[ef]	^{3}He/^{4}He (x 10^{-6})[e]	Ne (x 10^{-7})[f]	Ar (x 10^{-4})[f]	Kr (x 10^{-8})[f]	Xe (x 10^{-8})[f]	ΔNe_{UA} (%)	NGT_{UA} (ºC)	ΔNe_{CE} (%)	NGT_{CE} (ºC)	CE *F* value	$L_{ex,CE}$[g]	ΔNe_{PR} (%)	NGT_{PR} (ºC)	PR *R* value	$L_{ex,PR}$[g]
101267	SFBA	Y	15.7	0.995	12.6	1.29	1.31	4.20	6.16	9.33	1.20	-	-	-	-	-	-	-	-	-	-
101268	SFBA	Y	15.6	0.989	8.8	1.37	1.74	4.97	7.18	10.7	1.34	-	-	-	-	-	-	-	-	-	-
101269	SFBA	Y	15.6	0.989	12.2	1.69	1.39	6.27	8.14	11.0	1.41	-	-	-	-	-	-	-	-	-	-
101271	SFBA	Y	15.6	0.989	22.6	3.26	5.06	4.03	6.30	9.66	1.30	-	-	-	-	-	-	-	-	-	-
101272	SFBA	Y	15.6	0.989	11.6	1.14	1.88	4.18	6.20	9.33	1.27	-	-	-	-	-	-	-	-	-	-
101274	NCV	N	16.5	0.992	1.7	11.3	0.244	2.54	3.53	7.78	0.984	37	18.8	38	19.6	0.42	0.274	39	20.6	0.99	0.125
101275	NCV	N	16.5	0.992	26.2	15.2	0.320	6.19	5.86	10.7	1.27	229	15.0	231	17.7	0.09	0.276	235	19.1	0.54	0.182
101277	NCV	N	16.0	0.998	2.9	6.32	0.472	2.16	3.57	8.18	1.05	14	15.8	17	20.2	0.85	0.243	21	24.1	3.85	0.013
101278	NCV	N	16.0	0.998	1.7	12.6	0.477	2.87	4.22	9.44	1.16	-	-	50	16.2	0.56	0.253	56	20.8	2.41	0.038
101279	NCV	N	16.0	0.998	0.3	5.23	0.526	2.56	3.85	8.54	1.14	33	14.4	33	15.3	0.51	0.268	34	15.9	1.06	0.113
101280	NCV	N	16.0	0.998	0.3	11.6	0.452	2.34	3.56	7.92	1.09	23	16.4	22	16.4	0.00	0.288	22	16.3	0.00	0.288
101281	NCV	N	16.0	0.998	2.8	4.27	0.730	4.15	6.01	12.5	1.71	-	-	99	6.2	0.35	0.251	102	7.6	1.44	0.073
101282	NCV	N	16.0	0.998	1.8	14.5	0.486	2.98	4.32	9.34	1.26	51	11.6	52	13.0	0.42	0.265	53	13.7	1.03	0.114
101283	NCV	N	16.0	0.998	0.2	13.4	0.460	2.55	3.85	8.48	1.15	32	14.3	32	15.1	0.49	0.269	33	15.5	0.88	0.133
101284	NCV	N	16.0	0.998	1.3	19.7	0.480	2.95	4.38	9.50	1.29	48	10.8	49	12.2	0.46	0.262	50	12.9	1.13	0.104
101285	NCV	N	16.0	0.998	2.6	3.15	0.883	2.65	3.86	8.52	1.15	37	14.6	38	15.0	0.32	0.277	38	15.3	0.51	0.184
101286	NCV	N	16.0	0.998	2.3	3.63	0.820	2.49	3.65	7.95	1.11	31	16.3	30	16.2	0.00	0.288	30	16.2	0.00	0.288
101287	SCV	N	15.6	0.998	14.4	1.96	1.94	2.45	3.98	8.19	1.20	-	-	28	14.9	0.68	0.255	-	-	-	-
101288	SCV	N	15.6	0.998	21.9	4.41	2.10	2.27	3.84	8.03	1.13	-	-	20	17.0	0.80	0.246	20	16.6	2.04	0.049
101289	SCV	N	15.6	0.998	29.5	1.17	2.90	2.43	3.81	7.69	1.11	-	-	-	-	-	-	-	-	-	-
101290	SCV	N	15.6	0.998	11.6	-	-	2.39	3.84	7.77	1.11	-	-	-	-	-	-	-	-	-	-
101291	SCV	N	15.6	0.998	26.0	1.14	2.49	2.53	3.93	8.01	1.14	32	14.7	33	16.6	0.64	0.257	-	-	-	-
101292	SCV	N	15.6	0.998	16.6	1.25	1.95	2.41	3.94	8.10	1.17	25	13.7	26	15.5	0.71	0.253	-	-	-	-
101293	SCV	N	15.8	0.999	4.0	1.70	1.70	2.55	4.13	8.84	1.19	-	-	33	16.1	0.70	0.247	35	17.0	2.28	0.040
101294	SCV	N	15.8	0.999	1.6	1.10	1.57	2.45	4.01	8.15	1.20	-	-	-	-	-	-	-	-	-	-
101295	SCV	N	15.8	0.999	1.0	3.88	0.918	2.52	3.98	8.63	1.19	30	13.1	30	14.5	0.63	0.258	31	15.0	1.36	0.087
101296	SCV	N	15.8	0.999	7.4	0.770	1.73	3.13	4.45	9.33	1.28	59	11.5	60	13.2	0.40	0.264	61	13.8	0.98	0.119
101297	SCV	N	15.8	0.999	18.7	0.844	2.18	3.44	4.80	9.78	1.32	-	-	76	13.2	0.40	0.258	78	14.2	1.27	0.093
101298	SCV	N	15.8	0.999	13.2	0.836	1.87	3.24	4.66	9.40	1.28	-	-	68	14.4	0.46	0.256	69	15.3	1.43	0.081
101299	SCV	N	15.8	0.999	3.2	0.915	1.64	2.72	4.16	8.68	1.20	40	12.9	41	14.9	0.57	0.257	42	15.3	1.34	0.088
101300	SCV	N	15.8	0.999	2.9	0.837	1.53	2.79	4.31	9.00	1.23	-	-	45	14.9	0.59	0.252	46	15.7	1.72	0.063
101301	SCV	N	15.8	0.999	9.8	1.27	2.04	2.94	4.40	9.11	1.27	49	11.5	51	13.7	0.51	0.257	52	14.2	1.27	0.092
101302	SCV	N	15.8	0.999	2.1	0.823	1.93	3.38	4.71	9.77	1.30	-	-	73	13.3	0.40	0.259	75	14.4	1.29	0.091
101303	SCV	N	15.8	0.999	1.0	0.868	1.44	2.81	4.29	9.11	1.23	43	11.9	45	14.5	0.58	0.254	47	15.5	1.67	0.066
101304	SCV	N	16.4	0.999	19.7	3.54	1.47	11.4	8.76	13.7	1.58	496	14.4	500	17.0	0.03	0.281	505	17.5	0.24	0.235
101305	SCV	N	16.4	0.999	0.3	4.67	1.56	2.29	3.67	8.05	1.10	20	15.4	20	16.5	0.73	0.258	21	17.0	1.50	0.078
101306	SCV	N	15.8	0.999	0.8	2.87	1.56	2.99	4.22	9.06	1.18	54	13.4	56	15.4	0.45	0.263	57	16.7	1.31	0.092
101307	SCV	N	16.4	0.999	0.4	9.32	0.906	7.02	6.20	11.3	1.31	269	15.4	271	17.2	0.05	0.280	274	18.2	0.35	0.213
101308	SCV	N	16.4	0.999	0.2	17.4	0.690	2.15	3.39	7.65	1.02	14	17.7	14	17.8	0.30	0.285	15	18.0	0.46	0.195
101309	SCV	N	16.4	0.999	0.1	3.94	0.924	2.22	3.62	7.79	1.05	18	16.5	19	19.1	0.81	0.248	20	19.5	2.33	0.040
101310	SCV	N	16.4	0.999	0.5	16.8	0.672	2.34	3.55	8.04	1.02	24	17.3	25	18.5	0.67	0.262	27	21.3	2.28	0.043
101311	SCV	N	16.4	0.999	0.0	6.95	0.863	2.18	3.61	8.00	1.05	15	16.0	18	20.0	0.84	0.244	18	20.4	3.01	0.023
101312	SCV	N	16.4	0.999	0.7	15.6	0.673	2.25	3.57	7.87	1.05	19	16.6	19	17.7	0.74	0.259	20	18.4	1.68	0.068
101313	SCV	N	16.4	0.999	0.2	14.2	0.702	2.23	3.55	7.79	1.07	17	16.5	18	17.1	0.71	0.264	18	17.4	1.10	0.111
101314	SCV	N	16.4	0.999	15.8	3.71	1.40	2.29	3.67	7.96	1.06	21	16.0	22	18.5	0.77	0.250	23	19.3	2.26	0.042

Table S2. Measured data and model results for all 905 samples.

Sample Number	Region[a]	AR area[b]	MAAT[c] (ºC)	Atmo. pres.[d] (atm)	^{3}H (piC/L)[e]	^{4}He (x 10^{-7})[ef]	^{3}He/^{4}He (x 10^{-6})[e]	Ne (x 10^{-7})[f]	Ar (x 10^{-4})[f]	Kr (x 10^{-8})[f]	Xe (x 10^{-8})[f]	ΔNe_{UA} (%)	NGT_{UA} (ºC)	ΔNe_{CE} (%)	NGT_{CE} (ºC)	CE *F* value	$L_{ex,CE}$[g]	ΔNe_{PR} (%)	NGT_{PR} (ºC)	PR *R* value	$L_{ex,PR}$[g]
101315	SCV	N	16.4	0.999	0.8	10.1	1.06	2.66	4.10	8.54	1.12	-	-	43	19.1	0.65	0.249	45	20.3	2.28	0.042
101316	SCV	N	16.4	0.999	27.0	3.27	1.49	2.24	3.63	7.67	1.04	19	16.7	21	19.2	0.79	0.249	21	19.3	2.09	0.049
101317	SCV	N	16.4	0.999	4.8	7.45	1.18	1.81	3.15	6.96	0.965	0	19.6	0	19.6	0.00	-	0	19.6	0.00	-
101318	SCV	N	16.4	0.999	16.9	1.47	1.98	2.18	3.52	7.48	1.01	17	17.8	19	20.6	0.82	0.249	19	20.7	2.30	0.042
101320	SCV	N	16.4	0.999	22.7	4.25	1.54	2.43	3.70	7.91	1.09	28	16.1	28	17.1	0.59	0.265	29	17.3	0.96	0.126
101321	SCV	N	16.4	0.999	23.9	1.68	2.18	2.42	3.72	8.42	1.13	25	14.7	25	14.9	0.30	0.281	26	15.1	0.46	0.192
101322	SCV	N	16.4	0.999	16.7	2.82	1.74	2.33	3.66	8.48	1.14	20	14.5	20	14.5	0.00	0.288	20	14.6	0.10	0.263
101323	SCV	N	16.4	0.999	28.6	1.18	2.71	2.58	3.75	8.21	1.07	36	16.3	36	17.3	0.50	0.268	37	18.2	1.14	0.108
101324	SCV	N	16.4	0.999	36.7	0.872	2.86	2.51	3.71	8.38	1.10	31	15.6	32	16.0	0.36	0.278	32	16.5	0.72	0.154
101325	SCV	N	16.4	0.999	5.9	2.28	1.59	2.23	3.54	8.04	1.05	17	16.4	18	17.1	0.72	0.263	19	18.6	1.99	0.052
101326	SCV	N	16.4	0.999	48.2	1.19	3.17	2.42	3.68	8.34	1.11	26	15.3	26	15.6	0.36	0.279	26	16.0	0.64	0.164
101327	SCV	N	16.4	0.999	13.0	2.18	1.72	2.44	3.70	8.57	1.11	27	15.0	27	15.3	0.40	0.277	27	16.2	1.02	0.118
101328	SCV	N	16.4	0.999	3.2	3.13	0.912	2.46	3.81	8.65	1.18	26	13.7	26	13.8	0.18	0.284	26	13.9	0.29	0.222
101329	SCV	N	16.4	0.999	3.2	1.75	1.05	2.93	4.16	9.17	1.19	50	13.1	51	14.5	0.42	0.266	53	15.6	1.15	0.104
101330	SCV	N	16.4	0.999	3.1	2.22	1.01	3.06	4.26	9.37	1.28	54	11.9	55	12.1	0.11	0.283	55	12.2	0.21	0.239
101331	SCV	N	16.4	0.999	2.1	4.44	0.803	2.85	3.96	8.68	1.17	47	14.4	47	14.4	0.00	0.288	47	14.5	0.04	0.277
101332	SCV	N	16.4	0.999	12.1	20.6	0.719	2.48	3.88	8.53	1.19	27	13.5	28	14.0	0.50	0.271	28	14.1	0.63	0.164
101333	SCV	N	16.4	0.999	13.8	5.79	0.906	2.41	3.81	8.48	1.15	24	14.0	25	14.7	0.62	0.265	25	15.2	1.15	0.104
101334	SCV	N	15.8	0.999	20.3	0.981	2.52	2.92	4.27	9.28	1.27	48	11.6	49	12.6	0.40	0.268	49	13.1	0.83	0.137
101335	SCV	N	15.8	0.999	2.8	0.858	1.61	2.83	4.23	9.48	1.32	42	10.7	42	10.9	0.17	0.282	42	11.0	0.23	0.233
101336	SCV	N	15.8	0.999	0.5	6.94	0.829	2.63	4.14	9.60	1.32	31	10.3	31	10.4	0.09	0.286	31	10.6	0.28	0.223
101337	SCV	N	15.8	0.999	9.8	0.716	2.26	2.73	4.19	9.68	1.31	36	10.4	36	10.5	0.21	0.281	36	10.9	0.44	0.192
101338	SCV	N	15.8	0.999	1.8	0.729	1.47	2.99	4.39	9.93	1.34	49	9.9	49	10.5	0.29	0.275	49	10.9	0.63	0.162
101339	SCV	N	15.8	0.999	12.3	0.877	1.71	3.66	4.81	10.5	1.38	82	9.5	83	10.5	0.22	0.272	84	11.4	0.70	0.152
101340	SCV	N	15.8	0.999	32.0	0.783	3.54	3.12	4.37	9.61	1.30	57	11.1	57	11.8	0.25	0.275	58	12.1	0.53	0.178
101341	SCV	N	15.8	0.999	1.1	3.94	1.59	2.51	3.98	9.30	1.24	27	11.7	27	12.0	0.46	0.274	27	12.8	1.05	0.112
101342	SCV	N	15.8	0.999	0.4	3.36	1.19	2.61	4.11	9.36	1.26	32	11.3	32	12.2	0.55	0.264	33	13.1	1.32	0.088
101343	SCV	N	15.8	0.999	0.2	0.942	1.42	2.75	4.22	9.68	1.28	38	10.7	39	11.7	0.49	0.264	40	12.8	1.32	0.087
101344	SCV	N	16.4	0.999	1.0	3.67	1.01	2.59	4.12	9.43	1.27	30	11.0	31	11.8	0.56	0.263	32	12.8	1.35	0.085
101345	SCV	N	15.8	0.999	0.9	1.16	1.37	2.77	4.23	9.62	1.29	38	10.6	39	11.3	0.43	0.269	40	12.0	0.95	0.121
101346	SCV	N	15.8	0.999	6.9	3.17	0.942	2.62	4.12	9.31	1.28	32	11.1	32	11.7	0.49	0.268	33	12.2	0.92	0.124
101347	SCV	N	15.8	0.999	15.6	1.55	1.50	2.69	4.05	9.18	1.17	38	13.0	39	14.8	0.58	0.258	42	17.4	2.00	0.051
101348	SCV	N	15.8	0.999	19.2	0.704	2.65	3.04	4.29	9.46	1.20	56	12.6	57	14.6	0.44	0.262	60	16.6	1.49	0.078
101349	SCV	N	15.8	0.999	43.9	0.810	4.51	3.30	4.40	9.66	1.24	68	12.3	69	13.5	0.29	0.271	70	14.6	0.87	0.132
101350	SCV	N	15.8	0.999	31.3	0.796	3.39	3.21	4.44	9.76	1.26	63	11.6	64	13.2	0.37	0.265	66	14.5	1.16	0.103
101351	SCV	N	15.8	0.999	25.8	0.842	3.18	3.42	4.57	9.85	1.25	74	11.8	76	14.0	0.35	0.264	78	15.8	1.26	0.095
101352	SCV	N	15.8	0.999	14.5	0.722	2.01	2.97	4.20	9.29	1.20	52	12.8	53	14.2	0.40	0.266	55	15.4	1.15	0.104
101353	SCV	N	15.8	0.999	0.1	4.77	1.00	2.62	4.05	9.26	1.27	32	11.5	32	11.6	0.22	0.282	32	11.8	0.36	0.208
101354	SCV	N	16.4	0.999	32.5	1.70	2.32	2.50	3.79	8.68	1.13	30	14.5	30	15.2	0.51	0.270	31	16.3	1.30	0.092
101355	SCV	N	16.4	0.999	21.9	1.65	2.00	2.46	3.75	8.45	1.13	28	14.7	28	15.0	0.34	0.279	28	15.3	0.54	0.178
101356	MDB	N	16.0	0.896	0.4	2.98	0.454	2.96	4.13	8.98	1.20	65	10.1	66	11.3	0.32	0.268	67	12.1	0.87	0.131
101357	MDB	N	16.0	0.896	0.1	1.94	0.582	2.91	4.08	8.77	1.18	63	10.6	64	12.1	0.36	0.265	66	12.9	0.98	0.119
101358	MDB	N	16.0	0.896	0.1	6.42	0.269	2.66	3.76	8.14	1.09	52	12.9	53	14.0	0.37	0.269	54	14.6	0.85	0.136
101359	MDB	N	16.0	0.896	0.2	2.47	0.498	2.99	4.14	9.08	1.21	66	9.8	67	10.9	0.30	0.269	68	11.6	0.81	0.137
101360	MDB	N	16.0	0.896	0.2	5.58	0.308	2.95	4.13	8.91	1.20	64	10.0	65	11.3	0.33	0.267	66	11.9	0.86	0.131

Table S2. Measured data and model results for all 905 samples.

Sample Number	Region[a]	AR area[b]	MAAT[c] (ºC)	Atmo. pres.[d] (atm)	^{3}H (piC/L)[e]	^{4}He (x 10^{-7})[ef]	^{3}He/^{4}He (x 10^{-6})[e]	Ne (x 10^{-7})[f]	Ar (x 10^{-4})[f]	Kr (x 10^{-8})[f]	Xe (x 10^{-8})[f]	ΔNe_{UA} (%)	NGT_{UA} (ºC)	ΔNe_{CE} (%)	NGT_{CE} (ºC)	CE *F* value	$L_{ex,CE}$[g]	ΔNe_{PR} (%)	NGT_{PR} (ºC)	PR *R* value	$L_{ex,PR}$[g]
101361	MDB	N	16.0	0.896	0.2	5.88	1.26	17.8	9.07	15.3	1.64	-	-	-	-	-	-	-	-	-	-
101362	MDB	N	16.0	0.896	1.3	17.7	0.184	2.05	3.39	7.42	1.05	18	13.7	18	14.6	0.74	0.258	19	14.7	1.20	0.099
101363	MDB	N	16.0	0.896	0.3	149.2	0.156	2.42	3.66	8.20	1.08	38	12.4	38	13.6	0.53	0.262	40	14.8	1.39	0.084
101364	MDB	N	16.0	0.898	1.4	6.75	0.297	2.91	4.16	9.20	1.21	61	9.5	62	11.0	0.38	0.264	64	12.1	1.15	0.101
101365	MDB	N	16.0	0.896	0.3	3.70	0.345	2.54	3.66	7.96	1.10	45	12.8	45	13.1	0.21	0.281	45	13.2	0.24	0.232
101366	MDB	N	16.0	0.898	12.9	0.737	1.59	2.86	4.05	8.38	1.20	60	10.8	61	11.8	0.31	0.270	61	11.8	0.51	0.181
101367	MDB	N	16.0	0.896	5.9	0.890	1.37	3.74	4.81	9.33	1.23	-	-	114	13.6	0.30	0.259	118	15.1	1.25	0.095
101368	MDB	N	16.0	0.898	0.7	4.37	0.375	3.07	4.30	9.22	1.24	70	9.1	71	10.7	0.34	0.264	72	11.6	1.00	0.115
101369	MDB	N	16.0	0.896	0.3	2.06	0.474	2.36	3.46	7.63	1.01	37	14.8	37	15.6	0.44	0.271	38	16.2	0.91	0.130
101370	MDB	N	16.0	0.896	1.7	0.133	3.31	2.49	3.78	8.28	1.14	40	11.3	41	12.3	0.47	0.265	42	12.8	0.94	0.123
101371	MDB	N	16.0	0.896	1.5	1.18	0.763	2.27	3.51	7.76	1.05	31	13.5	31	14.5	0.57	0.264	32	15.1	1.20	0.100
101372	MDB	N	16.0	0.898	0.4	31.3	0.185	2.51	3.66	7.83	1.04	45	13.9	46	15.6	0.51	0.262	47	16.6	1.30	0.092
101373	MDB	N	16.0	0.898	0.2	0.916	1.46	3.77	4.80	9.69	1.33	106	8.1	108	10.0	0.23	0.267	110	10.5	0.74	0.145
101374	MDB	N	16.0	0.898	0.2	148.6	0.191	2.36	3.64	8.01	1.12	34	12.1	34	12.6	0.40	0.274	34	12.7	0.52	0.180
101375	MDB	N	16.0	0.896	4.7	0.935	1.21	2.90	4.18	9.13	1.23	60	9.2	62	10.6	0.38	0.264	63	11.5	1.06	0.109
101376	MDB	N	16.0	0.896	0.0	0.914	1.13	2.98	4.23	9.23	1.22	65	9.3	67	11.2	0.39	0.261	69	12.5	1.24	0.094
101377	MDB	N	16.0	0.896	0.2	1.41	0.637	2.51	3.52	7.50	1.05	45	14.7	45	14.7	0.00	0.288	45	14.7	0.00	0.288
101378	MDB	N	16.0	0.896	0.5	1.22	0.774	2.58	3.82	8.15	1.10	47	12.2	49	14.2	0.50	0.259	50	15.0	1.33	0.089
101379	MDB	N	16.0	0.896	10.1	0.689	1.42	2.96	4.30	9.50	1.26	62	8.2	64	10.1	0.41	0.259	66	11.5	1.33	0.085
101380	MDB	N	16.0	0.896	1.2	0.672	1.29	2.58	3.79	8.33	1.10	47	12.1	48	13.7	0.48	0.262	49	14.9	1.34	0.088
101381	MDB	N	16.0	0.896	6.2	0.797	1.72	3.30	4.52	9.71	1.33	79	7.4	80	8.6	0.26	0.269	81	9.1	0.69	0.150
101383	MDB	N	16.0	0.896	0.2	0.713	1.33	2.89	3.87	8.25	1.11	65	12.8	66	13.6	0.23	0.276	66	13.9	0.49	0.185
101384	MDB	N	16.0	0.898	0.3	22.9	0.191	1.91	2.93	6.50	0.872	15	19.7	14	19.6	0.00	0.288	15	19.6	0.00	0.288
101385	MDB	N	16.0	0.896	0.9	0.875	1.11	2.88	3.91	8.28	1.11	64	12.6	65	13.8	0.32	0.270	66	14.4	0.76	0.146
101386	MDB	N	16.0	0.896	0.1	0.791	1.16	2.64	3.62	7.91	1.04	53	14.4	53	14.9	0.25	0.277	53	15.4	0.54	0.179
101387	MDB	N	16.0	0.896	0.4	0.717	1.32	2.90	3.95	8.42	1.10	66	12.5	67	14.2	0.36	0.266	68	15.2	1.05	0.114
101388	MDB	N	16.0	0.896	0.1	0.933	0.782	2.23	3.27	7.08	0.973	31	16.6	31	16.6	0.08	0.287	31	16.6	0.01	0.287
101389	SCV	N	16.4	0.999	3.1	9.70	1.08	2.28	3.60	7.46	1.09	21	16.6	21	17.1	0.60	0.271	-	-	-	-
101390	SCV	N	16.4	0.999	0.0	14.3	0.904	2.31	3.66	7.62	1.14	21	15.6	-	-	-	-	-	-	-	-
101391	NCV	N	15.7	0.940	1.7	0.477	1.47	2.02	3.79	8.00	1.20	-	-	-	-	-	-	-	-	-	-
101392	NCV	N	16.5	0.991	6.2	0.695	1.47	2.31	3.42	7.20	1.03	25	18.6	24	18.5	0.00	0.288	23	18.5	0.00	0.288
101393	NCV	N	16.5	0.991	9.2	0.571	1.62	2.28	3.43	7.21	1.05	22	18.1	21	18.0	0.00	0.288	21	17.8	0.00	0.288
101394	NCV	N	16.5	0.991	12.2	0.541	1.86	2.31	3.48	7.17	1.05	24	18.1	-	-	-	-	-	-	-	-
101395	NCV	N	16.5	0.991	9.2	0.670	1.52	2.49	3.59	7.30	1.03	35	18.4	35	19.1	0.43	0.274	35	18.9	0.38	0.208
101396	SFBA	Y	15.2	0.982	0.7	1.79	0.929	4.37	5.40	10.8	1.41	-	-	124	11.5	0.24	0.263	127	12.8	1.00	0.116
101397	SCV	N	17.4	0.987	19.8	1.03	2.35	2.58	3.73	7.71	1.06	38	16.9	39	18.1	0.50	0.267	39	18.2	0.82	0.143
101398	SCV	N	17.4	0.987	4.7	0.677	1.42	2.48	3.69	7.80	1.05	33	16.7	34	18.2	0.59	0.262	35	18.7	1.25	0.099
101399	SCV	N	17.4	0.987	2.4	0.775	1.20	2.53	3.67	7.56	1.01	38	18.0	39	20.1	0.58	0.261	40	20.7	1.36	0.092
101400	SCV	N	17.4	0.987	2.4	0.771	1.19	2.35	3.40	7.22	0.955	29	19.9	29	20.8	0.56	0.270	30	21.2	0.95	0.130
101401	SCV	N	17.4	0.987	12.3	0.919	1.48	3.06	3.92	7.94	1.08	65	17.4	65	18.1	0.20	0.279	65	18.1	0.30	0.223
101402	SCV	N	17.4	0.987	2.4	0.599	1.44	2.50	3.61	7.83	1.02	35	17.5	35	18.4	0.49	0.270	36	19.1	1.02	0.120
101403	SCV	N	17.4	0.987	0.1	1.31	0.812	2.32	3.48	7.57	1.00	25	18.1	26	19.1	0.63	0.266	27	19.8	1.30	0.096
101404	SCV	N	17.4	0.987	6.1	0.694	1.60	2.69	3.73	7.98	1.05	44	17.0	45	17.7	0.34	0.275	45	18.1	0.60	0.171
101405	SCV	N	17.4	0.987	1.8	0.884	1.06	2.60	3.68	8.02	1.03	40	17.2	40	18.4	0.49	0.268	41	19.5	1.22	0.103
101406	SCV	N	17.4	0.987	4.1	0.679	1.52	2.61	3.68	8.06	1.05	39	16.8	40	17.3	0.35	0.276	40	17.8	0.66	0.162

Table S2. Measured data and model results for all 905 samples.

Sample Number	Region[a]	AR area[b]	MAAT[c] (ºC)	Atmo. pres.[d] (atm)	^{3}H (piC/L)[e]	^{4}He (x 10^{-7})[ef]	$^{3}He/^{4}He$ (x 10^{-6})[e]	Ne (x 10^{-7})[f]	Ar (x 10^{-4})[f]	Kr (x 10^{-8})[f]	Xe (x 10^{-8})[f]	ΔNe_{UA} (%)	NGT_{UA} (ºC)	ΔNe_{CE} (%)	NGT_{CE} (ºC)	CE *F* value	$L_{ex,CE}$[g]	ΔNe_{PR} (%)	NGT_{PR} (ºC)	PR *R* value	$L_{ex,PR}$[g]
101407	SCV	N	17.4	0.987	19.3	0.618	2.42	2.47	3.65	8.04	1.05	32	16.4	32	17.5	0.55	0.267	33	18.3	1.24	0.099
101408	SCV	N	17.4	0.987	18.2	0.589	1.75	2.27	3.43	7.52	1.01	23	18.0	23	18.2	0.45	0.278	23	18.4	0.48	0.191
101409	SCV	N	17.4	0.987	14.8	0.890	1.69	2.51	3.86	8.34	1.11	33	14.5	34	16.5	0.64	0.256	35	17.6	1.72	0.065
101410	SCV	N	17.4	0.987	10.6	2.19	0.883	2.38	3.52	7.76	1.02	28	17.6	28	18.1	0.47	0.274	29	18.6	0.81	0.145
101411	SCV	N	17.4	0.987	0.0	3.23	0.634	2.17	3.29	7.11	0.946	19	19.9	19	20.7	0.69	0.267	20	21.1	1.16	0.109
101412	SCV	N	17.4	0.987	2.1	1.31	0.881	2.31	3.40	7.36	0.985	25	19.0	26	19.3	0.45	0.277	26	19.5	0.52	0.185
101413	SCV	N	17.4	0.987	22.2	0.747	2.08	2.79	3.89	8.29	1.05	50	16.5	51	18.9	0.50	0.262	54	20.7	1.58	0.077
101414	SCV	N	17.4	0.987	3.8	4.74	0.635	2.38	3.41	7.33	1.01	29	18.8	27	18.8	0.00	0.288	27	18.7	0.00	0.288
101415	SCV	N	17.4	0.987	16.7	0.583	1.84	2.16	3.58	7.82	1.11	14	15.1	14	15.7	0.75	0.263	14	15.6	0.85	0.136
101416	SCV	N	17.4	0.987	22.3	0.624	3.28	2.54	3.87	8.46	1.11	33	14.4	35	16.4	0.63	0.256	36	17.8	1.81	0.060
101417	SCV	N	17.4	0.987	5.2	0.623	1.61	2.51	3.77	7.95	1.08	34	15.8	35	17.6	0.60	0.260	35	18.1	1.34	0.091
101418	SCV	N	17.4	0.987	6.9	0.753	1.61	2.74	4.07	8.87	1.11	-	-	47	17.5	0.59	0.253	51	20.7	2.29	0.042
101419	SCV	N	17.4	0.987	17.1	0.625	2.35	2.55	3.64	8.19	1.03	37	17.0	37	17.9	0.46	0.271	38	19.3	1.26	0.099
101420	SCV	N	17.4	0.987	2.7	0.848	1.25	2.71	3.98	8.52	1.11	43	14.5	45	16.8	0.55	0.258	47	18.2	1.62	0.072
101421	SCV	N	17.4	0.987	11.2	0.637	2.25	2.55	3.76	8.07	1.07	36	16.0	37	17.5	0.56	0.263	38	18.3	1.31	0.094
101422	SCV	N	17.4	0.987	19.3	0.558	2.24	2.27	3.54	7.89	1.07	20	16.1	21	16.5	0.53	0.275	21	16.7	0.68	0.159
101423	SCV	N	17.4	0.987	11.0	0.676	1.88	2.71	4.34	8.55	1.13	-	-	50	20.6	0.63	0.248	-	-	-	-
101424	SCV	N	17.4	0.987	8.5	0.648	1.64	2.55	3.85	8.30	1.11	35	14.8	36	16.5	0.59	0.260	37	17.4	1.48	0.080
101425	SCV	N	17.4	0.987	4.1	0.708	1.60	2.77	3.95	8.70	1.17	44	13.8	44	14.1	0.24	0.279	45	14.4	0.42	0.199
101426	SCV	N	17.4	0.987	0.1	3.98	0.603	2.15	3.32	7.25	0.940	18	19.6	19	21.3	0.78	0.256	20	22.8	2.29	0.044
101427	SCV	N	17.4	0.987	16.4	0.717	1.52	2.17	3.60	8.22	1.13	13	14.3	14	14.5	0.60	0.276	14	14.7	0.78	0.144
101428	SCV	N	17.4	0.987	46.3	0.631	4.19	2.46	3.78	8.30	1.06	31	15.4	33	18.4	0.69	0.252	35	20.9	2.42	0.038
101429	SCV	N	17.4	0.987	-	0.862	1.68	2.56	4.04	7.59	1.00	-	-	-	-	-	-	-	-	-	-
101430	SCV	N	17.4	0.987	13.3	0.759	1.41	2.83	3.95	8.66	1.10	49	15.0	50	16.5	0.44	0.266	52	17.9	1.27	0.097
101431	SCV	N	17.4	0.987	1.1	3.90	0.596	2.21	3.37	7.66	1.02	18	17.7	18	17.7	0.00	0.288	18	17.7	0.00	0.288
101432	SCV	N	17.4	0.987	9.8	0.638	1.90	2.37	3.43	7.76	1.03	27	17.8	25	17.6	0.00	0.288	26	17.7	0.00	0.288
101433	SCV	N	17.4	0.987	16.1	0.863	1.93	3.30	4.03	8.68	1.12	75	16.1	74	16.0	0.00	0.288	75	16.1	0.00	0.288
101434	SCV	N	17.4	0.987	16.1	0.848	1.83	3.28	4.18	8.43	1.07	77	16.6	78	19.3	0.36	0.266	81	20.7	1.16	0.109
101435	SCV	N	17.4	0.987	23.1	0.739	2.57	2.87	3.94	8.38	1.12	52	15.3	52	16.2	0.33	0.273	53	16.6	0.67	0.161
101436	SCV	N	17.4	0.987	16.7	0.777	2.10	2.81	3.73	8.13	1.06	50	17.2	50	17.3	0.06	0.286	50	17.6	0.19	0.245
101437	SCV	N	17.4	0.987	10.0	0.762	1.92	2.94	4.03	8.62	1.10	56	15.1	57	17.0	0.43	0.265	58	18.3	1.26	0.098
101438	SCV	N	17.4	0.987	24.9	4.24	1.42	15.3	11.4	17.6	1.77	-	-	737	19.7	0.03	0.276	770	24.5	0.57	0.182
101439	SCV	N	17.4	0.987	11.5	0.574	1.72	2.47	3.52	7.39	1.05	33	18.0	32	17.9	0.00	0.288	31	17.8	0.00	0.288
101440	SCV	N	17.4	0.987	28.7	0.703	2.40	3.08	3.88	7.78	1.05	67	18.2	67	18.9	0.19	0.280	67	18.8	0.26	0.232
101441	SCV	N	17.4	0.987	6.9	0.604	1.51	2.35	3.46	7.87	1.02	26	17.6	26	17.6	0.00	0.288	26	17.9	0.32	0.219
101442	SCV	N	17.4	0.987	18.5	0.780	2.00	2.79	3.85	8.44	1.12	47	15.2	47	15.4	0.14	0.284	47	15.7	0.25	0.230
101443	SCV	N	17.4	0.987	18.4	0.755	1.69	3.12	3.97	8.49	1.08	67	16.5	67	17.1	0.20	0.279	68	17.7	0.50	0.187
101444	SCV	N	17.4	0.987	20.1	0.825	2.46	3.11	4.16	9.11	1.19	62	13.4	62	13.9	0.18	0.279	62	14.3	0.45	0.193
101445	SCV	N	17.4	0.987	9.4	0.835	1.49	3.32	4.02	8.43	1.09	78	17.0	78	17.3	0.08	0.284	78	17.6	0.21	0.241
101446	SCV	N	17.4	0.987	15.9	0.662	1.74	2.74	3.72	8.01	1.04	47	17.4	48	18.1	0.31	0.276	48	18.6	0.63	0.168
101447	NCV	N	16.7	0.995	10.6	0.759	2.05	2.54	3.80	8.25	1.11	33	15.2	34	16.1	0.52	0.268	34	16.5	0.94	0.126
101448	NCV	N	16.7	0.995	7.3	0.703	1.83	2.41	3.67	7.90	1.05	28	16.7	29	18.3	0.66	0.259	30	19.2	1.62	0.073
101449	NCV	N	16.7	0.995	16.9	0.556	2.15	2.30	3.62	8.23	1.09	21	15.5	21	16.1	0.64	0.267	22	17.1	1.48	0.080
101451	NCV	N	16.7	0.995	20.8	0.667	2.47	2.52	3.71	8.28	1.11	32	15.5	32	15.5	0.07	0.287	32	15.7	0.17	0.247
101452	NCV	N	16.5	0.991	12.1	0.637	1.97	2.65	3.73	8.11	1.06	41	16.7	42	17.4	0.36	0.275	42	17.9	0.70	0.157

Table S2. Measured data and model results for all 905 samples.

Sample Number	Region[a]	AR area[b]	MAAT[c] (ºC)	Atmo. pres.[d] (atm)	^{3}H (piC/L)[e]	^{4}He (x 10^{-7})[ef]	^{3}He/^{4}He (x 10^{-6})[e]	Ne (x 10^{-7})[f]	Ar (x 10^{-4})[f]	Kr (x 10^{-8})[f]	Xe (x 10^{-8})[f]	ΔNe_{UA} (%)	NGT_{UA} (ºC)	ΔNe_{CE} (%)	NGT_{CE} (ºC)	CE *F* value	$L_{ex,CE}$[g]	ΔNe_{PR} (%)	NGT_{PR} (ºC)	PR *R* value	$L_{ex,PR}$[g]
101453	NCV	N	16.5	0.991	15.6	0.636	2.03	2.60	3.62	7.99	1.04	39	17.4	39	17.5	0.14	0.284	39	17.8	0.30	0.222
101454	NCV	N	16.5	0.991	12.4	0.623	1.65	2.57	3.49	7.71	1.05	38	18.3	35	17.9	0.00	0.288	35	17.9	0.00	0.288
101455	NCV	N	16.1	0.997	11.3	0.851	1.52	3.24	4.48	9.83	1.24	-	-	67	14.0	0.41	0.261	70	16.2	1.50	0.078
101456	NCV	N	16.7	0.995	13.5	0.886	2.00	2.87	3.96	8.69	1.15	49	14.7	50	15.1	0.21	0.280	50	15.4	0.42	0.199
101457	NCV	N	16.2	0.995	1.3	2.13	0.502	2.85	3.87	8.24	1.12	50	15.9	50	16.0	0.04	0.287	50	15.9	0.01	0.286
101458	NCV	N	16.2	0.995	3.7	0.914	1.28	2.57	3.83	8.55	1.15	34	14.3	34	14.7	0.34	0.277	34	15.0	0.56	0.176
101459	NCV	N	16.2	0.995	1.6	0.786	1.24	2.60	3.84	8.73	1.17	34	13.8	34	13.8	0.00	0.288	34	13.8	0.00	0.288
101460	NCV	N	16.7	0.995	1.1	4.78	0.751	2.34	3.64	8.42	1.13	21	14.7	21	14.7	0.00	0.288	21	14.7	0.00	0.288
101461	NCV	N	16.7	0.995	0.1	13.3	0.570	2.44	3.69	8.44	1.12	27	14.9	26	14.9	0.00	0.288	27	14.9	0.04	0.278
101462	MDB	N	16.7	0.916	4.8	0.687	1.47	2.77	4.00	8.62	1.13	54	11.9	56	14.2	0.48	0.259	58	15.7	1.50	0.077
101463	MDB	N	15.2	0.916	0.0	1.25	0.769	1.80	3.01	6.91	0.960	4	17.3	3	17.1	0.00	0.288	3	17.1	0.00	0.288
101464	MDB	N	15.2	0.916	0.5	9.70	0.289	2.23	3.26	7.33	1.01	27	16.4	26	16.1	0.00	0.288	26	16.1	0.00	0.288
101465	MDB	N	17.1	0.916	0.6	11.6	0.241	2.22	3.41	7.86	1.05	25	14.3	24	14.3	0.00	0.288	25	14.3	0.00	0.288
101466	MDB	N	17.1	0.916	0.0	12.8	0.166	2.34	3.67	8.37	1.11	30	12.2	30	13.2	0.58	0.262	32	14.4	1.52	0.074
101467	MDB	N	16.2	0.896	0.1	0.488	1.36	1.91	3.36	7.93	1.12	8	11.8	7	11.6	0.00	0.288	7	11.7	0.00	0.288
101468	MDB	N	15.2	0.884	0.0	1.58	1.24	5.43	5.02	9.88	1.28	209	12.1	201	11.7	0.00	0.288	201	11.7	0.00	0.288
101469	MDB	N	16.2	0.896	0.0	25.0	0.475	2.51	3.54	7.96	1.04	45	14.2	45	14.4	0.17	0.283	45	14.8	0.41	0.199
101470	MDB	N	16.2	0.896	0.1	24.2	0.453	2.06	3.25	7.34	0.982	20	15.4	20	15.9	0.60	0.271	21	16.4	1.08	0.112
101471	MDB	N	16.7	0.896	0.0	1.46	1.21	2.58	3.79	8.46	1.10	46	12.0	47	13.5	0.48	0.262	49	15.0	1.43	0.081
101472	MDB	N	16.7	0.916	0.4	2.11	1.17	2.40	3.55	7.83	1.04	36	14.6	37	15.5	0.47	0.269	37	16.1	0.99	0.121
101473	MDB	N	16.2	0.896	0.0	22.4	0.403	2.03	3.28	7.45	1.01	17	14.6	18	15.0	0.62	0.271	18	15.3	1.01	0.118
101474	MDB	N	17.1	0.916	0.0	5.23	0.670	8.66	7.36	12.6	1.35	-	-	406	18.7	0.07	0.272	423	22.7	0.75	0.155
101475	MDB	N	16.2	0.896	1.0	1.17	0.696	2.04	3.17	7.02	0.940	21	16.9	21	17.5	0.63	0.269	21	17.9	1.07	0.115
101476	MDB	N	16.7	0.916	0.0	0.721	1.22	2.33	3.52	7.88	1.05	32	14.3	32	15.0	0.48	0.270	33	15.6	0.98	0.122
101477	MDB	N	16.7	0.916	3.6	0.687	1.41	2.83	4.18	8.92	1.16	-	-	59	14.1	0.51	0.253	62	16.1	1.85	0.057
101478	MDB	N	16.7	0.916	13.0	0.715	1.38	2.77	3.79	8.29	1.11	55	13.4	55	13.8	0.19	0.280	56	14.1	0.39	0.204
101479	MDB	N	16.2	0.896	0.2	2.83	1.36	11.0	8.48	13.9	1.49	-	-	544	16.0	0.03	0.278	556	18.2	0.43	0.200
101480	MDB	N	16.2	0.896	7.0	0.547	1.38	2.17	3.23	7.54	0.977	26	15.8	26	15.7	0.00	0.288	26	15.8	0.00	0.288
101481	NCV	N	16.2	0.995	7.8	0.954	1.34	2.73	3.83	8.67	1.13	42	15.0	42	15.0	0.00	0.288	42	15.2	0.14	0.255
101482	NCV	N	16.2	0.995	1.6	2.07	0.496	2.89	3.86	8.38	1.09	52	16.3	53	16.7	0.19	0.281	53	17.0	0.39	0.206
101484	NCV	N	16.2	0.995	8.9	0.725	1.69	2.57	3.90	8.87	1.18	32	13.3	33	13.7	0.40	0.274	33	14.3	0.82	0.138
101485	NCV	N	16.2	0.995	3.6	1.85	0.600	2.68	3.83	8.58	1.10	41	15.3	41	16.0	0.38	0.274	42	16.8	0.91	0.130
101486	NCV	N	16.1	0.993	11.0	0.657	2.17	2.69	4.00	9.00	1.18	39	13.0	39	13.9	0.46	0.268	40	14.8	1.11	0.108
101487	NCV	N	16.1	0.993	0.6	0.556	1.32	2.14	3.30	7.74	1.02	14	17.9	13	17.7	0.00	0.288	13	17.7	0.00	0.288
101488	NCV	N	16.1	0.993	0.1	0.962	0.948	1.97	3.17	7.55	1.04	4	17.9	-	-	-	-	-	-	-	-
101489	NCV	N	16.1	0.993	2.7	0.582	1.37	2.21	3.44	7.87	1.05	17	16.8	17	16.8	0.00	0.288	17	16.8	0.00	0.288
101490	NCV	N	16.1	0.993	10.4	0.697	1.92	2.86	4.20	9.39	1.25	45	11.5	46	12.4	0.39	0.270	47	13.1	0.90	0.128
101491	NCV	N	16.1	0.993	4.3	0.638	1.79	2.61	4.00	9.06	1.19	34	12.6	35	13.7	0.55	0.263	36	14.9	1.45	0.079
101492	NCV	N	16.1	0.993	0.8	0.594	1.49	2.53	3.80	8.47	1.12	32	14.7	33	15.4	0.50	0.269	33	16.1	1.04	0.116
101493	NCV	N	16.1	0.993	1.3	0.593	1.50	2.33	3.70	8.27	1.11	22	14.8	22	15.6	0.67	0.263	23	16.4	1.45	0.081
101494	NCV	N	16.1	0.993	0.0	0.580	1.37	2.36	3.39	7.50	1.05	26	18.3	24	17.9	0.00	0.288	24	17.9	0.00	0.288
101495	NCV	N	16.1	0.993	7.6	0.680	1.62	2.73	3.84	8.43	1.10	44	15.6	44	16.4	0.36	0.274	45	17.0	0.78	0.146
101496	NCV	N	16.1	0.993	1.1	0.623	1.27	2.25	3.42	7.80	1.05	19	17.2	18	17.0	0.00	0.288	18	17.0	0.00	0.288
101497	NCV	N	16.1	0.993	0.5	0.586	1.41	2.40	3.81	8.49	1.18	24	13.4	24	13.9	0.52	0.272	24	14.0	0.66	0.159
101498	NCV	N	16.1	0.993	1.4	0.584	1.47	2.42	3.72	8.41	1.12	26	14.6	26	15.1	0.50	0.273	27	15.6	0.92	0.128

Table S2. Measured data and model results for all 905 samples.

Sample Number	Region[a]	AR area[b]	MAAT[c] (ºC)	Atmo. pres.[d] (atm)	^{3}H (piC/L)[e]	^{4}He (x 10^{-7})[ef]	^{3}He/^{4}He (x 10^{-6})[e]	Ne (x 10^{-7})[f]	Ar (x 10^{-4})[f]	Kr (x 10^{-8})[f]	Xe (x 10^{-8})[f]	ΔNe_{UA} (%)	NGT_{UA} (ºC)	ΔNe_{CE} (%)	NGT_{CE} (ºC)	CE *F* value	$L_{ex,CE}$[g]	ΔNe_{PR} (%)	NGT_{PR} (ºC)	PR *R* value	$L_{ex,PR}$[g]
101499	NCV	N	16.1	0.993	1.1	0.567	1.43	2.41	3.69	8.59	1.15	25	14.2	23	14.0	0.00	0.288	24	14.1	0.00	0.288
101500	NCV	N	16.1	0.993	0.8	0.600	1.41	2.54	3.89	8.93	1.22	30	12.6	29	12.6	0.00	0.288	29	12.6	0.00	0.288
101501	NCV	N	16.1	0.993	9.8	0.654	1.73	2.75	4.15	9.09	1.21	41	12.2	42	13.8	0.54	0.260	43	14.8	1.42	0.082
101502	NCV	N	16.1	0.993	13.9	0.726	2.23	3.18	4.45	9.64	1.31	61	10.7	61	11.7	0.31	0.270	62	12.2	0.72	0.150
101503	NCV	N	16.1	0.993	5.4	0.543	1.90	2.31	3.69	8.09	1.14	20	14.6	21	15.0	0.54	0.274	21	15.0	0.45	0.194
101504	NCV	N	16.1	0.993	11.0	0.568	2.20	2.48	4.30	8.07	1.15	-	-	-	-	-	-	-	-	-	-
101505	NCV	N	16.1	0.993	10.3	0.613	1.83	2.75	3.85	8.32	1.15	44	15.1	43	15.1	0.00	0.288	43	15.0	0.00	0.288
101506	NCV	N	16.1	0.993	8.0	0.532	2.18	2.29	3.65	8.22	1.12	19	14.8	20	15.1	0.55	0.274	20	15.4	0.78	0.144
101507	NCV	N	16.1	0.993	9.1	0.522	2.51	2.29	3.68	8.37	1.16	19	14.0	18	14.0	0.00	0.288	18	14.0	0.00	0.288
101508	NCV	N	16.1	0.993	4.6	0.520	1.71	2.30	3.68	8.20	1.13	20	14.5	20	14.9	0.58	0.272	20	15.1	0.69	0.157
101509	NCV	N	16.1	0.993	2.5	0.563	1.69	2.41	3.76	8.12	1.11	26	15.0	27	16.2	0.65	0.260	28	16.7	1.29	0.093
101510	NCV	N	16.1	0.993	12.6	0.641	2.21	2.65	3.85	8.39	1.11	39	15.1	40	16.2	0.47	0.268	41	16.9	1.04	0.117
101511	NCV	N	16.1	0.993	1.0	0.566	1.60	2.40	3.81	8.55	1.15	25	13.7	25	14.6	0.64	0.262	26	15.4	1.45	0.080
101512	NCV	N	16.1	0.993	11.9	0.498	8.13	2.30	3.56	8.04	1.12	20	15.4	19	15.3	0.00	0.288	19	15.3	0.00	0.288
101513	NCV	N	16.1	0.993	9.5	0.686	1.54	2.77	4.27	9.13	1.18	-	-	47	16.4	0.61	0.249	50	18.5	2.26	0.042
101514	NCV	N	16.1	0.993	11.0	0.550	1.90	2.27	3.65	8.12	1.08	20	15.5	21	17.0	0.76	0.254	22	18.4	2.20	0.044
101515	NCV	N	16.1	0.993	10.0	0.612	6.71	2.68	3.78	8.25	1.08	42	16.1	42	16.9	0.38	0.273	43	17.5	0.77	0.147
101516	NCV	N	16.1	0.993	7.7	0.624	1.88	2.90	3.87	8.44	1.15	51	15.3	49	15.2	0.00	0.288	49	15.1	0.00	0.288
101517	NCV	N	16.1	0.993	8.5	0.564	2.26	2.31	3.80	8.40	1.17	20	13.4	20	14.2	0.71	0.260	20	14.4	1.22	0.097
101518	NCV	N	16.1	0.993	0.0	0.531	2.39	2.42	3.58	8.29	1.18	25	14.7	-	-	-	-	-	-	-	-
101519	NCV	N	16.1	0.993	8.2	0.509	1.77	2.08	3.68	8.43	1.18	7	12.9	7	13.4	0.90	0.252	7	13.7	1.96	0.049
101520	NCV	N	16.1	0.993	12.4	0.516	2.08	2.30	3.58	7.95	1.12	20	15.5	19	15.4	0.00	0.288	19	15.4	0.00	0.288
101521	NCV	N	16.1	0.993	10.9	0.609	1.98	2.56	3.81	8.44	1.08	35	15.3	36	17.1	0.59	0.260	38	18.9	1.80	0.062
101522	NCV	N	16.1	0.993	6.4	0.627	1.83	2.76	3.97	8.90	1.22	41	13.0	40	12.9	0.00	0.288	40	12.9	0.00	0.288
101523	NCV	N	16.1	0.993	4.6	0.534	1.73	2.45	3.70	8.30	1.18	27	14.3	25	14.1	0.00	0.288	25	14.1	0.00	0.288
101524	NCV	N	16.1	0.993	4.2	0.580	1.62	2.62	3.79	8.53	1.15	36	14.6	35	14.5	0.00	0.288	36	14.5	0.00	0.288
101525	NCV	N	16.1	0.993	5.5	0.521	1.75	2.32	3.61	8.18	1.16	20	14.6	19	14.5	0.00	0.288	19	14.5	0.00	0.288
101526	NCV	N	16.1	0.993	2.3	0.960	1.12	2.28	3.44	7.80	1.07	21	17.0	19	16.8	0.00	0.288	19	16.8	0.00	0.288
101527	NCV	N	16.1	0.993	2.9	0.523	1.52	2.23	3.25	8.39	1.20	-	-	-	-	-	-	-	-	-	-
101528	NCV	N	16.1	0.993	0.5	1.87	0.801	1.94	2.92	7.65	1.06	-	-	-	-	-	-	-	-	-	-
101529	NCV	N	16.1	0.993	4.3	0.499	1.78	2.31	2.79	8.00	1.21	-	-	-	-	-	-	-	-	-	-
101530	NCV	N	16.1	0.993	9.6	0.514	2.08	2.34	3.66	8.31	1.15	22	14.3	20	14.2	0.00	0.288	21	14.3	0.00	0.288
101551	MDB	N	16.7	0.916	0.7	0.870	1.11	2.49	3.92	8.88	1.18	36	10.3	37	11.8	0.58	0.257	39	13.2	1.67	0.064
101552	MDB	N	15.2	0.916	0.0	1.80	0.838	2.33	3.33	7.43	0.984	34	16.7	34	16.7	0.00	0.288	34	16.7	0.00	0.288
101553	MDB	N	16.2	0.916	0.1	1.44	0.767	2.48	3.72	8.31	1.10	38	12.8	39	13.9	0.51	0.264	40	15.0	1.30	0.091
101554	MDB	N	16.2	0.916	0.4	3.83	0.536	2.45	3.53	7.84	1.05	38	14.7	39	14.7	0.08	0.286	39	14.9	0.16	0.249
101555	MDB	N	16.7	0.916	0.1	1.00	1.20	2.81	3.98	8.70	1.13	56	12.0	58	13.7	0.42	0.263	59	15.1	1.26	0.094
101556	MDB	N	15.2	0.896	11.6	0.790	1.40	3.20	4.41	9.81	1.21	-	-	80	11.6	0.38	0.258	84	14.6	1.65	0.066
101557	MDB	N	17.1	0.916	0.0	3.08	0.230	2.05	3.47	8.10	1.14	13	12.0	12	11.9	0.00	0.288	12	11.9	0.00	0.288
101558	MDB	N	16.2	0.916	0.1	23.3	0.450	2.52	3.58	7.98	1.09	41	14.0	40	13.9	0.00	0.288	40	13.9	0.00	0.288
101559	MDB	N	16.2	0.916	0.0	8.69	0.404	2.41	3.54	7.90	1.07	35	14.1	35	14.2	0.07	0.287	36	14.3	0.14	0.255
101560	MDB	N	16.2	0.916	0.0	3.17	0.553	2.76	4.31	9.39	1.26	-	-	51	11.0	0.55	0.251	53	12.4	1.80	0.056
101561	MDB	N	17.1	0.916	0.0	12.1	0.121	2.57	3.35	7.23	0.929	51	18.9	51	19.0	0.05	0.287	51	19.3	0.17	0.249
101562	MDB	N	17.1	0.916	0.1	25.2	0.109	2.17	3.47	8.09	1.15	20	12.3	18	12.1	0.00	0.288	18	12.1	0.00	0.288
101563	MDB	N	16.2	0.916	0.4	2.59	0.402	2.88	3.90	8.58	1.15	59	12.3	60	12.4	0.05	0.286	60	12.6	0.14	0.254

Table S2. Measured data and model results for all 905 samples.

Sample Number	Region[a]	AR area[b]	MAAT[c] (ºC)	Atmo. pres.[d] (atm)	^{3}H (piC/L)[e]	^{4}He (x 10^{-7})[ef]	^{3}He/^{4}He (x 10^{-6})[e]	Ne (x 10^{-7})[f]	Ar (x 10^{-4})[f]	Kr (x 10^{-8})[f]	Xe (x 10^{-8})[f]	ΔNe_{UA} (%)	NGT_{UA} (ºC)	ΔNe_{CE} (%)	NGT_{CE} (ºC)	CE *F* value	$L_{ex,CE}$[g]	ΔNe_{PR} (%)	NGT_{PR} (ºC)	PR *R* value	$L_{ex,PR}$[g]
101567	SFBA	Y	15.2	0.979	25.5	1.69	1.59	7.16	7.16	12.9	1.47	-	-	281	15.5	0.13	0.265	295	19.7	1.09	0.114
101573	NCV	N	16.1	0.993	0.2	0.748	1.12	2.04	3.39	7.54	1.03	9	17.2	9	17.8	0.87	0.257	10	18.1	1.78	0.062
101576	SFBA	Y	15.2	0.979	19.9	1.10	1.58	4.10	4.68	9.68	1.20	116	13.7	117	15.0	0.15	0.276	119	16.0	0.58	0.174
101579	NCV	N	16.1	0.993	15.1	0.534	2.37	2.29	3.71	8.17	1.15	19	14.2	20	14.6	0.58	0.272	20	14.6	0.52	0.182
101582	NCV	N	16.1	0.993	0.0	0.569	1.32	2.11	3.46	7.94	1.05	11	16.3	12	17.0	0.83	0.256	15	20.3	3.25	0.019
101583	NCV	N	16.1	0.993	0.4	0.658	1.21	2.07	3.43	7.68	1.07	10	16.4	10	16.5	0.58	0.280	10	16.5	0.26	0.229
101584	NCV	N	16.1	0.993	7.2	0.542	2.06	2.27	3.72	8.39	1.14	18	13.9	18	14.6	0.73	0.260	19	15.2	1.51	0.076
101585	NCV	N	16.1	0.993	11.0	0.514	2.13	2.13	3.60	8.17	1.15	11	14.2	11	14.2	0.34	0.285	11	14.2	0.10	0.263
101586	NC	N	7.8	0.836	10.6	9.05	0.391	2.18	3.76	8.70	1.22	26	6.9	27	8.0	0.67	0.252	28	8.8	1.70	0.058
101587	NC	N	7.8	0.836	10.2	47.9	0.338	2.36	4.06	9.27	1.25	-	-	38	8.5	0.66	0.241	41	10.5	2.43	0.030
101588	NC	N	7.8	0.831	7.0	0.401	1.39	1.71	3.58	8.76	1.26	0	5.6	0	5.6	0.00	-	0	5.6	0.00	-
101589	NC	N	7.8	0.812	7.9	0.744	1.29	2.64	4.27	9.65	1.32	-	-	56	6.1	0.51	0.248	58	7.8	1.80	0.052
101590	NC	N	7.8	0.809	10.3	0.777	1.71	3.08	4.77	10.7	1.33	-	-	85	8.3	0.46	0.241	96	13.6	2.51	0.030
101591	NC	N	7.8	0.807	29.1	3.59	0.595	3.07	4.68	10.3	1.40	-	-	79	5.0	0.41	0.249	83	6.8	1.62	0.061
101594	NCV	N	16.1	0.993	0.6	1.22	0.885	1.96	3.31	7.55	1.07	4	16.7	4	16.7	0.00	0.288	4	16.7	0.00	0.288
101595	NCV	N	16.1	0.993	6.7	0.573	1.83	2.43	3.76	8.19	1.16	26	14.4	26	14.6	0.33	0.280	26	14.5	0.15	0.252
101596	NCV	N	16.1	0.993	3.0	0.532	1.55	2.27	3.48	7.86	1.09	19	16.4	18	16.2	0.00	0.288	18	16.2	0.00	0.288
101597	NCV	N	16.1	0.993	3.3	0.648	1.59	2.86	3.95	8.63	1.18	49	14.3	48	14.2	0.00	0.288	48	14.2	0.00	0.288
101598	NCV	N	16.1	0.993	16.8	0.516	1.55	2.08	3.32	7.63	1.06	10	17.1	9	16.9	0.00	0.288	9	16.9	0.00	0.288
101600	NCV	N	16.1	0.993	0.3	0.476	1.41	2.12	3.25	7.63	1.03	13	18.1	12	17.8	0.00	0.288	12	17.8	0.00	0.288
101601	NCV	N	16.5	0.995	12.8	0.779	1.43	2.53	3.68	8.41	1.09	33	15.7	32	15.7	0.00	0.288	33	16.0	0.22	0.237
101602	NCV	N	16.5	0.995	25.3	0.614	2.27	2.69	3.82	8.50	1.13	40	15.1	40	15.1	0.04	0.287	40	15.3	0.16	0.250
101603	NCV	N	16.5	0.995	27.8	0.622	2.22	2.77	3.81	8.47	1.09	46	16.0	46	16.3	0.19	0.282	47	16.8	0.46	0.193
101604	NCV	N	16.1	0.993	1.6	0.469	1.40	2.08	3.30	7.54	1.06	10	17.3	10	17.1	0.00	0.288	10	17.1	0.00	0.288
101605	NCV	N	16.1	0.993	10.1	0.525	2.13	2.29	3.57	8.02	1.09	21	15.8	21	15.9	0.18	0.285	21	16.0	0.24	0.234
101606	NCV	N	16.1	0.993	9.1	0.490	1.84	2.14	3.59	8.19	1.17	11	13.9	10	13.9	0.00	0.288	10	13.9	0.00	0.288
101607	NCV	N	16.1	0.993	6.8	0.487	1.83	2.15	3.57	8.20	1.18	11	14.0	11	13.9	0.00	0.288	11	13.9	0.00	0.288
101608	NCV	N	16.1	0.993	0.8	0.505	1.47	2.21	3.60	8.13	1.16	15	14.4	14	14.3	0.00	0.288	14	14.3	0.00	0.288
101610	NCV	N	16.5	0.988	0.8	0.538	1.51	2.41	3.85	8.94	1.27	22	11.5	21	11.2	0.00	0.288	21	11.2	0.00	0.288
101620	SCV	Y	18.4	0.986	20.1	2.01	1.55	7.42	7.25	13.3	1.47	-	-	292	15.6	0.12	0.266	308	20.2	1.08	0.116
101621	SCV	Y	18.4	0.986	17.9	1.00	1.37	3.42	4.17	8.46	1.09	84	16.7	85	18.1	0.23	0.274	86	18.8	0.64	0.167
101622	SCV	Y	18.4	0.986	19.2	1.31	1.70	4.64	4.76	9.00	1.21	147	16.2	146	16.2	0.00	0.288	145	16.1	0.00	0.288
101623	SCV	Y	18.4	0.986	23.5	1.09	1.97	3.68	4.53	9.14	1.17	94	14.2	96	16.5	0.27	0.268	98	17.6	0.92	0.130
101624	SCV	Y	18.4	0.986	30.0	0.938	2.79	3.46	4.29	8.61	1.18	82	14.8	83	15.6	0.16	0.279	83	15.6	0.28	0.225
101625	SCV	Y	18.4	0.986	9.6	0.674	1.54	2.47	3.66	7.68	1.03	34	17.2	35	19.0	0.60	0.261	35	19.5	1.33	0.093
101626	SCV	Y	18.4	0.986	11.1	0.683	1.56	2.56	3.68	7.90	1.06	37	16.6	37	17.3	0.40	0.274	38	17.5	0.61	0.170
101627	SCV	Y	18.4	0.986	10.5	0.845	1.43	3.05	4.15	8.95	1.12	61	14.3	63	16.6	0.42	0.263	65	18.5	1.42	0.085
101628	SCV	Y	18.4	0.986	38.1	1.14	3.19	4.62	5.39	10.1	1.26	-	-	148	17.3	0.24	0.263	153	19.5	1.21	0.103
101629	SCV	Y	18.4	0.986	5.7	0.852	1.49	2.75	3.87	8.30	1.09	46	15.6	47	17.0	0.45	0.267	48	17.9	1.09	0.112
101630	SCV	Y	18.4	0.986	13.9	0.577	2.10	2.25	3.52	7.57	1.05	21	16.8	21	17.4	0.63	0.268	21	17.5	0.75	0.151
101631	SCV	Y	18.4	0.986	9.8	0.664	1.71	2.47	3.79	8.10	1.13	30	14.7	31	15.6	0.56	0.266	31	15.8	0.88	0.133
101632	SCV	Y	18.4	0.986	9.7	0.645	1.55	2.57	3.66	8.27	1.11	35	15.5	34	15.3	0.00	0.288	34	15.4	0.00	0.288
101633	SCV	Y	18.4	0.986	0.3	2.28	0.416	2.23	3.70	8.10	1.12	17	14.3	18	15.7	0.78	0.252	19	16.0	1.78	0.060
101634	SCV	Y	18.4	0.986	8.2	0.918	1.74	3.24	4.29	8.89	1.12	-	-	74	17.6	0.40	0.262	77	19.5	1.41	0.087
101635	SCV	Y	18.4	0.986	4.3	0.549	1.57	2.10	3.53	7.90	1.10	11	15.0	11	15.4	0.80	0.263	11	15.5	1.04	0.115

Table S2. Measured data and model results for all 905 samples.

Sample Number	Region[a]	AR area[b]	MAAT[c] (ºC)	Atmo. pres.[d] (atm)	^{3}H (piC/L)[e]	^{4}He (x 10^{-7})[ef]	$^{3}He/^{4}He$ (x 10^{-6})[e]	Ne (x 10^{-7})[f]	Ar (x 10^{-4})[f]	Kr (x 10^{-8})[f]	Xe (x 10^{-8})[f]	ΔNe_{UA} (%)	NGT_{UA} (ºC)	ΔNe_{CE} (%)	NGT_{CE} (ºC)	CE *F* value	$L_{ex,CE}$[g]	ΔNe_{PR} (%)	NGT_{PR} (ºC)	PR *R* value	$L_{ex,PR}$[g]
101636	SCV	Y	18.4	0.986	22.5	0.662	2.34	2.57	3.78	8.07	1.07	37	15.9	38	17.4	0.55	0.263	39	18.2	1.27	0.097
101637	SCV	Y	18.4	0.986	4.5	0.658	1.66	2.47	3.73	8.22	1.09	31	15.3	31	16.5	0.58	0.264	32	17.4	1.38	0.088
101638	SCV	Y	18.4	0.986	27.3	0.568	2.23	2.13	3.41	7.37	0.981	16	18.2	17	20.3	0.82	0.251	18	20.9	2.29	0.042
101639	SCV	Y	18.4	0.986	16.3	0.866	1.50	3.19	4.09	8.12	1.10	71	16.5	72	17.8	0.27	0.273	73	18.0	0.55	0.180
101640	SCV	Y	18.4	0.986	21.0	3.36	1.44	9.74	8.04	13.2	1.45	-	-	432	19.4	0.06	0.275	445	22.3	0.61	0.175
101641	SCV	Y	18.4	0.986	12.4	2.08	1.42	7.98	6.11	10.7	1.30	328	18.9	-	-	-	-	-	-	-	-
101642	SCV	Y	18.4	0.986	31.7	1.56	2.22	6.14	6.22	11.3	1.31	-	-	232	18.3	0.15	0.267	242	21.7	1.05	0.121
101643	SCV	Y	18.4	0.986	15.3	0.590	1.63	2.37	3.80	8.06	1.12	25	14.4	26	16.1	0.71	0.254	26	16.3	1.52	0.076
101644	SCV	Y	18.4	0.986	14.4	1.01	1.35	3.59	4.13	8.30	1.06	95	18.2	96	19.1	0.13	0.280	96	19.5	0.36	0.212
101645	SCV	Y	18.4	0.986	29.4	0.991	2.59	3.59	4.33	8.83	1.20	89	14.6	89	14.8	0.06	0.285	89	14.8	0.08	0.268
101646	SCV	Y	18.4	0.986	20.1	1.19	1.95	4.70	5.37	9.86	1.25	-	-	153	17.7	0.22	0.264	158	19.6	1.08	0.115
101647	SCV	Y	18.4	0.986	25.2	0.974	3.04	3.45	4.17	8.45	1.11	85	16.5	85	17.3	0.15	0.280	86	17.5	0.33	0.216
101648	SCV	Y	18.4	0.986	17.1	0.786	1.57	2.96	3.85	8.30	1.14	56	15.8	54	15.7	0.00	0.288	54	15.6	0.00	0.288
101649	SCV	Y	18.4	0.986	18.4	0.694	2.15	2.79	4.02	8.66	1.13	47	14.2	48	16.3	0.51	0.260	50	17.7	1.50	0.079
101660	SCV	Y	18.4	0.986	19.1	1.04	1.56	3.56	4.26	8.79	1.17	87	15.1	88	15.3	0.04	0.286	88	15.3	0.06	0.274
101661	SCV	Y	18.4	0.986	18.8	2.13	1.47	7.48	6.30	10.9	1.28	305	17.2	307	18.9	0.03	0.282	309	19.5	0.24	0.235
101662	SCV	Y	18.4	0.986	23.8	1.31	1.87	4.75	5.63	10.9	1.26	-	-	157	18.5	0.27	0.258	169	24.2	1.73	0.071
101663	SCV	Y	18.4	0.986	30.2	3.10	1.92	9.49	8.06	13.7	1.50	-	-	408	17.0	0.06	0.273	421	20.1	0.66	0.165
101664	SCV	Y	18.4	0.986	11.5	0.711	1.94	2.71	4.03	8.65	1.10	-	-	46	17.7	0.59	0.253	49	20.1	2.11	0.048
101665	SFBA	Y	15.6	0.989	14.9	0.859	1.61	3.96	4.41	9.11	1.22	106	14.9	103	14.6	0.00	0.288	102	14.6	0.00	0.288
101666	SFBA	Y	15.6	0.991	11.1	1.08	1.49	4.95	5.01	9.67	1.29	157	14.5	155	14.4	0.00	0.288	155	14.3	0.00	0.288
101667	SFBA	Y	15.6	0.991	11.1	1.35	1.50	6.40	5.84	10.8	1.34	234	14.1	234	14.6	0.02	0.285	235	14.7	0.09	0.265
101668	SFBA	Y	15.6	0.989	2.2	1.28	1.45	5.83	5.49	10.6	1.30	205	14.4	205	14.7	0.02	0.286	206	15.0	0.11	0.262
101673	SFBA	Y	15.6	0.989	15.6	67.6	0.176	4.76	4.91	9.48	1.27	149	14.7	147	14.6	0.00	0.288	147	14.6	0.00	0.288
101677	SCV	Y	18.4	0.986	20.2	2.14	1.53	8.04	6.90	12.4	1.46	318	12.4	319	14.0	0.04	0.281	323	14.9	0.29	0.222
101678	SCV	Y	18.4	0.986	28.5	1.32	2.41	5.42	5.84	10.8	1.34	-	-	186	15.5	0.16	0.267	192	17.4	0.91	0.131
101679	SCV	Y	18.4	0.986	9.6	0.933	1.56	3.20	4.37	9.41	1.18	-	-	69	15.6	0.42	0.260	72	18.1	1.60	0.073
101680	SCV	Y	18.4	0.986	11.3	0.761	2.08	3.12	4.34	9.03	1.18	63	13.0	65	15.8	0.44	0.259	67	17.2	1.43	0.083
101681	SCV	Y	18.4	0.986	0.8	0.584	1.52	2.35	3.71	8.00	1.16	23	14.3	23	14.4	0.26	0.283	23	14.3	0.00	0.288
101682	SCV	Y	18.4	0.986	28.4	1.30	2.11	5.04	5.54	10.4	1.33	-	-	165	14.5	0.16	0.269	168	15.7	0.74	0.150
101683	SCV	Y	18.4	0.986	30.4	1.20	3.24	4.79	5.50	10.5	1.26	-	-	157	17.2	0.23	0.262	164	20.5	1.32	0.095
101684	SCV	Y	18.4	0.986	9.7	1.98	1.23	6.00	6.03	11.3	1.33	-	-	218	15.9	0.12	0.270	224	18.1	0.80	0.144
101686	NC	N	9.1	0.880	13.4	0.475	1.95	1.97	3.68	8.64	1.26	9	7.7	9	8.0	0.83	0.258	9	8.0	1.13	0.099
101687	NC	N	9.1	0.880	0.4	3.58	7.00	2.08	3.69	8.89	1.27	14	7.6	13	7.5	0.00	0.288	13	7.5	0.00	0.288
101688	NC	N	9.8	0.880	7.7	1.29	6.56	2.10	3.79	9.21	1.31	14	6.6	14	6.6	0.00	0.288	14	6.7	0.07	0.269
101690	NC	N	9.8	0.877	-	0.545	2.81	2.01	3.80	9.31	1.30	9	6.2	10	6.8	0.87	0.245	14	10.6	3.83	0.008
101691	NC	N	9.8	0.880	1.3	2.31	3.17	1.93	3.42	8.14	1.10	10	10.9	11	11.8	0.87	0.245	15	16.1	3.84	0.010
101692	NC	N	10.3	0.877	0.0	1.17	2.79	2.09	3.50	8.24	1.14	19	10.4	19	10.4	0.00	0.288	19	10.5	0.11	0.259
101693	NC	N	10.3	0.905	15.9	1.29	1.30	2.80	4.12	9.31	1.21	54	9.4	55	10.9	0.43	0.261	57	12.5	1.40	0.081
101694	NC	N	10.3	0.905	11.8	0.611	1.36	2.50	3.80	8.80	1.19	37	10.3	37	10.4	0.12	0.285	38	10.7	0.33	0.212
101695	NC	N	10.3	0.905	13.2	0.726	1.37	2.60	3.86	8.50	1.18	44	10.9	45	11.3	0.28	0.277	45	11.4	0.40	0.199
101696	NC	N	8.1	0.848	1.5	2.20	1.92	1.89	3.22	7.46	1.03	13	12.3	14	12.6	0.70	0.269	14	13.0	1.24	0.094
101697	NC	N	8.1	0.848	1.4	1.98	1.68	1.93	3.37	7.78	1.08	14	10.7	15	11.6	0.81	0.250	16	12.6	2.21	0.039
101698	NC	N	8.1	0.848	1.4	2.41	1.82	1.91	3.26	7.75	1.07	13	11.2	12	11.2	0.00	0.288	13	11.2	0.00	0.288
101699	NC	N	8.1	0.848	2.2	2.47	1.77	1.89	3.29	7.75	1.06	12	11.1	12	11.4	0.73	0.267	13	12.3	1.86	0.053

Table S2. Measured data and model results for all 905 samples.

Sample Number	Region[a]	AR area[b]	MAAT[c] (ºC)	Atmo. pres.[d] (atm)	^{3}H (piC/L)[e]	^{4}He (x 10^{-7})[ef]	$^{3}He/^{4}He$ (x 10^{-6})[e]	Ne (x 10^{-7})[f]	Ar (x 10^{-4})[f]	Kr (x 10^{-8})[f]	Xe (x 10^{-8})[f]	ΔNe_{UA} (%)	NGT_{UA} (ºC)	ΔNe_{CE} (%)	NGT_{CE} (ºC)	CE *F* value	$L_{ex,CE}$[g]	ΔNe_{PR} (%)	NGT_{PR} (ºC)	PR *R* value	$L_{ex,PR}$[g]
101700	NC	N	8.2	0.863	0.0	0.520	1.81	2.00	2.96	6.55	0.898	23	18.0	22	17.9	0.00	0.288	22	17.9	0.00	0.288
101701	NC	N	8.2	0.863	0.2	0.521	1.81	1.92	2.97	6.54	0.919	18	17.3	16	17.2	0.00	0.288	16	17.1	0.00	0.288
101702	NC	N	8.2	0.862	0.4	0.518	1.79	2.08	3.33	7.51	1.05	23	12.6	23	12.7	0.27	0.283	23	12.8	0.20	0.240
101703	NC	N	8.2	0.863	0.3	0.490	1.49	1.88	2.89	6.42	0.903	16	17.9	13	17.8	0.00	0.288	13	17.7	0.00	0.288
101704	NC	N	8.2	0.862	0.1	0.653	2.16	2.25	3.39	7.57	1.06	33	12.9	33	12.8	0.00	0.288	33	12.8	0.00	0.288
101705	NC	N	8.2	0.862	1.2	0.529	1.48	2.07	3.11	6.85	0.958	26	16.0	25	15.9	0.00	0.288	24	15.9	0.00	0.288
101706	NC	N	8.9	0.863	0.7	0.688	3.53	2.29	3.55	8.00	1.15	32	10.7	31	10.6	0.00	0.288	31	10.6	0.00	0.288
101707	NC	N	6.8	0.856	1.4	0.770	2.71	2.12	3.64	8.32	1.20	21	8.5	21	8.9	0.59	0.267	22	9.0	0.72	0.147
101708	NC	N	6.8	0.856	6.0	0.621	1.63	2.64	3.78	8.36	1.14	54	10.3	55	10.8	0.22	0.277	55	11.1	0.44	0.193
101709	NC	N	8.8	0.887	8.5	0.441	1.47	1.98	3.78	9.14	1.37	6	6.1	6	6.0	0.00	0.288	6	6.0	0.00	0.288
101710	NC	N	8.8	0.887	9.4	0.442	1.48	1.94	3.79	9.19	1.34	4	6.1	4	6.1	0.00	0.288	4	6.1	0.00	0.288
101711	NC	N	8.8	0.887	9.5	0.437	1.48	1.98	3.74	9.11	1.35	6	6.4	6	6.4	0.00	0.288	6	6.4	0.00	0.288
101747	SFBA	Y	15.2	0.979	25.5	1.04	1.52	4.54	4.65	9.11	1.12	147	17.4	147	18.3	0.07	0.282	148	18.9	0.30	0.223
101754	SFBA	Y	15.2	0.979	0.9	1.38	0.870	4.01	4.76	9.66	1.21	112	13.1	113	15.4	0.22	0.269	116	16.8	0.89	0.133
101755	SFBA	Y	15.2	0.979	38.6	1.60	1.70	7.40	5.95	10.6	1.28	299	17.7	292	17.4	0.00	0.288	291	17.4	0.00	0.288
101756	SFBA	Y	15.2	0.979	5.7	1.07	1.11	3.70	4.55	9.06	1.24	94	13.1	95	14.2	0.18	0.275	96	14.4	0.42	0.199
101757	SFBA	Y	15.2	0.979	9.9	1.08	1.44	4.24	5.08	10.2	1.35	118	10.4	119	12.3	0.19	0.270	121	12.9	0.66	0.158
101758	SFBA	Y	15.2	0.979	8.3	1.31	1.05	3.67	4.42	9.03	1.26	91	13.2	90	13.1	0.00	0.288	90	13.1	0.00	0.288
101759	SFBA	Y	15.2	0.979	17.9	1.15	1.65	4.66	4.91	9.53	1.27	145	14.0	146	14.2	0.02	0.286	146	14.1	0.03	0.281
101760	SFBA	Y	15.2	0.979	12.9	1.26	1.40	4.25	4.89	9.79	1.28	121	12.3	122	13.6	0.14	0.275	124	14.1	0.48	0.188
101761	SFBA	Y	15.2	0.979	4.3	1.71	0.849	3.69	4.63	9.99	1.29	90	11.1	91	12.0	0.17	0.276	92	12.7	0.56	0.174
101763	SFBA	Y	15.2	0.979	37.8	0.800	1.86	3.27	4.03	8.86	1.10	75	15.8	75	16.2	0.12	0.282	76	16.9	0.42	0.199
101764	SFBA	Y	15.2	0.979	21.3	135.1	0.222	3.48	4.07	8.62	1.09	87	16.9	87	17.0	0.02	0.287	88	17.2	0.13	0.258
101765	SFBA	Y	15.2	0.979	15.4	0.512	1.35	2.21	3.61	7.87	1.03	19	15.8	22	20.4	0.80	0.245	23	20.7	2.84	0.026
103118	LAB	Y	17.8	0.983	3.8	3.00	0.728	4.28	4.83	9.61	1.19	127	14.2	129	16.4	0.18	0.272	131	17.7	0.76	0.150
103119	LAB	Y	18.0	0.964	20.9	0.656	1.29	2.51	3.66	7.87	1.02	38	16.5	39	18.6	0.58	0.260	41	20.0	1.65	0.071
103120	LAB	Y	16.8	0.957	7.7	1.32	1.29	4.84	5.60	10.7	1.34	-	-	160	13.9	0.21	0.263	166	16.0	1.10	0.110
103121	LAB	Y	17.8	0.976	4.7	7.32	0.313	4.59	4.93	9.86	1.24	142	13.6	143	14.6	0.09	0.280	144	15.2	0.36	0.210
103122	LAB	Y	18.3	0.986	16.2	0.763	1.28	2.37	3.55	7.66	1.01	28	17.7	29	19.2	0.65	0.261	30	20.2	1.58	0.076
103123	LAB	Y	17.8	0.984	7.0	1.31	1.07	4.03	4.98	9.66	1.16	-	-	121	20.0	0.33	0.259	129	24.1	1.72	0.071
103124	LAB	Y	16.8	0.958	16.4	0.853	1.11	2.37	3.61	8.00	1.07	29	15.1	29	16.0	0.58	0.265	30	16.8	1.26	0.096
103125	LAB	Y	18.2	0.989	1.0	1.69	1.25	3.91	4.55	9.25	1.18	106	14.7	107	15.8	0.15	0.277	108	16.4	0.48	0.189
103126	LAB	Y	18.2	0.993	21.4	0.708	1.64	2.83	3.83	8.08	1.04	51	17.3	52	18.8	0.41	0.269	53	19.7	1.03	0.121
103127	LAB	Y	18.2	0.973	-	0.667	1.52	2.67	3.75	8.27	1.04	45	16.2	46	17.6	0.47	0.266	47	19.3	1.37	0.089
103128	LAB	Y	18.0	0.957	15.8	2.56	1.41	9.35	8.03	13.4	1.53	-	-	408	15.3	0.06	0.273	420	17.7	0.61	0.170
103129	LAB	Y	18.0	0.957	15.8	1.97	1.42	7.55	6.97	12.4	1.44	-	-	308	14.7	0.08	0.272	317	16.9	0.68	0.160
103130	LAB	Y	17.6	0.971	11.0	1.73	1.43	6.56	6.31	11.7	1.37	-	-	250	15.0	0.10	0.272	256	17.0	0.69	0.159
103132	LAB	Y	18.2	0.980	16.1	1.57	1.37	6.55	6.65	12.1	1.43	-	-	247	15.1	0.13	0.266	257	18.1	0.98	0.124
103133	LAB	Y	18.2	0.984	4.3	1.93	1.17	3.55	4.31	9.06	1.13	88	15.1	89	16.5	0.22	0.273	91	17.6	0.74	0.152
103134	LAB	Y	18.2	0.986	1.1	1.08	1.06	3.29	4.27	8.97	1.12	75	14.7	76	17.1	0.35	0.265	79	18.8	1.22	0.102
103135	LAB	Y	13.4	0.976	13.5	0.831	1.36	3.39	4.24	9.17	1.19	78	13.6	78	13.9	0.09	0.283	79	14.2	0.27	0.226
103136	LAB	Y	16.8	0.973	-	1.04	1.39	4.36	5.01	9.31	1.12	-	-	145	21.3	0.26	0.263	151	24.5	1.38	0.095
103137	LAB	Y	18.0	0.973	9.1	2.43	0.527	3.07	3.94	8.31	1.10	66	16.0	66	16.4	0.15	0.281	66	16.7	0.30	0.223
103138	LAB	Y	18.2	0.973	0.9	5.23	0.286	2.74	3.90	8.52	1.13	46	14.2	46	15.0	0.38	0.271	47	15.6	0.81	0.141
103139	LAB	Y	18.2	0.973	1.1	5.31	0.292	2.83	3.90	8.41	1.11	51	14.9	52	15.7	0.32	0.274	52	16.1	0.65	0.163

Table S2. Measured data and model results for all 905 samples.

Sample Number	Region[a]	AR area[b]	MAAT[c] (°C)	Atmo. pres.[d] (atm)	^{3}H (piC/L)[e]	^{4}He (x 10^{-7})[ef]	$^{3}He/^{4}He$ (x 10^{-6})[e]	Ne (x 10^{-7})[f]	Ar (x 10^{-4})[f]	Kr (x 10^{-8})[f]	Xe (x 10^{-8})[f]	ΔNe_{UA} (%)	NGT_{UA} (°C)	ΔNe_{CE} (%)	NGT_{CE} (°C)	CE *F* value	$L_{ex,CE}$[g]	ΔNe_{PR} (%)	NGT_{PR} (°C)	PR *R* value	$L_{ex,PR}$[g]
103140	LAB	Y	18.2	0.984	1.5	1.10	1.13	3.54	4.52	9.54	1.22	84	12.6	86	14.5	0.28	0.268	88	15.7	0.96	0.123
103141	LAB	Y	18.2	0.984	12.8	1.17	1.42	4.69	5.00	10.1	1.25	145	13.4	146	14.5	0.09	0.279	147	15.2	0.39	0.204
103142	LAB	Y	18.2	0.993	23.0	1.50	1.38	5.88	6.60	12.6	1.37	-	-	217	19.1	0.21	0.258	-	-	-	-
103143	LAB	Y	18.2	0.985	14.6	1.72	1.40	6.61	6.05	11.4	1.38	244	12.8	245	13.7	0.03	0.283	246	14.3	0.22	0.237
103144	LAB	Y	17.8	0.972	8.1	1.07	1.49	4.20	4.97	9.87	1.21	-	-	126	16.2	0.25	0.264	131	18.5	1.16	0.106

[a] San Francisco Bay Area (SFBA), Los Angeles Basin (LAB), Northern California (NC), Mojave Desert Basin (MDB), northern portion of the Central Valley (NCV), and southern portion of the Central Valley (SCV)

[b] artificial recharge impacted area (Yes/No)

[c] mean annual air temperatures (MAAT) for station nearest the well, from the Western Regional Climate Center (http://www.wrcc.dri.edu/)

[d] calculated atmospheric pressure based on wellhead elevation using $P=P_o[(288.15/(288.15-(0.0065*H)))^{-5.25588}]$ where P_o is pressure at sea level (101 325 Pa) and H is the height above sea level in meters

[e] "-" indicates data unavailable

[f] values given in cm^3 STP g^{-1}

[g] L_{ex} is the He to Ne ratio of the excess air component (= He_{ex}/Ne_{ex})